Draft Report

Review of BEIS3 Formulation and Consequences Relative to Air Quality Standards

Task 1 – Review of BEIS3 Methodology for Estimating Emissions of Methane, Carbon Monoxide, and Nitric Oxide

EPRI Agreement EP-P5243/C2592

Prepared for:

Dr. Alan Hansen
Electric Power Research Institute
3412 Hillview Avenue
Palo Alto, CA 94304-1395

Prepared by:

James G. Wilkinson and Armistead G. Russell
Georgia Tech Research Corporation
Atlanta, GA

Steven Hanna
Hanna Consultants
Kennebunkport, ME

Jeffrey Vukovich
MCNC Environmental Programs
Research Triangle Park, NC

H. Christopher Frey
North Carolina State University
Raleigh, NC

17 September 2001

TABLE OF CONTENTS

1.0 Introduction

For at least the past twenty years, the U.S. EPA has used emissions observations and estimates from emissions models as one input to Chemical Transport Models (CTMs) to assist in making policy decisions concerning emissions controls for man-made (anthropogenic) pollutant sources such as industrial processes and motor vehicles. Equally important to this modeling process are emissions estimates from naturally occurring sources, broadly referred to as biogenic sources (e.g. vegetative material, soil microbes) and geogenic sources (e.g. lightning, petroleum seeps. The contribution of natural sources to an airshed's emissions load has significant implications towards the choice and extent of controls needed on anthropogenic sources in order to attain the National Ambient Air Quality Standards (NAAQS).

The CTMs are linked with estimates of pollutant emissions based on observations, projections and interpolations, and various types of models (e.g., statistical and deterministic) for anthropogenic, geogenic, and biogenic sources. An issue of concern is that the EPA's decision process treats pollutant standards as absolute numbers, whereas there is much uncertainty in both the observations and the models. An objective of the current project is to estimate the magnitudes of uncertainties in predictions of ozone by CTMs caused by uncertainties in biogenic emissions. The primary focus is on the EPA's third version of the Biogenic Emissions Inventory System (BEIS3 [Pierce, 2001a]), which is used to estimate biogenic emissions for input to CTMs.

BEIS3 estimates spatially and temporally resolved emissions of the following:

- Isoprene, monoterpenes, oxygenated and other volatile organic compounds, collectively named biogenic volatile organic compounds (BVOCs), due to biological activity in vegetative species;
- Carbon monoxide (CO) induced by photochemical transformation on or in vegetative species; and
- Nitric oxide (BNO) due to microbial, predominantly from the genera *pseudomonas* and *bacillus*, denitrification processes in soils.

Though some plant species are known to emit sesquiterpenes, there are no data configured for use in BEIS3 to estimate these compounds. Biogenic emissions are dominated by isoprene (31%), monoterpenes (22%), and methyl butenol (5%), although several other oxygenated compounds have also been identified (Lamb et al., 1999).

In contrast to its ability to estimate BVOC emissions, BEIS3 has no capability to estimate biogenically derived emissions of methane and limited capabilities to estimate biogenically derived emissions of oxides of nitrogen and carbon monoxide. Methane, carbon monoxide, and oxides of nitrogen are important participants in photochemistry. Therefore, accurate models to estimate these emissions are important to the overall success of air quality modeling studies.

BEIS3 does not estimate methane emissions from any naturally occurring source such as wetlands, termites, or biomass burning. Though BEIS3 has the capability to estimate carbon monoxide that results from biological activity with the plant species, it is unclear whether the BEIS3 model formulation is an appropriate representation of this process. However, BEIS3 does not estimate CO emissions due to processes occurring in soils or from biomass burning. Though BEIS3 estimates NO emissions from soils, it does not estimate NO_X emissions from biomass burning. For a discussion on why plants emit at all, a subject that is not entirely understood, Lamb et al. (1999) and Guenther et al. (2000) offer brief descriptions of the biological functions that are believed to result in emissions from plants. Also, Lamb et al., (1999 – Chapter 2) provide a synopsis of the history of biogenic emissions modeling.

The four primary inputs to BEIS3 are as follows:

- Spatially and temporally resolved temperatures;
- Spatially and temporally resolved photosynthetically active radiation (PAR);
- Spatially resolved, species-specific vegetation; and
- Species-specific biogenic emissions factors.

Each component as well as the model formulation has varying degrees of uncertainty, which in total, contribute to the overall uncertainty in the biogenic emissions estimated by BEIS3. To determine the uncertainty in the biogenic emissions that are estimated as a result of the application of the BEIS3, it is first necessary to develop an understanding of the BEIS3 model formulation, its inherent limitations, and the data that are input to the model.

The purpose of this report is two-fold: one, to review the current BEIS3 formulation; and two, to examine formulations that can be used to estimate emissions of CO, NO_X, and methane from biogenic sources, which are currently not covered within the BEIS3 framework. In Chapter 2, we present a comparative overview of global emissions from natural sources and anthropogenic sources. In Chapter 3, we identify the plant species and chemical species for which BEIS3 estimates emissions. In Chapter 4, we review the BEIS3 formulation. In Chapter 5, we describe formulations that might be possibly used to estimate CO emissions from biogenic sources. In Chapter 6, we describe formulations that might be possibly used to estimate NO_X emissions from biogenic sources. Finally, in Chapter 7, we describe formulations that might be possibly used to estimate methane emissions from biogenic sources.

2.0 Global Estimates Of Anthropogenic And Naturally Occurring Emissions

First and foremost, the BEIS family of models estimates emissions of BVOCs that are the result of biological activity from land-based vegetative species and BNO that are the result of microbial activity from certain soil types (Guenther et al., 2000, 1999, 1993, 1991; Geron et al., 1994; Lamb et al., 1993; Williams et al., 1992; Pierce and Waldruff, 1991; Pierce et al., 1990). The third generation of the BEIS models, BEIS3, is also able to estimate CO emissions, which are the result of photochemical transformation, from vegetative species (Pierce, 2001a). Other sources of biogenic and geogenic emissions are currently outside the framework of the BEIS family of models. This includes such emissions as methane from termites, wetlands, and biomass burning, as well as, carbon monoxide from biomass burning and soils.

Table 2-1 presents a comparative overview of the global natural sources and anthropogenic sources inventories for methane (CH_4), non-methane volatile organic compounds (NMVOC), CO, and NO_X for 1990. The purpose of Table 2-1 is to contrast the magnitudes of emissions from anthropogenic and naturally occurring sources. Further, Table 2-1 identifies the source categories for which BEIS3 estimates emissions. The identification of sources in Table 2-1 follows that of the IPCC (2000). Among the source categories that require further explanation are as follows:

- Natural Sources – Other, includes emissions from other geogenic sources such as volcanoes and other biogenic sources such as enteric fermentation, a digestive process under anaerobic conditions in the intestines of animals, from wildlife and emissions from wildlife waste; and
- Anthropogenic Sources – Other, includes emissions from residential, commercial, and other industrial processes as well as production of CO from VOC oxidation.

In Table 2-1, both the nominal emissions estimate and the possible range, in parentheses, of the emissions estimate are shown. If an entry has a question mark, either the nominal value or the range is unknown. The highlighted entries for NMVOC from vegetation and NO_X from soils indicate the biogenic sources for which BEIS3 is formulated to estimate emissions.

The methods that were used to estimate the NMVOC from vegetation are the same methods that are embedded in BEIS3. The methods account for 20% to 25% of the 1990 global NMVOC emissions. CO emissions have also been observed from plants and are believed to be the result of direct photochemical transformation on the plant leaf or in the plant matrix (Tarr et al., 1995). Though BEIS3 is formulated to estimate CO from vegetative species, the formulation is suspect since Tarr et al. (1995) report that the processes controlling CO production from plants are directly correlated with light whereas the BEIS3 employs a temperature-based formulation to estimate CO emissions from plants. Further, the methods used to estimate global CO emissions from vegetative species are different than those embedded in BEIS3 (Khalil and Rasmussen, 1990). Regardless, it appears that CO from plants accounts for 10% to 16% of the total global CO emissions load. Also, CO emissions from plants may be higher since Tarr et al. (1995) report that CO emissions rates from deadfall, which appear to be missing from the estimates

from Khalil and Rasmussen (1991) and Khalil et al. (1999), are upwards of an order of magnitude higher than for growing and senescent vegetative species. Finally, there is no evidence to suggest that methane or NO_X is released from vegetative species as a result of biological activity.

Because different methods than those embedded in BEIS3 were used to inventory the 1990 global NO_X emissions from soils, it is unknown how global NO_X emissions from soils estimated by BEIS3 compare to those shown in Table 2-1. Regardless, NO_X emissions from soils are about 25% to 30% of the 1990 global NO_X emissions.

If all sources of biospheric NO_X, NMVOC, methane, and CO are included as biogenic sources, the fraction of carbon and nitrogen emissions from biogenic sources jump to well over 50% of the total global load. Given the importance that these pollutants have in atmospheric chemistry, it is prudent to accurately characterize their contributions to the total emissions load.

The emissions estimates presented in Table 2-1 are not necessarily equally distributed throughout the globe. For example, though global BVOC emissions are roughly equally divided between the northern and southern hemisphere, 51% and 49% respectively, 90% of the BVOC emissions in the southern hemisphere occur between the equator and 25°S latitude. In the northern hemisphere, 65% of the BVOC emissions occur between the equator and 25°N latitude, 27% between 25°N and 50°N latitudes, and 8% between 50°N and 80°N latitudes (Guenther et al., 1995). Mobile source CO emissions are even more disparate with approximately 90% produced in the northern hemisphere (Bradley et al., 1999).

Table 2-1. Global emissions estimates of CH_4, NMVOC, CO, and NO_X for natural and anthropogenic sources for 1990. Emissions estimates are in terragrams carbon (Tg C) or terragrams nitrogen (Tg N). Question marks (?) indicate that either the nominal emissions estimate or the range, shown in parentheses, of the emissions estimate is unknown. Shaded boxes (i.e. NMVOC, CO, and NO_X) indicate the source sectors for which BEIS3 has been formulated to estimate emisstions.

Source	Pollutant (Tg C or N per year)				References
	CH_4	NMVOC	CO	NO_X	
Natural Sources					
Wetlands	110-115 (50-170)[1,2]				1. IPCC, 1994, 1995 2. Mathews, 2000
Termites	20 (10-50)[1]				1. IPCC, 1994, 1995 2. Sanderson, 1995
Oceans	10-14 (5-50)[1,2,3]	5 (2-15)[4]	13-100 (6-190)[5,6,7]		1. IPCC, 1994, 1995 2. Fang et al., 1991 3. Lambert and Schmidt, 1995 4. Guenther et al., 1995 5. Seiler and Crutzen, 1990 6. Bates et al., 1995 7. Khalil and Rasmussen, 1990
Soils			30 (?-?)[1]	19 (4-21)[2,3]	1. Khalil et al., 1999 2. Yienger and Levy, 1995 3. Davidson and Kingerlee, 1997
Vegetation (including agricultural lands)		Isoprene: 503 (200-800)[1] Monoterpenes: 127 (50-500)[1] Other VOCs: 515 (20-1800)[1]	75-230 (20-400)[2,3]		1. Guenther et al., 1995 2. Khalil and Rasmussen, 1990 3. Khalil et al., 1999
Lightning				17 (2-25)[1,2]	1. Price et al., 1997a, 1997b 2. Pickering et al., 1997
Petroleum Seeps	? (8-65)[1]	1 (0.2-6)[2]			1. Hovland et al., 1993 2. Wilson et al., 1994
Fires		2360(?-?)[1] -- includes methane	35 (25-75)[2,3]	-- included in Biomass Burning	1. UNEP, 1999 2. Olivier et al., 1999 3. Seiler and Crutzen, 1990
Other	15 (10-40)[1]				1. IPCC, 1994, 1995

Source	Pollutant (Tg C or N per year)				References
	CH_4	NMVOC	CO	NO_X	
Anthropogenic Sources					
Natural Gas Production and Combustion	40 (25-50) [1]	7 (?-?) [2]		1 (0.5-2) [2,3]	1. IPCC, 1994, 1995 2. Olivier et al., 1999, 2000 3. Lee et al., 1997
Coal Mining	30 (15-45) [1]				1. IPCC, 1994, 1995
Petroleum Industry	15 (5-30) [1]	22 (?-?) [2]	<1 (?-?) [2]	<1 (?-?) [2]	1. IPCC, 1994, 1995 2. Olivier et al., 1999, 2000
Coal Combustion	? (1-30) [1]	<1 (?-?) [2]	1 (?-?) [2]	5 (2-7) [2,3]	1. IPCC, 1994, 1995 2. Olivier et al., 1999, 2000 3. Lee et al., 1997
Enteric Fermentation	80-85 (65-100) [1]				1. IPCC, 1994, 1995
Rice Paddies	60 (20-100) [1]				1. IPCC, 1994, 1995
Biomass Burning	40 (20-80) [1]	1540 (?-?) [2]	500 (300-700) [3,4]	8 (3-15) [5]	1. IPCC, 1994, 1995 2. UNEP, 1999 3. IPCC, 2000 4. Olivier et al., 1999, 2000 5. Lee et al., 1997
Landfills	40 (20-70) [1]				1. IPCC, 1994, 1995
Animal Waste Treatment And Decomposition	25 (20-30) [1]				1. IPCC, 1994, 1995
Domestic Sewage Treatment And Decomposition	25 (15-80) [1]				1. IPCC, 1994, 1995
On-road And Non-road Mobile Sources	<1 (?-?) [1]	34 (?-?) [1]	210-500 (200-600) [1,2,3]	5 (3-8) [4]	1. Olivier et al., 1999, 2000 2. Bradley et al., 1999 3. Khalil et al., 1999 4. Lee et al., 1997
Other	15 (?-?) [1]	64 (?-?) [1]	300-1100 (200-1500) [1,2,3]	10 (5-14) [1,4]	1. Olivier et al., 1999, 2000 2. IPCC, 2000 3. Khalil et al., 1999 4. Lee et al., 1997

3.0 BEIS3 Plant Species And Chemical Species

Appendix A lists the 230 species for which BEIS3 estimates emissions (Pierce, 2001a). These 230 plant species are believed to represent the vast majority of plant species, at least in the North America, that emit one or more chemical species which impact atmospheric chemistry from the urban scale to the global scale. However, at least one gap in our knowledge of biogenic emissions needs to be closed. For some plant species, emission factors for specific terpenes, sesquiterpenes, and oxygenated compounds need to be determined (Lamb et al., 1999). This is needed since in some cases, the emissions factors for some compounds from some plant species are based on taxonomical assignment from those plant species whose emissions factors are relatively well known (e.g. Benjamin et al., 1996).

Also listed in Appendix A are the BEIS3 species codes, leaf area indices, dry leaf biomass factors, wintertime adjustment factors, and biogenic emissions factors (Pierce, 2001a). These are inputs to the BEIS3 model.

Leaf area index (LAI) is defined as the total one-sided, or one half of the total all-sided, green leaf area per unit ground surface area (Chen and Black, 1992). LAI describes a fundamental property of the plant canopy in its interaction with the atmosphere, especially concerning radiation, energy, momentum and gas exchange (Monteith and Unsworth, 1990). Leaf area plays a key role in the absorption of radiation, in the deposition of photosynthates during the diurnal and seasonal cycles, and in the pathways and rates of biogeochemical cycling within the canopy-soil system (Bonan, 1995). Globally, LAI varies from less than one to above ten but also exhibits significant variation within biomes at regional, landscape, and local levels (Monteith and Unsworth, 1990). In the context of BEIS3, LAI is used to adjust the isoprene emissions for the effects of PAR penetrating through the leaf canopy.

Leaf biomass provides the energy that drives the growth of the tree stand and as such, is the subject of several models (Valentine, 1985; Makela, 1986). It is also possible to describe changes in leaf biomass using less formal techniques including expert knowledge, which is subject to verification using visual estimation or photogrametric techniques. The leaf biomass values that are listed in Appendix A reflect peak foliar density (i.e. these values are the maximum leaf biomass factors that occur during the growing season).

The wintertime adjustment factor indicates the fraction of the emissions factors to use when estimating biogenic emissions in the winter months (e.g. zero indicates that the plant species does not emit in the winter months; 0.5 indicates that the plant species emits at one-half the listed emissions factors in the winter months). It is unclear how this factor was determined, and is therefore likely to be highly uncertain.

The isoprene, monoterpene, OVOC, and NO emissions factors are the flux-rate that each species emits under standard environmental conditions (i.e. 30°C and 1000 $umol \cdot m^{-2} \cdot s^{-1}$ PAR).

The biogenic emissions factors are based primarily on enclosure flux measurements (Guenther et al, 2000). The enclosure flux methods include static branch chamber (e.g. Lamb et al., 1985), dynamic flow branch chamber with and without environmental control (e.g. Dement et al., 1975; Arey et al., 1995), dynamic whole plant chamber with and without environmental control (e.g. Tingey, 1981; Pier, 1995), dynamic leaf cuvette with and without environmental control (e.g. Geron et al. 1997; Harley et al., 1996, 1997), and leaf cuvette (e.g. Harley et al., 1996).

Though the current release of BEIS3 is formulated to estimate emissions of isoprene, monoterpenes, OVOCs, and nitric oxide, Pierce (2001b) indicates that the BEIS3 formulation allows for the estimation of the discrete chemical compounds that comprise the monoterpene and OVOC classes. Pierce (2001b) also indicates that the BEIS3 formulation also allows for the estimation of biogenic carbon monoxide (BCO). Although BCO is released both as a biomass combustion by-product and as the result of less than well-understood direct photoproduction processes that occur on the plant tissues or within the plant matrix (Lamb et al., 1999; Tarr et al., 1995), BEIS3 is only formulated to estimate BCO from the latter process (Pierce, 2001b). However, as indicated earlier, the BEIS3 BCO formulation is suspect since Tarr et al. (1995) report that BCO production is regulated by light, but the BEIS3 formulation controls BCO production via a temperature-dependent mechanism. Appendix B lists the emissions factors for the discrete OVOC chemical compounds for each plant species listed in Appendix A. Appendix C lists the emissions factors for the discrete monoterpene chemical compounds and BCO for each plant species listed in Appendix A.

Though BEIS3 has been formulated to estimate BNO from soils, the BEIS3 formulation uses only the "agricultural soils" BNO model described by Williams et al., (1992). BEIS3 does not utilize the BNO formulations for grassland soils, forest soils, wetland soils, or "other agricultural soils" that are also discussed by Williams et al., (1992).

As identified in Table 2-1, BEIS3 is not formulated to estimate methane from any biogenic source sector including:

- Wetlands – under anaerobic conditions, methane is released due to the bacterial remineralization of labile organic matter (IPCC, 1995, 2000);
- Termites – in their digestive tracts, methane is produced during the breakdown of cellulose by symbiotic microorganisms (Seiler et al., 1984; Fraser et al., 1986); and
- Naturally occurring combustion of biomass – methane is released as a by-product of incomplete combustion (UNEP, 1999);

Under international protocol, the following biogenic source sectors are classified as anthropogenic due to the human management of the root plant or animal species and are not included in BEIS3 (IPCC, 1994, 1995, 2000):

- Enteric fermentation (commonly known as belching cows) – methane is produced in the intestines of domesticated species such as cattle and sheep as a result of

digestive processes under anaerobic conditions (Johnson et al., 1994; Moss et al., 1994; Johnson and Johnson, 1995); and

- Rice paddies – same process that produces methane from wetlands (van der Gon et al., 1999, 2000)

Further BEIS3 is not formulated to estimate emissions of NMVOC, CO and NOX that are released during the combustion of biomass. In Section 4, we discuss possible models to accommodate the estimation of these biogenic source sectors within the framework of BEIS3.

4.0 BEIS3 Model Formulation

Numerous peer-reviewed papers have been written on the BVOC and BNO model formulations that are embedded in BEIS3 including most recently Lamb et al. (1999) and Guenther et al. (1999, 2000). All three papers provide more detailed information concerning the most recent biogenic emissions models. However, there has been some confusion generated as a result of the Lamb et al. (1999) study which identifies the model formulations therein as representative of the BEIS3 model formulations that are used by Pierce (2001a). Pierce (2001a) uses an earlier form of the model formulations reported in Lamb et al. (1999) and Guenther et al. (2000), more specifically those reported in Guenther et al. (1993), and the deviations in the models used by Pierce (2001a) are identified here.

4.1 Isoprene

Early studies (e.g. Tingey et al., 1979) showed that short-term variation in isoprene emissions from vegetative species were influenced by leaf temperature and the amount of PAR reaching the leaves. Isoprene is emitted only during daylight hours from specific deciduous species, such as oak (e.g. Anderson et al., 2000), willow (e.g. Isebrands et al., 1999), aspen (e.g. Baldocchi et al., 1999), and poplar (e.g. Isebrands et al., 1999), and only from spruce (Kempf et al., 1996) among coniferous species. Though the biochemical pathway is well known (Sharkey et al., 1991; Fall and Wildermuth, 1998), the reasons why plants emit isoprene are not well understood. Sharkey and Singaas (1995) suggest that isoprene is emitted as a thermal stress relief mechanism, whereas Guenther et al. (1993, 2000) suggest that isoprene emissions are related to chloroplast production, which are necessary for chlorophyll storage. Regardless, it appears that the ability to model isoprene emissions from vegetative species is relatively good (Lamb et al., 1996; Guenther et al., 1996; Fuentes et al., 1996; Baldocchi et al., 1995)

Pierce (2001a) uses a slightly modified form of the Guenther et al. (1993) formulations to estimate isoprene emissions based on leaf temperature and PAR (Eq. 1):

$$E = \xi \cdot E_s \cdot C_L^A \cdot C_T \cdot A \qquad \textbf{(1)}$$

where E ($\mu g \cdot hr^{-1}$) is the emissions rate of isoprene; ξ is the seasonal adjustment coefficient (ξ is one for the spring, summer, and fall or the "wintertime adjustment factor" identified in Appendix A); E_s ($\mu g \cdot ha^{-1} \cdot hr^{-1}$) is the species-specific emissions flux at 30°C and 1000 $\mu mol \cdot m^{-2} \cdot s^{-1}$ PAR (the biogenic emissions factors identified in Appendices A, B, and C); C_L^A is the environmental correction factor that accounts for changes in PAR as attenuated by the leaf; C_T is the environmental correction factor that accounts for changes in leaf temperature; and A (ha) is the areal extent of the species

However, Guenther et al. (1995, 1999, 2000) have refined their model to estimate isoprene emissions (Eq. 2):

$$E = \varepsilon \cdot D_P \cdot D_f \cdot \gamma_P \cdot \gamma_T \cdot \gamma_A \cdot \rho \cdot A \quad \textbf{(2)}$$

where ε is a landscape average emission capacity ($\mu g \cdot g \cdot hr^{-1}$); D_P is the annual peak foliar density (i.e. biomass) ($g \cdot ha^{-1}$); D_f is the fraction of foliage present at a particular time of year; the emission activity factors γ_P, γ_T, and γ_A account for the influence of photosynthetic photon flux density (PPFD), temperature, and leaf age, respectively; and ρ is the canopy escape efficiency that represents the fraction of emissions released into the above-canopy atmosphere.

$\varepsilon \cdot D_P$ in the Guenther et al. (2000) formulation is equivalent to E_s in BEIS3 (the biomass factors, ε, and biogenic emissions factors, E_s, in Appendices A, B, and C where $D_P = E_s / \varepsilon$); γ_T is equivalent to C_T; and γ_P is equivalent to C_L^A. However, though the parameters are equivalent, the formulation of the parameters may be slightly different. This leaves the Guenther et al. (2000) terms D_f, γ_A, and ρ unaccounted for in the Pierce (2001a) BEIS3 formulation.

4.1.1 Fraction Of Foliage (D_f)

Guenther et al. (2000) introduce D_f to account for changes in biomass as the plant progresses through its growing season. Guenther et al. (2000) indicate that D_f is both a function of time of year and forest type. Though D_f is excluded from the BEIS3 formulation, Pierce (2001a) includes a simple approach for capturing the seasonal change in biomass with the introduction of the seasonal adjustment factor, ξ. During the spring, summer, and fall, Pierce (2001a) assumes that the seasonal adjustment factor, ξ, is one. This treats the plant as if it exists under conditions of peak foliar density at all time during the spring, summer, and fall. During the winter, Pierce (2001a) assumes that for most plants, there is no biomass (i.e. ξ=0.0), and for a few plants, the biomass is one-half of (i.e. ξ=0.5) or equal to (i.e. ξ=1.0) to the peak foliar density. However, this is a very limited approximation of the seasonally changing biomass.

Though Guenther et al. (2000) indicate that D_f is both a function of time of year and forest type, GLOBEIS (Environ, 2001), a biogenic emissions model based on the work of Guenther et al. (1999), uses a lookup table based on geographic location to define D_f. It is unclear which approach (i.e. Guenther et al. [2000] or Environ [2001]) is better suited to model D_f, but either could be adapted for use in BEIS3. Because the assumption in the BEIS3 formulation is that plants emit as if they are at peak foliar density during the spring, summer and fall, from a qualitative perspective, the exclusion of D_f from the BEIS3 formulation likely results in higher predicted isoprene emissions. Yet the magnitude of this overestimate is unknown since no study has been conducted to examine this issue.

4.1.2 Leaf Age (γ_A)

The biogenic emissions estimation algorithm that is used by Pierce (2001a) (Eq. 1) accounts only for the environmental conditions that a leaf has been exposed to in the past hour. The modified algorithm (Eq. 2) accounts for the influence of the environmental conditions that a leaf has been exposed to in the past several weeks (γ_A). γ_A accounts for the findings of Guenther et al. (1991) and Monson et al. (1994) that showed disparate isoprene emissions rates between young and old leaves. Results from Monson et al. (1994), Geron et al. (1997), and Goldstein et al. (1998) suggest that isoprene emissions begin 650 growing degree-days after leaf-out. Therefore, the onset of isoprene emissions can occur several days to several weeks after budbreak. Peak seasonal isoprene emissions occur after 1050 growing degree-days, oscillating with the rise and fall of temperature and PAR, and continue for on the order of 65 days (Goldstein et al., 1998). Thereafter, isoprene emissions decline to zero when temperatures fall below some minimum value or leaf death occurs (Goldstein et al., 1998).

Monson et al. (1994), Geron et al. (1997), Goldstein et al. (1998) and Lamb et al. (1999) use, or allude to, the term "heating degree-day." Technically, this is incorrect. The better term is "growing degree-day." Growing degree-day is defined as the amount of accumulated heat required for a plant to reach a certain stage of development (e.g. Griffith et al., 1997a, 1997b). This relationship holds true for most organisms if their growth and development is regulated by temperature (e.g., weeds, insects, pathogens) (e.g. Griffith et al., 1997a, 1997b). The basic concept is that development will only occur if the temperature exceeds some minimum developmental threshold, or base temperature (T_b). The base temperature is determined experimentally and is different for each plant (e.g. Griffith et al., 1997a, 1997b). However, in the case of isoprene emissions from plants, it appears that the community has agreed to a base temperature of 65°F for all plant species (Lamb et al. 1999). The number of growing degree-days is the day-to-day accumulated difference between the average temperature for the day (T_a =(T_{max}-T_{min})/2 where T_{max} is the maximum observed temperature and T_{min} is the minimum observed temperature for a day) and T_b for T_a greater than T_b. For days where Ta is less than Tb, no growing degree-days are accumulated. The growing degree-days are accumulated starting from January 1 and continue through the end of the year.

Guenther et al. (1999) suggest that the effects of leaf age can be modeled as a function of D_f(Eq. 3).

$$\gamma_A = a_1 \cdot \frac{\left|D_f^i - D_f^{i-1}\right|}{MAX(D_f^i, D_f^{i-1})} + a_2 \cdot \left(1 - \frac{\left|D_f^i - D_f^{i-1}\right|}{MAX(D_f^i, D_f^{i-1})}\right) \quad \textbf{(3)}$$

where a_1 = 0.33 and is the average of the emissions activity of young and old leaves; a_2 = 0.95 and is the fraction of mature foliage present during the month of peak foliar density; and D_f^i and

D_f^{t-1} are the fraction of peak foliar densities present for the current month and the previous month respectively. Guenther et al. (1999) expect the coefficients a_1 and a_2 to change with landscape type but have no data to develop such relationships. The model is based on the assumption that increasing D_f indicates the presence of a greater proportion of younger leaves and decreasing D_f indicates the greater proportion of older leaves. Given that D_f ranges from zero to one, the maximum value for γ_A in Eq. 3 is 0.95 and occurs during periods of peak foliar density. Because the assumption in the BEIS3 formulation is that plants emit as if they are at peak foliar density, from a qualitative perspective, the exclusion of γ_A from the BEIS3 formulation results in slightly higher predicted isoprene emissions. Though during periods other than times of peak foliar density, the magnitude of this overprediction is not known since no study has been conducted to examine this issue.

4.1.3 Canopy Escape Efficiency (ρ)

ρ is used to account for discrepancies between observed emissions rates at the leaf-level and measured above-canopy flux rates with the former typically being higher. Guenther et al. (1999) rigorously model ρ as a function of canopy ventilation rate and isoprene deposition rate based on the work of Jacob and Bakwin (1991). They assume that the canopy ventilation rate is proportional to the mean wind speed within the canopy. They base the isoprene deposition rate on observations of microbial consumption of isoprene in soils reported by Cleveland and Yavitt (1997). In contrast, Guenther et al. (2000) assign a default value of 0.95 to ρ due to a lack of BVOC deposition or canopy loss data. Regardless, in both Guenther et al. (1999) and Guenther et al. (2000), they conclude that their isoprene model performance (i.e. comparison of observed to predicted isoprene emissions) is acceptable. Because there is no information in the literature that contrasts these two approaches against the same data set, it is unclear which approach is a better physical description. However, exclusion of ρ from the BEIS3 formulation results in an overestimate of predicted isoprene emissions, but the magnitude of the overestimate is unknown since no study has been conducted to examine this issue. Incorporation of a constant, such as that used by Guenther et al (2000), into the BEIS3 framework is relatively straightforward.

4.1.4 Light Correction Factor (C_L and γ_P)

Pierce (2001a) follows the formulation of Guenther et al. (1993) to estimate the light correction factor in BEIS3 (Eq. 4).

$$\gamma_P = C_L = \frac{\alpha \cdot c_{L1} \cdot L}{\sqrt{1 + \alpha^2 \cdot L^2}} \qquad (4)$$

where $\alpha = 0.0027$ and $c_{L1} = 1.066$ are empirical coefficients; and L is the PAR flux rate ($\mu mol \cdot m^{-2} \cdot s^{-1}$). Guenther et al. (1993) explain the derivation of the terms in Eq. 4. The light correction factor exhibits a nearly linear response through very low-light conditions, approximately 0 to 700

umol·m^{-2}·s^{-1} (Figure 4-1). From approximately 700 to 2700 umol·m^{-2}·s^{-1}, conditions of low to moderate light, Equation 4 sub-linearly transitions to an almost constant value and remains so through the solar spectra of interest. The structure of Equation 4 is similar to that used to model the dependence of photosynthesis on light (e.g. Harley and Tenhunen, 1991).

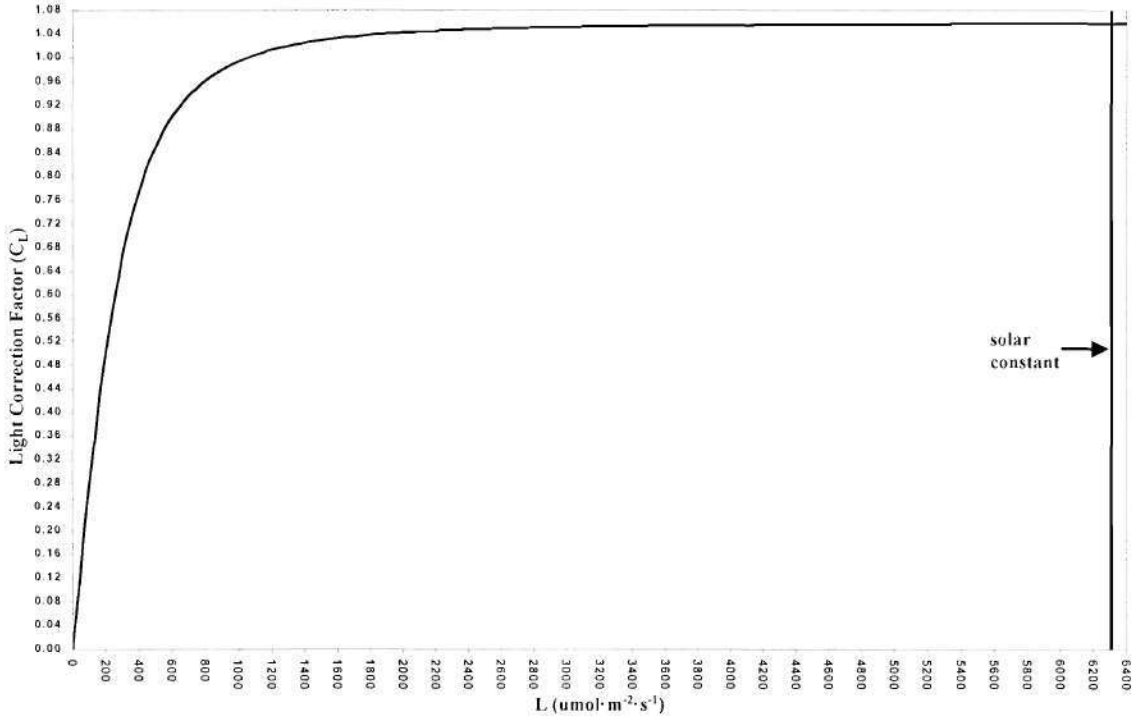

Figure 4-1. Light correction factor as a function of PAR defined by Equation 3. Note that the solar constant (~1370 W·m-2) is based on a conversion factor of 4.6 (Pierce and Geron, 1996).

PAR can be expressed in energy terms (i.e. W·m-2) and in photon terms (μmol·m^{-2}·s^{-1}). In energy terms, PAR is expressed as PAR irradiance, which is the total energy in the PAR range (400 nm to 700 nm). When measured in photon terms, PAR is also called Photosynthetic Photon Flux Density (PPFD), which is a measure of the number of photons in the 400 nm to 700 nm waveband that are incident per unit time on a unit surface. When expressed in photon terms, all the photons are considered equal, independent of their energy. The quantity of photons is measured in moles of photons (1 mole of photons = $6.022 \cdot 10^{23}$ photons). Since a photon carries energy that is inversely proportional to its wavelength, it is necessary to integrate the PPFD across the PAR waveband to accurately compute PAR in energy terms. PAR in terms of photon terms is used due to the dependence of photosynthesis and related processes on specific wavelengths of light in the 400 nm to 700 nm spectra and not on the total energy available in the spectra.

Though Pierce (2001a) treats α and c_{LI} as did Guenther et al. (1993, 1995), Harley et al. (1996, 1997) have shown that the empirical coefficients α and c_{LI} vary with past PAR levels experienced by the leaf. Therefore, Guenther et al. (1999) updated the formulation of α (Eq. 5) and c_{LI} (Eq. 6) to account for variations in these coefficients as a function of LAI.

$$\alpha = 0.001 + 0.00085 \cdot LAI \tag{5}$$

$$c_{L1} = 1.42 \cdot \exp(-0.31 \cdot LAI) \tag{6}$$

Incorporation of these additional extensions results in a light correction factor of about one for PAR of 1000 $\mu mol \cdot m^{-2} \cdot s^{-1}$ and LAI depth of less that 0.5 (i.e. near the top of the canopy). For a leaf in the lower canopy (i.e. LAI depth greater than five) and PAR of 1000 $\mu mol \cdot m^{-2} \cdot s^{-1}$, the light correction factor is less than 0.30 (Guenther et al., 1999). Because these extensions are missing from the Pierce (2001a) formulation, BEIS3 is likely to slightly overestimate isoprene emissions. The magnitude of this overestimate, however, is unknown since no study has been conducted to examine this issue. Incorporation of these extensions into BEIS3 is relatively straightforward.

4.1.5 Temperature Correction Factor (C_T and γ_T)

Pierce (2001a) follows the formulation of Guenther et al. (1993) to estimate the temperature correction factor in BEIS3 (Eq. 7).

$$C_T = \frac{\exp\left(\frac{c_{T1} \cdot (T - T_S)}{R \cdot T_S \cdot T}\right)}{1 + \exp\left(\frac{c_{T2} \cdot (T - T_M)}{R \cdot T_S \cdot T}\right)} \tag{7}$$

where $c_{T1} = 95000$ J·mol^{-1}, $c_{T2} = 230000$ J·mol^{-1}, and $T_M = 314$ are empirical coefficients; R is the ideal gas constant (8.314 J·K^{-1}·mol^{-1}); T_S is the normalizing temperature (303 K); and T is the leaf temperature which is taken to be the ambient temperature (K). Guenther et al. (1993) explain the derivation of the terms in Eq. 7. The response of the light correction factor is shown in Figure 4-2. The light correction factor is relatively small for temperatures below about 16°C but rapidly increases thereafter peaking about 39°C and then rapidly declining. The form of Equation 7 has been used to simulate the temperature response of enzymatic activity (e.g. Johnson et al., 1942; Sharpe and DeMichelle, 1977).

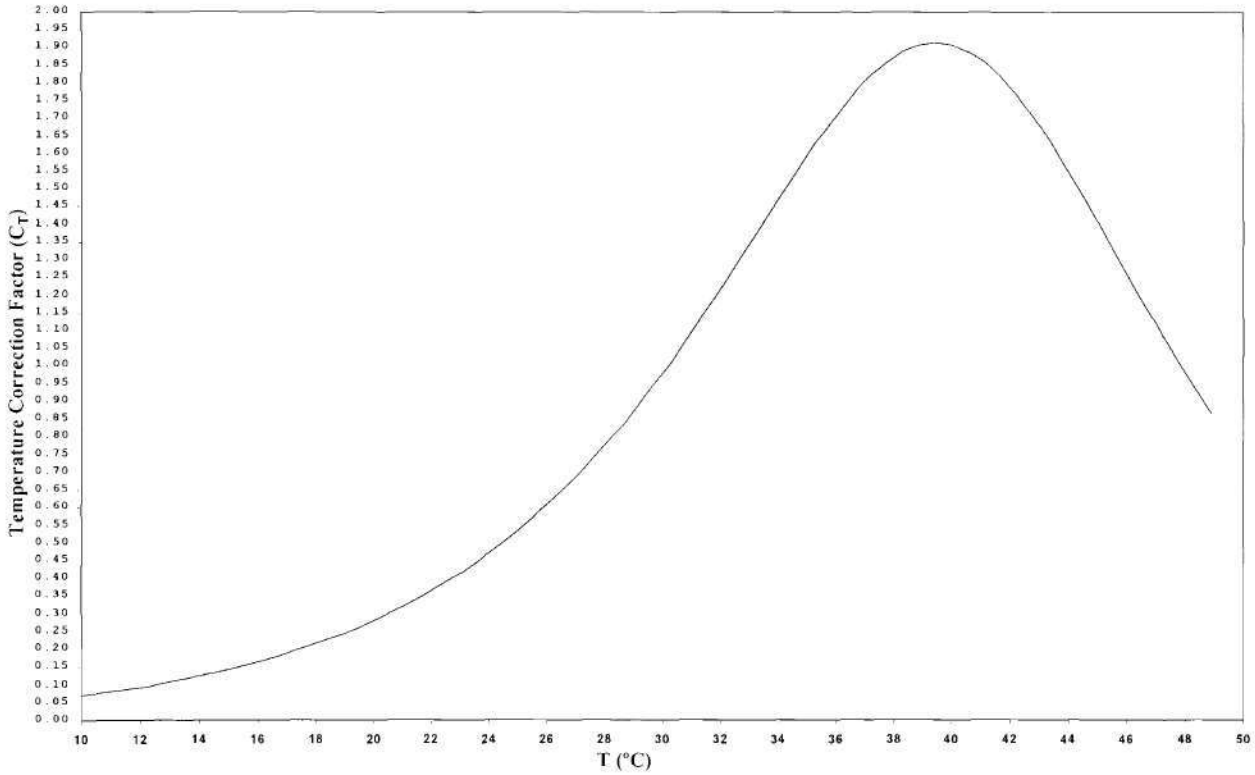

Figure 4-2. Temperature correction factor as a function of ambient temperature defined by Equation 7.

Guenther et al. (1999) updated the temperature correction formulation to account for findings by Sharkey et al. (1999) that the temperature correction factor is dependent on temperatures during the past several days (Eq. 8).

$$\gamma_T = \frac{E_{opt} \cdot c_{T2} \cdot \exp\left(\frac{c_{T1}}{R}\left[\frac{1}{T_{opt}} - \frac{1}{T}\right]\right)}{\left(c_{T2} - c_{T1}\right)\left(1 - \exp\left(\frac{c_{T2}}{R}\left[\frac{1}{T_{opt}} - \frac{1}{T}\right]\right)\right)} \quad \textbf{(8)}$$

where $E_{opt} = 1.9 \cdot \exp(0.125[T_d - 301])$ and $T_{opt} = 312.5 + 0.5(T_d - 301)$ are empirical coefficients; and T_d is the mean temperature of the last fifteen days (K). Guenther et al (1999) show that for values of $E_{opt} = 1.9$ and $T_{opt} = 312.5$, Eq. 8 is almost identical to Eq. 7. Also, though Guenther et al. (1999) suggest a lapse period of fifteen days, Sharkey et al. (1999) and Lamb et al. (1999) suggest that this period may be from eighteen hours to several weeks. It is unclear what the overall effect on the BEIS3 isoprene emissions estimates is due to the exclusion of the updated Guenther et al. (2000) temperature correction factor since the mean temperature of the prior fifteen days can vary considerable depending on the time of year. Further,

incorporation of the revised formulation into the BEIS3 framework may be difficult given the requirement for fairly extensive prior knowledge of temperatures.

4.1.6 Canopy Adjusted PAR (C_L^A)

In BEIS3, C_L^A is computed via a canopy model that accounts for the effects of PAR as it penetrates the leaf canopy (Pierce, 2001a). The canopy model in BEIS3, which is a function of LAI and is based on a leaf energy balance, is a modified form of that used in BEIS (Pierce and Waldruff, 1991) and better accounts for visible and near-infrared scattered, direct, and diffuse radiation on both sunlit and shaded leaves. C_L^A differs from γ_P in that the PAR used in C_L^A is adjusted via a leaf energy balance as PAR migrates through the canopy. The application of γ_P assumes that whatever the PAR is at the top of the canopy is the PAR that is experienced by all leaves within the canopy. Pierce (2001a) computes the canopy adjusted PAR for the sunlit and shaded leaves based on the work of Campbell and Norman (1998) (Eq. 9).

$$C_L^A = L_S^f \cdot C_L\left(L = PAR_S\right) + L_D^f \cdot C_L\left(L = PAR_D\right) \quad \textbf{(9)}$$

where L_S^f is the fraction of sunlit leaves defined by Eq. 10; L_D^f is the fraction of shaded leaves defined by Eq. 11; PAR_D is the amount of PAR on the shaded leaves defined by Eq. 16 ($\mu mol \cdot m^{-2} \cdot s^{-1}$); PAR_S is the amount of PAR on the sunlit leaves defined by Eq. 17 ($\mu mol \cdot m^{-2} \cdot s^{-1}$); and C_L is the light correction factor defined by Eq. 4.

$$L_S^f = \frac{1 - \exp(-K \cdot LAI)}{K \cdot LAI} \quad \textbf{(10)}$$

$$L_D^f = 1 - L_S^f \quad \textbf{(11)}$$

where K is the direct beam solar radiation extinction coefficient defined by Eq. 12.

$$K = \frac{\sqrt{1 + \left[\tan(\theta)\right]^2}}{2} \quad \textbf{(12)}$$

where θ is the solar zenith angle. Pierce (2001a) computes the solar zenith angle from Eq. 13 (Duffie and Beckman, 1980).

$$\theta = a\cos\left(\delta_s \cdot \sin\left(\frac{\pi\phi}{180}\right) + \sqrt{1.0-\delta_s^2}\cdot\cos\left(\frac{\pi\phi}{180}\right)\cdot\cos\left(\frac{15\pi}{180}\left|t+\frac{\lambda}{15}-0.123470\sin\left(t_r\right)+0.004289\cos\left(t_r\right)-0.153809\sin\left(t_r+t_r\right)-0.060783\sin\left(t_r+t_r\right)-12\right|\right)\right) \quad \textbf{(13)}$$

where ϕ is the latitude (°); λ is the longitude (°); t is local time converted to Greenwich Mean Time (hours); t_r is the terrestrial rotation angle (rad) defined by Eq. 14; and δ_s is a parameter of the earth's declination to the solar plane defined by Eq. 15.

$$t_r = \frac{\pi\,\Omega\,t}{180} \quad \textbf{(14)}$$

$$\delta_s = \sin\left(\frac{\pi\delta}{180}\right)\cdot\sin\left(t_r+\frac{\pi}{180}\left[279.9348+1.914827\sin\left(t_r\right)-0.079525\cos\left(t_r\right)+0.019938\sin\left(t_r+t_r\right)-0.00162\cos\left(t_r+t_r\right)\right]\right) \quad \textbf{(15)}$$

where Ω is the fraction of complete rotation per day (360/365.242); and δ is the earth's declination to the solar plane (23.443833°). Please note that though the formulation of Eq. 15 takes into account the time of day, it does not take into account the day of the year. Instead Eq. 15 treats radiation reaching the earth as if every day were the summer solstice in the northern hemisphere. To account for day of year, the first term in Eq. 11 should read $\sin\left(\frac{\pi\delta}{180}\sin\left[\frac{\pi}{180}\left(360\frac{284+n}{365}\right)\right]\right)$ (Duffie, 1980) where n is the julian day of the year (i.e. 1 to 365). By excluding the effect of the day of the year, BEIS3 will overestimate the amount of radiation reaching the canopy resulting in an overestimate of the isoprene emissions. Though the overestimate will likely be small during much of the summer, it will be noticeably large during winter days.

The PAR for shaded leaves is computed via Eq. 16, and the PAR for sunlit leaves is computed via Eq. 17.

$$PAR_D = \frac{PAR_d\left[1-\exp\left(-0.61\cdot LAI\right)\right]}{0.61\cdot LAI} + \frac{PAR_b\left[\exp\left(-0.894\cdot LAI\right)-\exp\left(-K\cdot LAI\right)\right]}{2} \quad \textbf{(16)}$$

$$PAR_S = K\cdot\left(PAR_b+PAR_d\right)\cdot PAR_D \quad \textbf{(17)}$$

where PAR_d is the amount of PAR from diffuse visible solar radiation defined by Eq. 18 ($\mu mol\cdot m^{-2}\cdot s^{-1}$); and PAR_b is the amount of PAR from direct beam, visible radiation defined by Eq. 19 ($\mu mol\cdot m^{-2}\cdot s^{-1}$).

$$PAR_b = I_r \cdot I_c^v \cdot I_b^v \cdot f \tag{18}$$

$$PAR_d = I_r \cdot I_c^v \cdot I_d^v \cdot f \tag{19}$$

where I_r is the ratio of the observed, or modeled, solar radiation to the clear sky total solar radiation defined by Eq. 26; I_b^v is the fraction of visible solar radiation that is from direct beam solar radiation defined by Eq. 20; I_d^v is the fraction of visible solar radiation that is from diffuse beam solar radiation defined by Eq. 21; I_c^v is the clear sky total visible solar radiation defined by Eq. 22 ($W \cdot m^{-2}$); and $f = 4.6$ is an empirical factor that converts solar radiation in terms of energy (i.e. $W \cdot m^{-2}$) to solar radiation in terms of photon flux (i.e. $\mu mol \cdot m^{-2} \cdot s^{-1}$).

$$I_b^v = \begin{cases} 0.009550 \dfrac{I_{cb}^v}{I_c^v} & for\ I_r \le 0.21 \\ \left(1.0 - \left(\dfrac{0.9 - I_r}{0.7}\right)^{2/3}\right) \dfrac{I_{cb}^v}{I_c^v} & for\ 0.21 < I_r < 0.89 \\ 0.941124 \dfrac{I_{cb}^v}{I_c^v} & for\ I_r \ge 0.89 \end{cases} \tag{20}$$

$$I_d^v = 1 - I_b^v \tag{21}$$

$$I_c^v = I_{cb}^v + I_{cd}^v \tag{22}$$

where I_{cb}^v is the clear sky, direct beam visible solar radiation defined by Eq. 23 ($W \cdot m^{-2}$); and I_{cd}^v is the clear sky, diffuse visible solar radiation defined by Eq. 24 ($W \cdot m^{-2}$).

$$I_{cb}^v = 600 \cdot \exp(-0.185m) \cdot \cos(\theta) \tag{23}$$

$$I_{cd}^v = 0.42 \cdot (600 - I_{cb}^v) \cdot \cos(\theta) \tag{24}$$

where m is the atmospheric optical thickness defined by Eq. 25.

$$m = \frac{P}{P_o \cdot \cos(\theta)} \tag{25}$$

where P is the observed pressure (mb); and P_o is standard pressure (1013.25 mb).

$$I_r = \frac{I}{I_c} \tag{26}$$

where I is the observed, or modeled incoming solar radiation; and I_c is the clear sky total solar radiation defined by Eq. 27 ($W \cdot m^{-2}$)

$$I_c = I_{cb}^i + I_{cd}^i + I_{cb}^v + I_{cd}^v \tag{27}$$

where I_{cb}^i is the clear sky, direct beam near-infrared solar radiation defined by Eq. 28 ($W \cdot m^{-2}$); and I_{cd}^i is the clear sky, diffuse near-infrared solar radiation defined by Eq. 29 ($W \cdot m^{-2}$).

$$I_{cb}^i = \left(720 \cdot \exp(-0.06m) - \omega\right) \cdot \cos(\theta) \tag{28}$$

$$I_{cd}^i = 0.65 \cdot \left(720 - \omega - I_{cb}^i\right) \cdot \cos(\theta) \tag{29}$$

where ω is absorption by water of solar radiation in the near-infrared spectrum defined by Eq. 30 ($W \cdot m^{-2}$).

$$\omega = 101.64 \cdot (2m)^{0.3} \tag{30}$$

Though Pierce (2001a) accounts for canopy attenuation of PAR, there is still some debate in the literature about how best to account for canopy effects not only for PAR but also for temperature (Lamb et al. [1999 – Chapter 2] summarizes the issues surrounding the debate). It is well known that discrepancies exist between the typically higher measured leaf-level isoprene emissions and lower measured above-canopy isoprene emissions. Even with the application of isoprene canopy escape efficiency, ρ, coupled with a canopy attenuation model (Goudriaan and van Laar, 1994), in a modified version of the GLOBEIS (Environ, 2001), that is more rigorous than that used by Pierce (2001a), Guenther et al. (1999) did not seem to necessarily improve isoprene model performance. Therefore, it seems that our knowledge of canopy effects is still incomplete and requires further investigation so that these effects can be better modeled.

4.2 Monoterpenes

Early studies show that short-term variation in terpenoid emissions from vegetative species was influenced by leaf temperature and relative humidty (e.g. Dement et al., 1975) as well as foliar moisture (Lamb et al., 1985; Schade et al., 1999) and to some degree, solar radiation (Steinbrecher et al., 1988). However, unlike isoprene emissions, no seasonal effects have been clearly established for monoterpene emissions (Lamb et al., 1999). Also, though the dependence of monoterpene emissions on solar radiation has been established, no quantitative description of this dependency appears to exist (Guenther et al., 1993). On the other hand, Schade et al. (1999) propose a model to account for humidity effects on monoterpene though this model has not been incorporated into BEIS3. Monoterpene emissions occur from coniferous species (Guenther et al., 1994) and some deciduous species (Keiser, 1997). However, the specific terpenoid species are not necessarily well characterized (Lamb et al., 1999). In fact, almost all studies report monoterpene emissions in terms of a small number of predominant compounds, typically α-pinene, β-pinene, limonene, and Δ^3-carene, along with a larger number of terpenes present only in trace amounts. Hence, many terpenoid species have been identified from plant species, but their biogenic emissions capacities for the chemical species are not well known (Lamb et al., 1999). The biochemical pathway for monoterpene production in needles is relatively well understood (Croteau, 1987), and it appears to be used in both tissue defense and chloroplast production (Guenther et al., 2000). Due to their temperature dependence, terpene emissions from vegetation follow a diurnal pattern with low emissions at night, increasing emissions during the day to a mid-afternoon maximum, and returning to low emissions rates in the late evening (Lamb et al., 1999). Further, because of the storage pools that exist in the needles, wounding of the needle, either due to mechanical stress or herbivory, can lead to large increases in the monoterpene emission rate (Lamb et al., 1999). Again, unlike isoprene, there have been few canopy-scale flux studies of terpene emissions suitable for use in model performance evaluation. Therefore, it is difficult to determine how well the BEIS family of models performs with respect to observed monoterpene emissions rates.

Pierce (2001a) follows the recommendation of Guenther et al. (1993) to estimate monoterpene emissions based on leaf temperature, which is taken to be ambient temperature (Eq. 31).

$$E = \xi \cdot E_s \cdot A \cdot \exp\left(\beta\left[T - T_S\right]\right) \tag{31}$$

where $\beta = 0.09\ K^{-1}$ is the empirical coefficient that establishes the temperature dependence of the emissions rate. Of note, Guenther et al. (1993) report that some variation exists in β, which may be due to such factors as leaf-to-leaf and seasonal emissions rate variability, different vapor pressure and solubilities for the monoterpenes, different chemical storage and emissions pathways, and experimental error. The form of Equation 31 appears to be based purely on a statistical fit of the measured emissions rate data (i.e. appears to have little or no basis to any biological process).

Much like the isoprene formulation, BEIS3 does not account for the effects of leaf age (γ_A) and seasonal changes in foliar density (D_f) on monoterpene emissions estimates. Guenther et al. (2000) suggest that it is appropriate to add these terms to the monoterpene formulation, and given the BEIS3 framework, these changes are relatively easy to implement. Further, the BEIS3 monterpene formulation does not account for solar radiation (γ_P) and canopy escape efficiency (ρ) though there is no recent evidence to support such dependencies nor is there evidence to support the attenuation of monoterpene emissions from the leaf canopy similar to what is done for isoprene. Also, as stated earlier, the effects of short-term changes in humidity on monoterpene emissions are not accommodated in BEIS3 (Schade et al., 1999). Finally, Guenther et al. (2000) model the monoterpenes that are related to chloroplast production using the isoprene formulation. Because BEIS3 excludes these environmental factors, BEIS3 is likely to overestimate monoterpene emissions. It is unclear, however, what the magnitude of the emissions change is for those monoterpenes modeled using the isoprene formulation since no study reports this comparison.

4.3 Oxygenated And Other Biogenic VOCs

It is well known that a wide variety of oxygenated and other BVOCs, which are collectively named OVOC, are emitted from vegetation including 2-methyl-3-buten-2-ol (MBO), a variety of hexene compounds, aldehydes, alcohols, ketones, and organic acids (e.g. Kesselmeier et al., 1997; Kirstine et al., 1998; MacDonald and Fall, 1993; Winer et al., 1992; Gabriel et al., 1999). While MBO is released from pines via a chloroplast mechanism (Guenther et al., 1999) and has similar environmental dependencies to isoprene (Goldan et al., 1993; Harley et al., 1998), most of the OVOCs appear to be emitted as defense mechanisms (Lamb et al., 1999). The hexene compounds have antibiotic properties (Croft et al., 1993) and are released as a result of plant damage through mechanical stress (de Gouw et al., 1999), infection, or herbivory (Lamb et al., 1999). However, Lamb et al. (1999) imply that though these emissions can be quite large, quantitative methods to estimate OVOC emissions from such plant damage is limited and requires further work before they can be included in regional inventory development efforts. Other OVOCs are emitted as well, sometimes in large quantities but typically in lower quantities as compared to damaged plants, in situations where plant damage is not apparent.

Pierce (2001a) uses the monoterpene formulation (Eq. 31) to estimate BVOC emissions. Except for MBO, this approach is the same as that used by Guenther et al. (1999, 2000) with the caveats that accompany the monoterpene formulation noted in the previous section. For MBO, Guenther et al. (2000) use the isoprene formulation to estimate emissions of this species. It is unclear what direction the predicted magnitude of the MBO emissions estimate will take using the isoprene formulation in-lieu of the monoterpene formulation since no studies have reported such a comparison.

4.4 Biogenic Nitric Oxide

BNO is emitted as a result of microbial nitrification-denitrification activities in soil and is enhanced through such practices as nitrogen-based fertilizer application (Williams et al, 1992), stubble burning (Levine, 1990), and soil tilling (Civerolo and Dickerson, 1998). Soil NO emissions are dependent on both long-term and short-term environmental conditions. Potter et al. (1996) include the following as long-term conditions that impact soil NO emissions: soil texture, organic matter content, soil pH, and nitrate levels; and the following as short-term conditions: soil temperature and water-filled pore space. The primary means for developing NO emission factors from soils has been through measurements with static or dynamic chambers (Williams et al., 1992; Thornton et al. 1997); however, Parrish et al. (1987) express concern over the results derived from such techniques since it is unclear whether the chambers represent a true NO_X ($NO + NO_2$) flux from the soil to the atmosphere, and there exist concerns about extrapolating the flux results from small field studies to regional-scale fluxes. Soil NO emissions factors range over two orders magnitudes or more (Williams et al., 1992; Yienger and Levy, 1995; Davidson and Kingerlee, 1997). In general, wetlands and tundra have very low soil NO emissions, forests have moderate soil NO emissions, and agricultural and grasslands have the highest soil NO emission rates.

Pierce (2001a) uses the model of Williams et al. (1992) to model NO emissions from soils (Eq. 32).

$$E = E_s \cdot A \cdot \exp(0.05112 \cdot T - 15.68248) \quad \textbf{(32)}$$

Eq. 32 presumably represents the agricultural soils model proposed by Williams et al. (1992); however, our calculations show that this model should actually be Eq. 33.

$$E = E_s \cdot A \cdot \exp(0.05112 \cdot T - 13.55009) \quad \textbf{(33)}$$

We are currently in contact with Mr. Pierce to resolve this apparent discrepancy. Further, though Pierce (2001a) uses the agricultural soils model of Williams et al. (1992), he does not use the grasslands (Eq. 34), forests (Eq. 35), wetlands (Eq. 36), or 'other' agricultural (Eq. 37) soils model in the BEIS3 formulation. Pierce (2001b) states that the use of only the agricultural soils model results in only small deviation from the results produced when the other soils models are rigorously applied.

$$E = E_s \cdot A \cdot \exp(0.04686 \cdot T - 12.17360) \quad \textbf{(34)}$$

$$E = E_s \cdot A \cdot \exp(0.05964 \cdot T - 16.03328) \quad \textbf{(35)}$$

$$E = E_s \cdot A \cdot \exp(0.06532 \cdot T - 17.52780) \quad \textbf{(36)}$$

$$E = E_s \cdot A \cdot \exp(0.07313 \cdot T - 19.76737) \quad \textbf{(37)}$$

5.0 Biogenic Methane And Carbon Monoxide

6.0 Conclusion

****NEED TO ADD****

7.0 References

Anderson, L.J., P. C. Harley, R. K. Monson, and R. B. Jackson, 2000. "Reduction of isoprene emissions from live oak (*Quercus fusiformis*) with oak wilt." *Tree Physiology* **20**:1199-1203.

Arey, J., D.E. Crowley, M. Crowley, M. Resketo, and J. Lester, 1995. "Hydrocarbon Emissions from Natural Vegetation in California's South Coast Air Basin." *Atmospheric Environment* **29**:2977-2998.

Baldocchi, D.D., J. D. Fuentes, D. R. Bowling, A. Turnipseed, and R. K. Monson, 1999. "Scaling isoprene fluxes from leaves to canopies: test cases over a boreal aspen and mixed-species temperate forest." *Journal of Applied Meteorology* **38**:885-898.

Baldocchi, D., A. Guenther, P. Harley, L. Klinger, P. Zimmerman, B. Lamb and H. Westberg, 1995. "The fluxes and air chemistry of isoprene above a deciduous hardwood forest," *Phil. Trans. R. Soc. Lond.* A, **350**:1-18.

Bates, T.S., K.C. Kelly, J.E Johnson, and R.H. Gammon, 1995. "Regional and seasonal variations in the flux of ocieanic carbon monoxide to the atmosphere," *J. Geophys. Res.*, **100**, 23093-23101.

Benjamin, M.T., M. Sudol, L. Bloch and A.M. Winer, 1996. "Low-emitting urban forests: a taxonomic methodology for assigning isoprene and monoterpene emission rates," *Atmos. Environ.*, **30**, 1437-1452.

Bonan, G.B. 1995. "Land-atmosphere interactions for climate system models: coupling biophysical, biogeochemical, and ecosystem dynamical processes," *Remote Sensing of Environment* **51**:57-73.

Bradley, K. S., D. H. Stedman, and G. A. Bishop, 1999. "A global inventory of carbon monoxide emissions from motor vehicles," *Chemosphere: Global Change Science*, **1**, 65-72.

Campbell, G. and J. Norman, 1998. An Introduction to Environmental Biophysics, 2nd ed., Springer-Verlag, New York, 286 pp

Chen, J.M. and T.A. Black. 1992. "Defining leaf area index for non-flat leaves," *Plant, Cell and Environment* **15**:421-429

Civerolo, K. and R. Dickerson, 1998. "Nitric oxide soil emissions from tilled and untilled cornfields," *Agric. and Forest Meteorol.* **90**, 307-311.

Cleveland, C. C. and J. B. Yavitt, 1997. "Consumption of atmospheric isoprene in soil," *Geophys. Rev. Lett.*, **24**:2379-2382.

Croft, K., F. Juttner and A. Slusarenko, 1993. "Volatile products of the lipoxygenase pathway evolved from *Phaseolus vulgaris* (L.) leaves inoculated with *Pseudomonas syringae pv phaseolicol*a," *Plant Physiol.*, **101**:13-24.

Croteau, R., 1987. "Biosynthesis and catabolism of monoterpenoids," *Chemical Revie*w, **87**:929-954.
Dabberdt. W.F. and E. Miller, 2000: Uncertainty, ensemble and air quality dispersion modeling: applications and challenges. *Atmos. Environ.* **34**, 4667-4673.

Davidson, E.A., and W. Kingerlee, 1997. "A global inventory of nitric oxide emissions from soils," *Nutrient Cycling in Agroecosystems*, **48**, 37-50.

de Gouw, J. A., C. J. Howard, T. G. Custer and R. Fall, 1999. "Emissions of volatile organic compounds from cut grass are enhanced during the drying process," *Geophys. Res. Lett.*, **26**:811-814.

Dement, W., B. Tyson and H. Money, 1975. "Mechanism of monterpene volatilization in *Salvia mellifera*," *Phytochemistry*, **14**:2555-2557.

Duffie, J. A. and W. A. Beckman (editors), 1980. Solar Engineering of Thermal Processes, John Wiley & Sons.

Environ (2001). "The Global Biosphere Emissions And Interactions System (GLOBEIS)," www.globeis.com

Fall, R. and M. Wildermuth, 1998. "Isoprene synthase: From biochemical mechanism to emission algorithm," *J. Geophys. Res.*, 103, 25599-25609.

Fraser, P.J., R. Rasmussen, J.W. Creffield, J.R. French and M.A.K. Khalil, 1986. "Termites and global methane: another assessment," *J. Atmos. Chem.*, 4:295-310.

Fuentes, J.D., D. Wang, H.H. Neumann, T.J. Gillespie, G.D. Hartog and T.F. Dann, 1996. "Ambient biogenic hydrocarbons and isoprene emissions from a mixed deciduous forest," *J. Atmos. Chem.*, **25**:67-95.

Fung, I., J. John, J. Lerner, E. Matthews, M. Prather, L.P. Steele, and P.J. Fraser, 1991. "Three-dimensional model synthesis of the global methane cycle," *J. Geophys. Res.*, **96**, 13033-13065.

Gabriel, R., L. Schafer, C. Gerlach, T. Rausch and J. Kesselmeier, 1999. "Factors controlling the emissions of volatile organic acids from leaves of *Quercus ilex* L. (Holm oak)" *Atmos. Environ.*, **33**:1347-1356.

Geron, C., D. Nie, R. Arnts, T. Sharkey, E. Singsaas, P. Vanderveer, A. Guenther, G. Katul, J. Sickles and T. Kleindienst, 1997. "Biogenic isoprene emission: model evaluation in a southeastern U.S. bottomland deciduous forest," *J. Geophys. Res.*, **102**, 18889-18901.

Geron, C. D., A. B. Guenther, T. E. Pierce, 1994. "An improved model for estimating emissions of volatile organic compounds from forests in the eastern United States," *J. Geophys. Res.* **99**, D6, 12773-12791.

Goldan, P., W. Kuster and F. Fehsenfeld, 1993. "The observation of a C_5 alcohol emission in a North American pine forest," *Geophys. Res. Lett.*, **20**:1039-1042.

Goldstein, A., M. Goulden, J.W. Munger, S. Wofsy and C. Geron, 1998. "Seasonal course of isoprene emissions from a midlatitude forest," *J. Geophys. Res.*, **103**, 31045-31056.

van der Gon, D., H.A.C., 2000. "Changes in CH4 Emissions from Rice Fields from 1960 to the 1990s. I. Impacts of modern rice technology," *Global Biogeochemical Cycles* 14:61-72.

van der Gon, D., H.A.C., 1999. "Changes in CH4 Emissions from Rice Fields from 1960 to the 1990s. II. The declining use of organic inputs in rice farming," *Global Biogeochemical Cycles* 13:1053-1062.

Goudriaan, J. and H. van Laar, 1994. Modeling Potential Crop Growth Processes, Kluwer Acad., Norwell, MA.

Griffith, S.M., S.C. Alderman, and D.J. Streeter. 1997a. "Italian ryegrass and N source fertilization in western Oregon in two contrasting climatic years. I. Growth and seed yield." *J. Plant Nutrition* **20**:419-428.

Griffith, S.M., S.C. Alderman, and D.J. Streeter. 1997b. "Italian ryegrass and N source fertilization in western Oregon in two contrasting climatic years. II. Plant N accumulation and soil N status." *J. Plant Nutrition* **20**:429-439.

Guenther, A., C. Geron, T. Pierce, B. Lamb, P. Harley, and R. Fall, 2000. "Natural emissions of non-methane volatile organic compounds, carbon monoxide, and oxides of nitrogen from North America," *Atmos. Environ.*, **34**, 2205-2230.

Guenther, A., B. Baugh, G. brasseur, J. Greenberg, P. Harley, L. Klinger, D. Serça, and L. Vierling, 1999. "Isoprene emission estimates and uncertainties for the Central African EXPRESSO study domain," *J. Geophys. Res.* **104** (D23):30625-30639.

Guenther, A., W. Baugh, K. Davis, G. Hampton, P. Harley, L. Klinger, L. Vierling, P. Zimmerman, E. Allwine, S. Dilts, B. Lamb, H. Westberg, D. Baldocchi, C. Geron and T. Pierce, 1996. "Isoprene fluxes measured by enclosure, relaxed eddy accumulation, surface layer gradient, mixed layer gradient, and mixed layer mass balance techniques," *J. Geophys. Res.*, **101**:18555-18567.

Guenther, A., C. N. Hewitt, D. Erickson, R. Fall, C. Geron, T. Graedel, P. Harley, L. Klinger, M. Lerdau, W. A. McKay, T. E. Pierce, B. Scholes, R. Steinbrecher, R. Tallamraju, J. Taylor, P. Zimmerman, 1995. "A global model of natural volatile organic compound emissions," *J. Geophys. Res.* **100**:D5, 8873-8892.

Guenther, A., P. Zimmerman and M. Wildermuth, 1994. "Natural volatile organic compound emission rate estimates for U.S. woodland landscapes," *Atmos. Environ.*, **28**:1197-1210.

Guenther, A., P. R. Zimmerman, P. C. Harley, R. K. Monson, R. Fall, 1993. "Isoprene and Monoterpene Emission Rate Variability: Model Evaluations and Sensitivity Analysis," *J. Geophys. Res.* **98**, 12609-12617.

Guenther, A., R. Monson, and R. Fall, 1991. "Isoprene and Monoterpene Emission Rate Variability: Observations with Eucalyptus and Emission Rate Algorithm Development," *J. Geophys. Res.* **96,** 10799-10808.

Harley, P., V. Fridd-Stroud, J. Greenberg, A. Guenther and P. Vasconcellos, 1998. "Emission of 2-methyl-3-buten-2-ol by pines: A potentially large natural source of reactive carbon to the atmosphere," *J. Geophys. Res.*, 103:25479-25486.

Harley, P., A. Guenther and P. Zimmerman, 1997. "Environmental controls over isoprene emission from sun and shade leaves in a mature white oak canopy," *Tree Phys.*, **17**, 705-712.

Harley, P., A. Guenther, and P. Zimmerman, 1996. "Effects of light, temperature and canopy position on net photosynthesis and isoprene emission from leaves of sweetgum *(Liquidambar styraciflua* L.)," *Tree Phys.*, **16**, 25-32.

Harley, P. and J. Tenhunen, 1991. "Modeling the photosynthetic response of C3 leaves to environmental factors," in *Modeling Crop Photosynthesis – from Biochemistry to Canopy. Crop Soc. Am. Spec. Publ.* 19, Madison, WI.

Houghton, J.T., G.J. Jenkins, and J.J. Ephraums, 1990. Climate Change: The IPCC Scientific Assessment, published for the Intergovernmental Panel on Climate Change by Cambridge Univ. Press, New York.

Hovland, M., A.G. Judd, and R.A. Burje Jr., 1993. "The global flux of methane from shallow submarine sediments," *Chemosphere*, **26**, 559-578.

IPCC, 1994. Climate Change 1994: Radiative Forcing of Climate Change and An Evaluation of the IPCC IS92 Emission Scenarios. J.T. Houghton et al., eds, Cambridge University Press 1995.

IPCC, 1995. Intergovernmental Panel on Climate Change 1995: The Science of Climate Change. J.T. Houghton et al., eds, Cambridge University Press 1996.

IPCC, 2000. Special Report On Emissions Scenarios. Nebojsa Nakicenovic and Rob Swart., eds. http://www.grida.no/climate/ipcc/emission/index.htm

Isebrands, J. G., A. B. Guenther, P. Harley, D. Helmig, L. Klinger, L. Vierling, P. Zimmerman and C. Geron, 1999. "Volatile organic compound emission rates from mixed deciduous and coniferous forests in Northern Wisconsin, USA." *Atmospheric Environment*, **33**(16):2527-2536.

Jacob, D. and P. Bakwin, 1991. "Cycling of NOX in tropical forest canopies," in Microbial Production and Consumption of Greenhouse Gases. Edited by J. Rogers and W. Whitman, pp. 237-253. Am. Soc. For Microbiol., Washington DC.

Johnson. F., H. Eyring, and R. Williams, 1942. "The nature of enzyme inhibitions in bacterial luminescence: Sulfanilamide, urethane, temperature, pressure." *J. Cell Comp. Physiol.*, **20**:247-268.

Johnson, K., M. Huyler et al., 1994. "Measurement of Methane Emissions from Ruminant Livestock Using a SF6 Tracer Technique," *Environ. Sci. Technol.*, **28**(2):359-362.

Johnson, K.A. and D.E. Johnson, 1995. "Methane emissions from cattle," *J. Anim. Sci.* **73**:2483-2492.

Kempf, K., E. Allwine, H. Westberg, C. Claiborn and B. Lamb, 1996. "Hydrocarbon emissions from spruce species using environmental chamber and branch enclosure methods," *Atmos. Environ.*, **30**, 1381-1389.

Keiser, B., 1997. "Monoterpene emissions from native Canadian maples," in *Workshop on Biogenic Hydrocarbons in the Atmospheric Boundary Laye*r, American Meteorological Society, Charlottesville, VA.

Kesselmeier, J., K. Bode, U. Hofmann, H. Muller, L. Schafer, A. Wolf, P. Ciccioli, E. Brancaleoni, A. Cecinato, M. Frattoni, P. Foster, C. Ferrari, V. Jacob, J. Fugit, L. Dutaur, V. Simon and L. Torres, 1997. "The BEMA project: Emission of short chained organic acids, aldehydes and monoterpenes from *Quercus ilex* L. and *Pinus pinea* L. in relation to physiological activities, carbon budget and emission algorithms," *Atmos. Environ.*, **31**, 119-133.

Khalil, M.A.K., J. P. Pinto, and M.J. Shearer, 1999. "Preface: Atmospheric carbon monoxide," *Chemosphere: Global Change Science*, **1**, ix-xi.

Khalil, M.A.K., and R.A. Rasmussen, 1990. "The global cycle of carbon monoxide: trends and mass balance," *Chemosphere* **20**, 227-242.

Kirstine, W., I. Galbally, Y. Ye and M. Hooper, 1998. "Emissions of volatile organic compounds (including oxygenated species) from pasture," *J. Geophys. Res.*, **103**:10605-10619.

Lamb, B., D. Grosjean, B. Pun and C. Seigneur, 1999. "Review of the Emissions, Atmospheric Chemistry, and Gas/Particle Partition of Biogenic Volatile Organic Compounds and Reaction Products," Document Number CP051-1b-99, CRC Project Number A-23, 219 Perimeter Center Parkway, Suite 400, Atlanta, GA 30346, 206 pages. Available at: www.crcao.com/reports/recentstudies00-01/A-23%20AER%20final%20report.pdf

Lamb, B., T. Pierce, D. Baldocchi, E. Allwine, S. Dilts, H. Westberg, C. Geron, A. Guenther, L. Klinger, P. Harley and P. Zimmerman, 1996. "Evaluation of forest canopy models for estimating isoprene emissions," *J. Geophys. Res.*, **101**:22787-22797.

Lamb, B. K., D. Gay, H. Westberg, and T. E. Pierce, 1993. "A Biogenic Hydrocarbon Emissions Inventory for the U.S.A Using a Simple Forest Canopy Model." *Atmospheric Environment*, **27A**:1673-1690.

Lamb, B., H. Westberg, and G. Allwine, 1985. "Biogenic hydrocarbon emissions from deciduous and coniferous trees in the United States," *J. Geophys. Res.*, **90**:2380-2390.

Lambert, G., and S. Schmidt, 1993. "Reevaluation of the oceanic flux of methane: Uncertainties and long term variations," *Chemosphere*, **26**, 579-589.

Lee, D. S., I. Kohler, E. Grobler, F. Rohrer, R. Sausen, L.Gallardo-Klenner, J. J. G. Olivier, F. J. Dentener, and A. F. Bouwman, 1997. "Estimates of global NOx emissions and their uncertainties," *Atmospheric Environment*, **31**, 1735-1749.

Levine, J.S., 1990. "Global biomass burning: atmospheric, climatic, and biospheric implications," *EOS* **71**, 1075-1077.

MacDonald, R.C. and R. Fall, 1993. "Detection of substantial emissions of methanol from plants to the atmosphere," *Atmos. Environ.* **27A**, 1709-1713.

Makela, A., 1986. "Implications of the pipe model theory on dry matter partitioning and height growth in trees," *J. Theor. Biol.* **123**: 103-120.

Matthews, E., 2000. In Atmospheric methane. Its Role in the Global Environment. M.A.K. Khalil (editor), Springer -Verlag, Heidelberg/New York. "Wetlands " pp. 202-233.

Monson, R., P. Harley, M. Litvak, M. Wildermuth, A. Guenther, P. Zimmerman, and R. Fall, 1994. "Environmental and developmental controls over the seasonal pattern of isoprene emission from aspen leaves," *Oecologia* **99**, 260-270.

Monteith, J.L. and Unsworth, M.H., 1990. Principles of environmental physics. Edward Arnold, London,

Moss, A.R., D.I. Givens, P.C. Garnsworthy, 1994. 'The effect of alkali treatment of cereal straws on digestibility and methane production by sheep," *Animal Feed Science and Technology* 49:245-259.

Olivier, J. G. J., J. J. M. Berdowski, J. A. H. W. Peters, J. Bakker, A. J. H. Visschedijk, and J.-P. J. Bloos, 2000. "Applications of EDGAR. Including a description of EDGAR 3.0: reference database with trend data for 1970-1995." RIVM, Bilthoven. RIVM report number 773301 001. Synopsis and data sets available at http://www.rivm.nl/env/int/coredata/edgar

Olivier, J.G.J, A.F. Bouwman, J.J.M. Berdowski, C. Veldt, J.P.J. Bloos, A.J.H. Visschedijk, C.W.M. van der Maas and P.Y.J. Zandveld, 1999. "Sectoral emission inventories of greenhouse gases for 1990 on a per country basis as well as on 1°x1°," *Environmental Science & Policy*, **2**, 241-264.

Parrish, D., E. Williams, D. Fahey, S. Liu and F. Fehsenfeld, 1987. "Measurement of nitrogen oxide fluxes from soils: intercomparison of enclosure and gradient measurement techniques," *J. Geophys. Res* **92**:2165-2171.

Pickering, K.E., Y. Wang, W.K. Tao, C. Price, and J.-F. Müller, 1998. "Vertical distributions of lightning NOX for use in regional and global chemical transport models," *J. Geophys. Res.* **1003**, 31203-31216.

Pier, P., 1995. "Isoprene emission rates from northern red oak using a whole-tree chamber." *Atmospheric Environment* **29**:1347-1353.

Pierce, T. E., B. K. Lamb, and A. R. Van Meter, 1990. "Development of a Biogenic Emissions Inventory System for Regional Scale Air Pollution Models." Paper 90-94.3. In the Proceedins of the 83rd Annual Meeting of the Air and Waste Management Association, 24-29 June, Pittsburgh, PA.

Pierce, T. and P. Waldruff, 1991. "PC-BEIS: A personal computer version of the biogenic emissions inventory system." *J. Air and Waste Manage. Assoc.*, **41**, 937-941.

Pierce, T. E. and C. D. Geron, 1996. The personal computer version of the Biogenic Emissions Inventory System (PCBEIS2.2). "AAREADME," via anonymous ftp at monsoon.rtpnc.epa.gov located in /pub/beis2/pcbeis22. Please also see Pierce et al. (1990), Lamb et al. (1993),Geron et al. (1994), and Pierce (1996).

Pierce, T. E., 1996a. "AAREADME" via anonymous ftp at monsoon.rtpnc.epa.gov located in /pub/beis2/SOS.

Pierce, T. E., 2001a. BEIS3 version 0.9. ftp://ftp.epa.gov/amd/asmd/beis3v09/. March 30.

Pierce, T. E., 2001b. Personal Communication. January 19.

Potter, C., P. Matson, P. Vitousek, E. Davidson, 1996. "Process modeling of controls on nitrogen trace gas emissions from soils worldwide," J. Geophys. Res., **101**:1361-1377.

Price, C.G., J.E. Penner, and M.J. Prather, 1997a. "NOX from lightning, Part I: Global distribution based on lightning physics," *J. Geophys. Res.*, **102**, 5929-5941.

Price, C.G., J.E. Penner, M.J. Prather, 1997b. "NOX from lightning, Part II: Constraints from the global atmospheric electric circuit," *J. Geophys. Res.*, **102**, 5943-5951.

RIVM, 2000. "Emission Database for Global Atmospheric Research – EDGAR,"

Sanderson, M.G., 1996. "Biomass of termites and their emissions of methane and carbon dioxide: A global database," *Global Biogeochem. Cycles*, **10**, 543-557.

Schade, G.W., A.H. Goldstein and M.S. Lamanna, 1999. "Are monoterpene emissions influenced by humidity," *Geophys. Res. Lett.*, **26**:2187-2190.

Seiler, W., R. Conrad, and D. Scharffe, 1984. "Field studies of methane emission from termite nests into the atmosphere and measurement of methane uptake by tropical soils," *J. Atmos. Chem.*, 1:171-186.

Seiler, W., and P.J. Crutzen, 1990. "Estimates of gross and net fluxes of carbon between the biosphere and the atmosphere from biomass burning," *Climatic Change* **2**, 207–247.

Sharkey, T.D., F. Loreto and D.F. Delwiche, *1991*. 'The biochemistry of isoprene emission from leaves during photosynthesis," Trace Gas Emissions from Plants, eds. T.D. Sharkey, E.A. Holland, and H.A. Mooney, Academic Press, San Diego, CA, pp. 153-184.

Sharkey, T. D. and E. L. Singsaas, 1995. "Why plants emit isoprene," *Nature*, 374, 769.

Sharkey,T.D., E.L. Singsaas, M. T. Lerdau, and C. Geron, 1999. "Effects of weather on the capacity for isoprene emission and applications in emissions modeling," *Ecological Applications* **9**:1132-1137.

Sharpe, P. and D. DeMichelle, 1977. "Reaction kinetics of poikilothermic development." *J. Theor. Biol.*, **64**:649-670.

Steinbrecher, R., R. Schonwitz, and H. Ziegler, 1988. "Emission of monoterpenes from needles of Picea abies (L.) Karst under field conditions,"*19th International Symp. Essential Oils Othjer Nat. Substrates*, Landenbergenhaus Greifensee.

Tarr, M. A., W. L. Miller, and R. G. Zepp, 1995. "Direct carbon monoxide photoproduction from plant matter." *Journal of Geophysical Research*, 100 (D6):11,403-11,413.

Thornton, F., P. Pier, and R.Valente, 1997. "NO emissions from soils in the southeastern United States," *J. Geophys. Res* **102**:21189-21195.

Tingey, D. T., M. Manning, L. C. Grothaus, and W. F. Burns, 1979. "Influence of Light and Temperature on Isoprene Emissions from Live Oaks," *Physiological Plantarum*, **47**:112-118.

Tingey, D., 1981. "The effect of environmental factors on the emission of biogenic hydrocarbons from live oak and slash pine." In: Bufalini, J., Arnts, R. (Eds.), Atmospheric Biogenic Hydrocarbons. Butterworth, Stoneham, MA, pp. 53-72.

UNEP, 1999. Levine, J.S., Bobbe, T., Ray, N., Singh, A. and R.G. Witt. "Wildland Fires and the Environment a Global Synthesis." UNEP/DEIAEW/TR.99-1. http://asd-www.larc.nasa.gov/biomass_burn/wildland.html

Valentine, H.T., 1985. "Tree-growth models: derivations employing the pipe-model theory," *J. Theor. Biol.*, **117**: 579-585.

Williams, E. J., A. Guenther, and F. C. Fehsenfeld, 1992. "An Inventory of Nitric Oxide Emissions from Soils in the United States," *J. Geophys. Res.* **97**, Number D7:7511-7519.

Wilson, R.D., P.H. Monoghan, A. Osanik, L.C. Price, and M.A. Rogers, 1994. "Natural marine oil seepage," *Science*, **184**, 857-865.

Winer, A., J. Arey, R. Atkinson, S. Aschman, W. Long, L. Morrison and D. Olszyk, 1992. "Emission rates of organics from vegetation in California's Central Valley," *Atmos.Environ.*, **26**A, 2647-2659.

Yienger, J.J., and H. Levy II, 1995. "Empirical model of global soil-biogenic NOX emissions," *J. Geophys. Res.*, **100**, 11447-11464.

Appendix A. BEIS3 species and emissions factors table.

BEIS3 Species Code	Species Name	Leaf Area Index	Dry Leaf Biomass Factor ($g \cdot m^{-2}$)	Wintertime Adjustment Factor	Biogenic Emissions Factors (g C or $N \cdot kg^{-2} \cdot hr^{-1}$)			
					Isoprene	Monoterpene	Oxygenated Volatile Organic Compounds	Nitric Oxide
USGS Species								
3	USGS_urban	0	100	0.5	10	20	83	6
4	USGS_drycrop	0	300	0.5	28	21	249	34
5	USGS_irrcrop	0	500	0.5	28	50	415	34
6	USGS_cropgrass	0	400	0.5	28	28	332	34
7	USGS_cropwdlnd	2	400	0.5	2650	80	332	21
8	USGS_grassland	0	300	0.5	49	21	249	27
9	USGS_shrubland	2	50	0.5	2859	1	42	2
10	USGS_shrubgrass	3	100	0.5	5741	40	83	27
11	USGS_savanna	1	100	0.5	1765	60	83	27
12	USGS_decidforest	5	300	0.5	8232	90	249	2
13	USGS_evbrdleaf	5	500	1.0	7941	250	415	2
14	USGS_coniferfor	6	550	1.0	11383	1375	457	2
15	USGS_mxforest	5	450	0.5	7729	225	374	2
16	USGS_water	0	0	0.0	0	0	0	0
17	USGS_wetwoods	6	400	0.5	5816	320	332	2
18	USGS_sprsbarren	0	50	0.5	0	3	42	0
19	USGS_woodtundr	3	200	0.5	3360	200	166	2
20	USGS_mxtundra	2	150	0.5	1680	15	125	5
21	USGS_snowice	0	0	0.0	0	0	0	0
Agricultural Species								
22	Alfalfa	0	300	0.0	17	7	249	27
23	Barley	0	300	0.0	7	17	249	45
24	Corn	0	300	0.0	1	0	249	68
25	Cotton	0	300	0.0	7	17	249	45
26	Grass	0	300	0.5	49	124	249	27
27	Hay	0	300	0.5	34	83	249	27
28	Misc_crop	0	300	0.5	7	17	249	40
29	Oats	0	300	0.0	7	17	249	45
30	Pasture	0	300	0.5	49	124	249	27
31	Peanuts	0	300	0.0	90	225	249	27

BEIS3 Species Code	Species Name	Leaf Area Index	Dry Leaf Biomass Factor ($g \cdot m^{-2}$)	Wintertime Adjustment Factor	Biogenic Emissions Factors ($g\ C$ or $N \cdot kg^{-2} \cdot hr^{-1}$)			
					Isoprene	Monoterpene	Oxygenated Volatile Organic Compounds	Nitric Oxide
32	Potatoes	0	300	0.0	9	21	249	120
33	Rice	0	300	0.5	90	225	249	0
34	Rye	0	300	0.0	7	17	249	27
35	Sorghum	0	300	0.0	7	18	249	68
36	Soybeans	0	300	0.0	19	0	249	27
37	Tobacco	0	300	0.0	0	52	249	45
38	Wheat	0	300	0.5	13	5	249	30
Tree Species								
39	Acacia	5	700	0.0	70	1851	581	2
40	Ailanthus	5	375	0.0	38	33	311	2
41	Alder	5	375	0.0	38	33	311	2
42	Apple	5	375	0.0	38	33	311	2
43	Ash	5	375	0.0	38	33	311	2
44	Basswood	5	375	0.0	38	33	311	2
45	Beech	5	375	0.0	38	192	311	2
46	Birch	5	375	0.0	38	66	311	2
47	Bumelia_gum	5	375	1.0	38	33	311	2
48	Cajeput	5	375	1.0	38	33	311	2
49	Califor_laurel	5	375	1.0	38	33	311	2
50	Cascara_buckthor	5	375	0.0	38	33	311	2
51	Castanea	5	375	0.0	38	33	311	2
52	Catalpa	5	375	0.0	38	33	311	2
53	Cedar_chamaecyp	7	1500	1.0	150	265	1245	2
54	Cedar_thuja	7	1500	1.0	150	793	1245	2
55	Chestnut_buckeye	5	375	0.0	38	33	311	2
56	Chinaberry	5	375	0.0	38	33	311	2
57	Cypress_cupress	3	375	1.0	70	33	311	2
58	Cypress_taxodium	5	375	0.0	38	609	311	2
59	Dogwood	5	375	0.0	38	530	311	2
60	Douglas_fir	7	1500	1.0	150	2118	1245	2
61	East_hophornbean	5	375	0.0	38	33	311	2
62	Elder	5	375	0.0	38	33	311	2
63	Elm	5	375	0.0	38	33	311	2
64	Eucalyptus	5	375	1.0	26250	993	311	2
65	Fir_balsam	7	1500	1.0	150	4221	1245	2

BEIS3 Species Code	Species Name	Leaf Area Index	Dry Leaf Biomass Factor ($g \cdot m^{-2}$)	Wintertime Adjustment Factor	Biogenic Emissions Factors (g C or $N \cdot kg^{-2} \cdot hr^{-1}$)			
					Isoprene	Monoterpene	Oxygenated Volatile Organic Compounds	Nitric Oxide
66	Fir_CA_red	7	1500	1.0	150	3971	1245	2
67	Fir_corkbark	7	1500	1.0	150	3971	1245	2
68	Fir_fraser	7	1500	1.0	150	3971	1245	2
69	Fir_grand	7	1500	1.0	150	3971	1245	2
70	Fir_noble	7	1500	1.0	150	4304	1245	2
71	Fir_Pacf_silver	7	1500	1.0	150	3971	1245	2
72	Fir_SantaLucia	7	1500	1.0	150	3971	1245	2
73	Fir_Shasta_red	7	1500	1.0	150	3971	1245	2
74	Fir_spp	7	1500	1.0	150	3971	1245	2
75	Fir_subalpine	7	1500	1.0	150	3971	1245	2
76	Fir_white	7	1500	1.0	150	3971	1245	2
77	Gleditsia_locust	5	375	0.0	38	33	311	2
78	Hackberry	5	375	0.0	38	66	311	2
79	Hawthorn	5	375	0.0	38	33	311	2
80	Hemlock	7	700	1.0	70	123	581	2
81	Hickory	5	375	0.0	38	530	311	2
82	Holly_American	5	375	1.0	38	66	311	2
83	Hornbeam	5	375	0.0	38	530	311	2
84	Incense_cedar	3	1500	1.0	70	132	1245	2
85	Juniper	7	700	1.0	70	371	581	2
86	KY_coffeetree	5	375	0.0	38	33	311	2
87	Larch	5	375	0.0	38	33	311	2
88	Loblolly_bay	5	375	1.0	38	33	311	2
89	Madrone	5	375	1.0	38	33	311	2
90	Magnolia	5	375	1.0	38	993	311	2
91	Mahogany	5	375	1.0	38	33	311	2
92	Maple_bigleaf	5	375	0.0	38	529	311	2
93	Maple_bigtooth	5	375	0.0	38	529	311	2
94	Maple_black	5	375	0.0	38	529	311	2
95	Maple_boxelder	5	375	0.0	38	529	311	2
96	Maple_FL	5	375	0.0	38	529	311	2
97	Maple_mtn	5	375	0.0	38	529	311	2
98	Maple_Norway	5	375	0.0	38	529	311	2
99	Maple_red	5	375	0.0	38	529	311	2
100	Maple_RkyMtn	5	375	0.0	38	529	311	2

BEIS3 Species Code	Species Name	Leaf Area Index	Dry Leaf Biomass Factor ($g \cdot m^{-2}$)	Wintertime Adjustment Factor	Biogenic Emissions Factors (g C or $N \cdot kg^{-2} \cdot hr^{-1}$)			
					Isoprene	Monoterpene	Oxygenated Volatile Organic Compounds	Nitric Oxide
101	Maple_silver	5	375	0.0	38	529	311	2
102	Maple_spp	5	375	0.0	38	529	311	2
103	Maple_striped	5	375	0.0	38	529	311	2
104	Maple_sugar	5	375	0.0	38	529	311	2
105	Mesquite	5	375	0.0	38	33	311	2
106	Misc_hardwoods	5	375	0.0	38	33	311	2
107	Mixed_conifer_sp	7	700	1.0	70	62	581	2
108	Mountain_ash	5	375	0.0	38	33	311	2
109	Mulberry	5	375	0.0	38	66	311	2
110	Nyssa	5	375	0.0	5250	199	311	2
111	Oak_AZ_white	5	375	1.0	26250	66	311	2
112	Oak_bear	5	375	0.0	26250	66	311	2
113	Oak_black	5	375	0.0	26250	66	311	2
114	Oak_blackjack	5	375	0.0	26250	66	311	2
115	Oak_blue	5	375	0.0	26250	66	311	2
116	Oak_bluejack	5	375	0.0	26250	66	311	2
117	Oak_bur	5	375	0.0	26250	66	311	2
118	Oak_CA_black	5	375	0.0	26250	66	311	2
119	Oak_CA_live	5	375	1.0	26250	66	311	2
120	Oak_CA_white	5	375	0.0	26250	66	311	2
121	Oak_canyon_live	5	375	1.0	26250	66	311	2
122	Oak_chestnut	5	375	0.0	26250	66	311	2
123	Oak_chinkapin	5	375	0.0	26250	66	311	2
124	Oak_delta_post	5	375	0.0	26250	66	311	2
125	Oak_Durand	5	375	0.0	26250	66	311	2
126	Oak_Emery	5	375	1.0	26250	66	311	2
127	Oak_Engelmann	5	375	1.0	26250	66	311	2
128	Oak_evergreen_sp	5	375	1.0	26250	66	311	2
129	Oak_Gambel	5	375	0.0	26250	66	311	2
130	Oak_interio_live	5	375	1.0	26250	66	311	2
131	Oak_laurel	5	375	1.0	26250	66	311	2
132	Oak_live	5	375	1.0	26250	66	311	2
133	Oak_Mexicanblue	5	375	1.0	26250	66	311	2
134	Oak_Northrn_pin	5	375	0.0	26250	66	311	2
135	Oak_Northrn_red	5	375	0.0	26250	66	311	2

BEIS3 Species Code	Species Name	Leaf Area Index	Dry Leaf Biomass Factor ($g \cdot m^{-2}$)	Wintertime Adjustment Factor	Biogenic Emissions Factors (g C or $N \cdot kg^{-2} \cdot hr^{-1}$)			
					Isoprene	Monoterpene	Oxygenated Volatile Organic Compounds	Nitric Oxide
136	Oak_nuttall	5	375	0.0	26250	66	311	2
137	Oak_OR_white	5	375	0.0	26250	66	311	2
138	Oak_overcup	5	375	0.0	26250	66	311	2
139	Oak_pin	5	375	0.0	26250	66	311	2
140	Oak_post	5	375	0.0	26250	66	311	2
141	Oak_scarlet	5	375	0.0	26250	66	311	2
142	Oak_scrub	5	375	0.0	26250	66	311	2
143	Oak_shingle	5	375	0.0	26250	66	311	2
144	Oak_Shumrd_red	5	375	0.0	26250	66	311	2
145	Oak_silverleaf	5	375	1.0	26250	66	311	2
146	Oak_Southrn_red	5	375	0.0	26250	66	311	2
147	Oak_spp	5	375	0.0	26250	66	311	2
148	Oak_swamp_cnut	5	375	0.0	26250	66	311	2
149	Oak_swamp_red	5	375	0.0	26250	66	311	2
150	Oak_swamp_white	5	375	0.0	26250	66	311	2
151	Oak_turkey	5	375	0.0	26250	66	311	2
152	Oak_water	5	375	0.0	26250	66	311	2
153	Oak_white	5	375	0.0	26250	66	311	2
154	Oak_willow	5	375	0.0	26250	66	311	2
155	Osage_orange	5	375	0.0	38	33	311	2
156	Paulownia	5	375	0.0	38	33	311	2
157	Pawpaw	5	375	0.0	38	33	311	2
158	Persimmon	5	375	0.0	38	33	311	2
159	Pine_Apache	3	700	1.0	70	1842	581	2
160	Pine_Austrian	3	700	1.0	70	1853	581	2
161	Pine_AZ	3	700	1.0	70	1853	581	2
162	Pine_Bishop	3	700	1.0	70	1853	581	2
163	Pine_blackjack	3	700	1.0	70	1853	581	2
164	Pine_brstlcone	3	700	1.0	70	1853	581	2
165	Pine_chihuahua	3	700	1.0	70	1853	581	2
166	Pine_Coulter	3	700	1.0	70	1857	581	2
167	Pine_digger	3	700	1.0	70	1853	581	2
168	Pine_Ewhite	3	700	1.0	70	1853	581	2
169	Pine_foxtail	3	700	1.0	70	1853	581	2
170	Pine_jack	3	700	1.0	70	1849	581	2

BEIS3 Species Code	Species Name	Leaf Area Index	Dry Leaf Biomass Factor ($g \cdot m^{-2}$)	Wintertime Adjustment Factor	Biogenic Emissions Factors (g C or $N \cdot kg^{-2} \cdot hr^{-1}$)			
					Isoprene	Monoterpene	Oxygenated Volatile Organic Compounds	Nitric Oxide
171	Pine_Jeffrey	3	700	1.0	70	1907	581	2
172	Pine_knobcone	3	700	1.0	70	1855	581	2
173	Pine_limber	3	700	1.0	70	1853	581	2
174	Pine_loblolly	3	700	1.0	70	1853	581	2
175	Pine_lodgepole	3	700	1.0	70	1853	581	2
176	Pine_longleaf	3	700	1.0	70	1851	581	2
177	Pine_Monterey	3	700	1.0	70	1855	581	2
178	Pine_pinyon	3	700	1.0	70	1853	581	2
179	Pine_pinyon_brdr	3	700	1.0	70	1853	581	2
180	Pine_pinyon_cmn	3	700	1.0	70	1779	581	2
181	Pine_pitch	3	700	1.0	70	1853	581	2
182	Pine_pond	3	700	1.0	70	1855	581	2
183	Pine_ponderosa	3	700	1.0	70	1853	581	2
184	Pine_red	3	700	1.0	70	1851	581	2
185	Pine_sand	3	700	1.0	70	1853	581	2
186	Pine_scotch	3	700	1.0	70	1853	581	2
187	Pine_shortleaf	3	700	1.0	70	1851	581	2
188	Pine_slash	3	700	1.0	70	1851	581	2
189	Pine_spruce	3	700	1.0	70	1853	581	2
190	Pine_sugar	3	700	1.0	70	1853	581	2
191	Pine_Swwhite	3	700	1.0	70	1853	581	2
192	Pine_tablemtn	3	700	1.0	70	1855	581	2
193	Pine_VA	3	700	1.0	70	1853	581	2
194	Pine_Washoe	3	700	1.0	70	1853	581	2
195	Pine_whitebark	3	700	1.0	70	1853	581	2
196	Pine_Wwhite	3	700	1.0	70	1851	581	2
197	Pine_yellow	3	700	1.0	70	1853	581	2
198	Populus	5	375	0.0	26250	33	311	2
199	Prunus	5	375	0.0	38	34	311	2
200	Redbay	5	375	1.0	38	33	311	2
201	Robinia_locust	5	375	0.0	5250	33	311	2
202	Sassafras	5	375	0.0	38	33	311	2
203	Sequoia	7	1500	1.0	150	133	1245	2
204	Serviceberry	5	375	0.0	38	33	311	2
205	Silverbell	5	375	0.0	38	33	311	2

BEIS3 Species Code	Species Name	Leaf Area Index	Dry Leaf Biomass Factor ($g \cdot m^{-2}$)	Wintertime Adjustment Factor	Biogenic Emissions Factors (g C or $N \cdot kg^{-2} \cdot hr^{-1}$)			
					Isoprene	Monoterpene	Oxygenated Volatile Organic Compounds	Nitric Oxide
206	Smoketree	5	375	0.0	38	33	311	2
207	Soapberry_westrn	5	375	1.0	38	33	311	2
208	Sourwood	5	375	0.0	38	198	311	2
209	Sparkleberry	5	375	0.0	38	33	311	2
210	Spruce_black	7	1500	1.0	21000	3971	1245	2
211	Spruce_blue	7	1500	1.0	21000	3975	1245	2
212	Spruce_Brewer	7	1500	1.0	21000	3971	1245	2
213	Spruce_Englemann	7	1500	1.0	21000	3971	1245	2
214	Spruce_Norway	7	1500	1.0	21000	3975	1245	2
215	Spruce_red	7	1500	1.0	21000	3967	1245	2
216	Spruce_Sitka	7	1500	1.0	21000	3971	1245	2
217	Spruce_spp	7	1500	1.0	21000	3971	1245	2
218	Spruce_white	7	1500	1.0	21000	3971	1245	2
219	Sweetgum	5	375	0.0	26250	991	311	2
220	Sycamore	5	375	0.0	13125	33	311	2
221	Tallowtree_chins	5	375	1.0	38	33	311	2
222	Tamarix	3	375	1.0	70	33	311	2
223	Tanoak	5	375	1.0	38	33	311	2
224	Torreya	7	700	1.0	150	62	581	2
225	Tung_oil_tree	5	375	1.0	38	33	311	2
226	Unknown_tree	5	375	0.0	38	33	311	2
227	Walnut	5	375	0.0	38	993	311	2
228	Water_elm	5	375	0.0	38	33	311	2
229	Willow	5	375	0.0	13125	33	311	2
230	Yellow_poplar	5	375	0.0	38	68	311	2
231	Yellowwood	5	375	0.0	38	33	311	2
232	Yucca_Mojave	5	375	1.0	38	33	311	2

Appendix B. BEIS3 discrete species emissions factors for the OVOC class.

BEIS3 Species Code	Biogenic Emissions Factors (g C·kg^{-2}·hr^{-1})															
	2-methyl-3-butenol (MBO)	Methanol	Ethene	Propene	Ethanol	Acetone	Hexanal	Hexenol	Hexenyl-acetate	Form-aldehyde	Acet-aldehyde	Butene	Ethane	Formic acid	Acetic acid	Butenone
3	100	200	10	10	10	10	10	10	10	3	3	3	1	1	1	1
4	10	600	30	30	30	30	30	30	30	9	9	9	3	3	3	3
5	10	1000	50	50	50	50	50	50	50	15	15	15	5	5	5	5
6	10	800	40	40	40	40	40	40	40	12	12	12	4	4	4	4
7	200	800	40	40	40	40	40	40	40	12	12	12	4	4	4	4
8	10	600	30	30	30	30	30	30	30	9	9	9	3	3	3	3
9	20	100	5	5	5	5	5	5	5	2	2	2	1	1	1	1
10	400	200	10	10	10	10	10	10	10	3	3	3	1	1	1	1
11	0	200	10	10	10	10	10	10	10	3	3	3	1	1	1	1
12	0	600	30	30	30	30	30	30	30	9	9	9	3	3	3	3
13	0	1000	50	50	50	50	50	50	50	15	15	15	5	5	5	5
14	1000	500	55	55	55	55	55	55	55	17	17	17	6	6	6	6
15	100	600	45	45	45	45	45	45	45	14	14	14	5	5	5	5
16	0	0	0	0	0	0	0	0	0	0	0	0	0	0	0	0
17	0	800	40	40	40	40	40	40	40	12	12	12	4	4	4	4
18	10	100	5	5	5	5	5	5	5	2	2	2	1	1	1	1
19	0	200	20	20	20	20	20	20	20	6	6	6	2	2	2	2
20	0	100	15	15	15	15	15	15	15	5	5	5	2	2	2	2
21	0	0	0	0	0	0	0	0	0	0	0	0	0	0	0	0
22	0	600	30	30	30	30	30	30	30	9	9	9	3	3	3	3
23	0	600	30	30	30	30	30	30	30	9	9	9	3	3	3	3
24	0	600	30	30	30	30	30	30	30	9	9	9	3	3	3	3
25	0	600	30	30	30	30	30	30	30	9	9	9	3	3	3	3
26	0	600	30	30	30	30	30	30	30	9	9	9	3	3	3	3
27	0	600	30	30	30	30	30	30	30	9	9	9	3	3	3	3
28	0	600	30	30	30	30	30	30	30	9	9	9	3	3	3	3
29	0	600	30	30	30	30	30	30	30	9	9	9	3	3	3	3
30	0	600	30	30	30	30	30	30	30	9	9	9	3	3	3	3
31	0	600	30	30	30	30	30	30	30	9	9	9	3	3	3	3
32	0	600	30	30	30	30	30	30	30	9	9	9	3	3	3	3
33	0	600	30	30	30	30	30	30	30	9	9	9	3	3	3	3
34	0	600	30	30	30	30	30	30	30	9	9	9	3	3	3	3
35	0	600	30	30	30	30	30	30	30	9	9	9	3	3	3	3
36	0	600	30	30	30	30	30	30	30	9	9	9	3	3	3	3
37	0	600	30	30	30	30	30	30	30	9	9	9	3	3	3	3
38	0	600	30	30	30	30	30	30	30	9	9	9	3	3	3	3
39	0	1400	70	70	70	70	70	70	70	21	21	21	7	7	7	7
40	0	750	38	38	38	38	38	38	38	11	11	11	4	4	4	4
41	0	750	38	38	38	38	38	38	38	11	11	11	4	4	4	4

BEIS3 Species Code	Biogenic Emissions Factors (g C·kg^{-2}·hr^{-1})															
	2-methyl-3-butenol (MBO)	Methanol	Ethene	Propene	Ethanol	Acetone	Hexanal	Hexenol	Hexenyl-acetate	Form-aldehyde	Acet-aldehyde	Butene	Ethane	Formic acid	Acetic acid	Butenone
42	0	750	38	38	38	38	38	38	38	11	11	11	4	4	4	4
43	0	750	38	38	38	38	38	38	38	11	11	11	4	4	4	4
44	0	750	38	38	38	38	38	38	38	11	11	11	4	4	4	4
45	0	750	38	38	38	38	38	38	38	11	11	11	4	4	4	4
46	0	750	38	38	38	38	38	38	38	11	11	11	4	4	4	4
47	0	750	38	38	38	38	38	38	38	11	11	11	4	4	4	4
48	0	750	38	38	38	38	38	38	38	11	11	11	4	4	4	4
49	0	750	38	38	38	38	38	38	38	11	11	11	4	4	4	4
50	0	750	38	38	38	38	38	38	38	11	11	11	4	4	4	4
51	0	750	38	38	38	38	38	38	38	11	11	11	4	4	4	4
52	0	750	38	38	38	38	38	38	38	11	11	11	4	4	4	4
53	0	750	150	150	150	150	150	150	150	45	45	45	15	15	15	15
54	0	750	150	150	150	150	150	150	150	45	45	45	15	15	15	15
55	0	750	38	38	38	38	38	38	38	11	11	11	4	4	4	4
56	0	750	38	38	38	38	38	38	38	11	11	11	4	4	4	4
57	0	750	38	38	38	38	38	38	38	11	11	11	4	4	4	4
58	0	750	38	38	38	38	38	38	38	11	11	11	4	4	4	4
59	0	750	38	38	38	38	38	38	38	11	11	11	4	4	4	4
60	0	750	150	150	150	150	150	150	150	45	45	45	15	15	15	15
61	0	750	38	38	38	38	38	38	38	11	11	11	4	4	4	4
62	0	750	38	38	38	38	38	38	38	11	11	11	4	4	4	4
63	0	750	38	38	38	38	38	38	38	11	11	11	4	4	4	4
64	0	750	38	38	38	38	38	38	38	11	11	11	4	4	4	4
65	0	750	150	150	150	150	150	150	150	45	45	45	15	15	15	15
66	0	750	150	150	150	150	150	150	150	45	45	45	15	15	15	15
67	0	750	150	150	150	150	150	150	150	45	45	45	15	15	15	15
68	0	750	150	150	150	150	150	150	150	45	45	45	15	15	15	15
69	0	750	150	150	150	150	150	150	150	45	45	45	15	15	15	15
70	0	750	150	150	150	150	150	150	150	45	45	45	15	15	15	15
71	0	750	150	150	150	150	150	150	150	45	45	45	15	15	15	15
72	0	750	150	150	150	150	150	150	150	45	45	45	15	15	15	15
73	0	750	150	150	150	150	150	150	150	45	45	45	15	15	15	15
74	0	750	150	150	150	150	150	150	150	45	45	45	15	15	15	15
75	0	750	150	150	150	150	150	150	150	45	45	45	15	15	15	15
76	0	750	150	150	150	150	150	150	150	45	45	45	15	15	15	15
77	0	750	38	38	38	38	38	38	38	11	11	11	4	4	4	4
78	0	750	38	38	38	38	38	38	38	11	11	11	4	4	4	4
79	0	750	38	38	38	38	38	38	38	11	11	11	4	4	4	4
80	0	350	70	70	70	70	70	70	70	21	21	21	7	7	7	7
81	0	750	38	38	38	38	38	38	38	11	11	11	4	4	4	4
82	0	750	38	38	38	38	38	38	38	11	11	11	4	4	4	4
83	0	750	38	38	38	38	38	38	38	11	11	11	4	4	4	4
84	0	750	150	150	150	150	150	150	150	45	45	45	15	15	15	15
85	0	350	70	70	70	70	70	70	70	21	21	21	7	7	7	7

BEIS3 Species Code	Biogenic Emissions Factors (g C·kg^{-2}·hr^{-1})															
	2-methyl-3-butenol (MBO)	Methanol	Ethene	Propene	Ethanol	Acetone	Hexanal	Hexenol	Hexenyl-acetate	Form-aldehyde	Acet-aldehyde	Butene	Ethane	Formic acid	Acetic acid	Butenone
86	0	750	38	38	38	38	38	38	38	11	11	11	4	4	4	4
87	0	750	38	38	38	38	38	38	38	11	11	11	4	4	4	4
88	0	750	38	38	38	38	38	38	38	11	11	11	4	4	4	4
89	0	750	38	38	38	38	38	38	38	11	11	11	4	4	4	4
90	0	750	38	38	38	38	38	38	38	11	11	11	4	4	4	4
91	0	750	38	38	38	38	38	38	38	11	11	11	4	4	4	4
92	0	750	38	38	38	38	38	38	38	11	11	11	4	4	4	4
93	0	750	38	38	38	38	38	38	38	11	11	11	4	4	4	4
94	0	750	38	38	38	38	38	38	38	11	11	11	4	4	4	4
95	0	750	38	38	38	38	38	38	38	11	11	11	4	4	4	4
96	0	750	38	38	38	38	38	38	38	11	11	11	4	4	4	4
97	0	750	38	38	38	38	38	38	38	11	11	11	4	4	4	4
98	0	750	38	38	38	38	38	38	38	11	11	11	4	4	4	4
99	0	750	38	38	38	38	38	38	38	11	11	11	4	4	4	4
100	0	750	38	38	38	38	38	38	38	11	11	11	4	4	4	4
101	0	750	38	38	38	38	38	38	38	11	11	11	4	4	4	4
102	0	750	38	38	38	38	38	38	38	11	11	11	4	4	4	4
103	0	750	38	38	38	38	38	38	38	11	11	11	4	4	4	4
104	0	750	38	38	38	38	38	38	38	11	11	11	4	4	4	4
105	0	750	38	38	38	38	38	38	38	11	11	11	4	4	4	4
106	0	750	38	38	38	38	38	38	38	11	11	11	4	4	4	4
107	0	350	70	70	70	70	70	70	70	21	21	21	7	7	7	7
108	0	750	38	38	38	38	38	38	38	11	11	11	4	4	4	4
109	0	750	38	38	38	38	38	38	38	11	11	11	4	4	4	4
110	0	750	38	38	38	38	38	38	38	11	11	11	4	4	4	4
111	0	750	38	38	38	38	38	38	38	11	11	11	4	4	4	4
112	0	750	38	38	38	38	38	38	38	11	11	11	4	4	4	4
113	0	750	38	38	38	38	38	38	38	11	11	11	4	4	4	4
114	0	750	38	38	38	38	38	38	38	11	11	11	4	4	4	4
115	0	750	38	38	38	38	38	38	38	11	11	11	4	4	4	4
116	0	750	38	38	38	38	38	38	38	11	11	11	4	4	4	4
117	0	750	38	38	38	38	38	38	38	11	11	11	4	4	4	4
118	0	750	38	38	38	38	38	38	38	11	11	11	4	4	4	4
119	0	750	38	38	38	38	38	38	38	11	11	11	4	4	4	4
120	0	750	38	38	38	38	38	38	38	11	11	11	4	4	4	4
121	0	750	38	38	38	38	38	38	38	11	11	11	4	4	4	4
122	0	750	38	38	38	38	38	38	38	11	11	11	4	4	4	4
123	0	750	38	38	38	38	38	38	38	11	11	11	4	4	4	4
124	0	750	38	38	38	38	38	38	38	11	11	11	4	4	4	4
125	0	750	38	38	38	38	38	38	38	11	11	11	4	4	4	4
126	0	750	38	38	38	38	38	38	38	11	11	11	4	4	4	4
127	0	750	38	38	38	38	38	38	38	11	11	11	4	4	4	4
128	0	750	38	38	38	38	38	38	38	11	11	11	4	4	4	4
129	0	750	38	38	38	38	38	38	38	11	11	11	4	4	4	4

BEIS3 Species Code	Biogenic Emissions Factors (g C·kg^{-2}·hr^{-1})															
	2-methyl-3-butenol (MBO)	Methanol	Ethene	Propene	Ethanol	Acetone	Hexanal	Hexenol	Hexenyl-acetate	Form-aldehyde	Acet-aldehyde	Butene	Ethane	Formic acid	Acetic acid	Butenone
130	0	750	38	38	38	38	38	38	38	11	11	11	4	4	4	4
131	0	750	38	38	38	38	38	38	38	11	11	11	4	4	4	4
132	0	750	38	38	38	38	38	38	38	11	11	11	4	4	4	4
133	0	750	38	38	38	38	38	38	38	11	11	11	4	4	4	4
134	0	750	38	38	38	38	38	38	38	11	11	11	4	4	4	4
135	0	750	38	38	38	38	38	38	38	11	11	11	4	4	4	4
136	0	750	38	38	38	38	38	38	38	11	11	11	4	4	4	4
137	0	750	38	38	38	38	38	38	38	11	11	11	4	4	4	4
138	0	750	38	38	38	38	38	38	38	11	11	11	4	4	4	4
139	0	750	38	38	38	38	38	38	38	11	11	11	4	4	4	4
140	0	750	38	38	38	38	38	38	38	11	11	11	4	4	4	4
141	0	750	38	38	38	38	38	38	38	11	11	11	4	4	4	4
142	0	750	38	38	38	38	38	38	38	11	11	11	4	4	4	4
143	0	750	38	38	38	38	38	38	38	11	11	11	4	4	4	4
144	0	750	38	38	38	38	38	38	38	11	11	11	4	4	4	4
145	0	750	38	38	38	38	38	38	38	11	11	11	4	4	4	4
146	0	750	38	38	38	38	38	38	38	11	11	11	4	4	4	4
147	0	750	38	38	38	38	38	38	38	11	11	11	4	4	4	4
148	0	750	38	38	38	38	38	38	38	11	11	11	4	4	4	4
149	0	750	38	38	38	38	38	38	38	11	11	11	4	4	4	4
150	0	750	38	38	38	38	38	38	38	11	11	11	4	4	4	4
151	0	750	38	38	38	38	38	38	38	11	11	11	4	4	4	4
152	0	750	38	38	38	38	38	38	38	11	11	11	4	4	4	4
153	0	750	38	38	38	38	38	38	38	11	11	11	4	4	4	4
154	0	750	38	38	38	38	38	38	38	11	11	11	4	4	4	4
155	0	750	38	38	38	38	38	38	38	11	11	11	4	4	4	4
156	0	750	38	38	38	38	38	38	38	11	11	11	4	4	4	4
157	0	750	38	38	38	38	38	38	38	11	11	11	4	4	4	4
158	0	750	38	38	38	38	38	38	38	11	11	11	4	4	4	4
159	0	350	70	70	70	70	70	70	70	21	21	21	7	7	7	7
160	0	350	70	70	70	70	70	70	70	21	21	21	7	7	7	7
161	17500	350	70	70	70	70	70	70	70	21	21	21	7	7	7	7
162	17500	350	70	70	70	70	70	70	70	21	21	21	7	7	7	7
163	17500	350	70	70	70	70	70	70	70	21	21	21	7	7	7	7
164	0	350	70	70	70	70	70	70	70	21	21	21	7	7	7	7
165	0	350	70	70	70	70	70	70	70	21	21	21	7	7	7	7
166	49000	350	70	70	70	70	70	70	70	21	21	21	7	7	7	7
167	49000	350	70	70	70	70	70	70	70	21	21	21	7	7	7	7
168	0	350	70	70	70	70	70	70	70	21	21	21	7	7	7	7
169	0	350	70	70	70	70	70	70	70	21	21	21	7	7	7	7
170	17500	350	70	70	70	70	70	70	70	21	21	21	7	7	7	7
171	17500	350	70	70	70	70	70	70	70	21	21	21	7	7	7	7
172	70	350	70	70	70	70	70	70	70	21	21	21	7	7	7	7
173	0	350	70	70	70	70	70	70	70	21	21	21	7	7	7	7

BEIS3 Species Code	Biogenic Emissions Factors (g C·kg^{-2}·hr^{-1})															
	2-methyl-3-butenol (MBO)	Methanol	Ethene	Propene	Ethanol	Acetone	Hexanal	Hexenol	Hexenyl-acetate	Form-aldehyde	Acet-aldehyde	Butene	Ethane	Formic acid	Acetic acid	Butenone
174	70	350	70	70	70	70	70	70	70	21	21	21	7	7	7	7
175	17500	350	70	70	70	70	70	70	70	21	21	21	7	7	7	7
176	7000	350	70	70	70	70	70	70	70	21	21	21	7	7	7	7
177	70	350	70	70	70	70	70	70	70	21	21	21	7	7	7	7
178	0	350	70	70	70	70	70	70	70	21	21	21	7	7	7	7
179	0	350	70	70	70	70	70	70	70	21	21	21	7	7	7	7
180	0	350	70	70	70	70	70	70	70	21	21	21	7	7	7	7
181	70	350	70	70	70	70	70	70	70	21	21	21	7	7	7	7
182	70	350	70	70	70	70	70	70	70	21	21	21	7	7	7	7
183	17500	350	70	70	70	70	70	70	70	21	21	21	7	7	7	7
184	0	350	70	70	70	70	70	70	70	21	21	21	7	7	7	7
185	70	350	70	70	70	70	70	70	70	21	21	21	7	7	7	7
186	0	350	70	70	70	70	70	70	70	21	21	21	7	7	7	7
187	0	350	70	70	70	70	70	70	70	21	21	21	7	7	7	7
188	70	350	70	70	70	70	70	70	70	21	21	21	7	7	7	7
189	70	350	70	70	70	70	70	70	70	21	21	21	7	7	7	7
190	0	350	70	70	70	70	70	70	70	21	21	21	7	7	7	7
191	0	350	70	70	70	70	70	70	70	21	21	21	7	7	7	7
192	70	350	70	70	70	70	70	70	70	21	21	21	7	7	7	7
193	0	350	70	70	70	70	70	70	70	21	21	21	7	7	7	7
194	17500	350	70	70	70	70	70	70	70	21	21	21	7	7	7	7
195	0	350	70	70	70	70	70	70	70	21	21	21	7	7	7	7
196	0	350	70	70	70	70	70	70	70	21	21	21	7	7	7	7
197	17500	350	70	70	70	70	70	70	70	21	21	21	7	7	7	7
198	0	750	38	38	38	38	38	38	38	11	11	11	4	4	4	4
199	0	750	38	38	38	38	38	38	38	11	11	11	4	4	4	4
200	0	750	38	38	38	38	38	38	38	11	11	11	4	4	4	4
201	0	750	38	38	38	38	38	38	38	11	11	11	4	4	4	4
202	0	750	38	38	38	38	38	38	38	11	11	11	4	4	4	4
203	0	750	150	150	150	150	150	150	150	45	45	45	15	15	15	15
204	0	750	38	38	38	38	38	38	38	11	11	11	4	4	4	4
205	0	750	38	38	38	38	38	38	38	11	11	11	4	4	4	4
206	0	750	38	38	38	38	38	38	38	11	11	11	4	4	4	4
207	0	750	38	38	38	38	38	38	38	11	11	11	4	4	4	4
208	0	750	38	38	38	38	38	38	38	11	11	11	4	4	4	4
209	0	750	38	38	38	38	38	38	38	11	11	11	4	4	4	4
210	0	750	150	150	150	150	150	150	150	45	45	45	15	15	15	15
211	0	750	150	150	150	150	150	150	150	45	45	45	15	15	15	15
212	0	750	150	150	150	150	150	150	150	45	45	45	15	15	15	15
213	0	750	150	150	150	150	150	150	150	45	45	45	15	15	15	15
214	0	750	150	150	150	150	150	150	150	45	45	45	15	15	15	15
215	0	750	150	150	150	150	150	150	150	45	45	45	15	15	15	15
216	0	750	150	150	150	150	150	150	150	45	45	45	15	15	15	15
217	0	750	150	150	150	150	150	150	150	45	45	45	15	15	15	15

BEIS3 Species Code	Biogenic Emissions Factors (g C·kg^{-2}·hr^{-1})															
	2-methyl-3-butenol (MBO)	Methanol	Ethene	Propene	Ethanol	Acetone	Hexanal	Hexenol	Hexenyl-acetate	Form-aldehyde	Acet-aldehyde	Butene	Ethane	Formic acid	Acetic acid	Butenone
218	0	750	150	150	150	150	150	150	150	45	45	45	15	15	15	15
219	0	750	38	38	38	38	38	38	38	11	11	11	4	4	4	4
220	0	750	38	38	38	38	38	38	38	11	11	11	4	4	4	4
221	0	750	38	38	38	38	38	38	38	11	11	11	4	4	4	4
222	0	750	38	38	38	38	38	38	38	11	11	11	4	4	4	4
223	0	750	38	38	38	38	38	38	38	11	11	11	4	4	4	4
224	0	350	70	70	70	70	70	70	70	21	21	21	7	7	7	7
225	0	750	38	38	38	38	38	38	38	11	11	11	4	4	4	4
226	0	750	38	38	38	38	38	38	38	11	11	11	4	4	4	4
227	0	750	38	38	38	38	38	38	38	11	11	11	4	4	4	4
228	0	750	38	38	38	38	38	38	38	11	11	11	4	4	4	4
229	0	750	38	38	38	38	38	38	38	11	11	11	4	4	4	4
230	0	750	38	38	38	38	38	38	38	11	11	11	4	4	4	4
231	0	750	38	38	38	38	38	38	38	11	11	11	4	4	4	4
232	0	750	38	38	38	38	38	38	38	11	11	11	4	4	4	4

Appendix C. BEIS3 carbon monoxide emissions factors and discrete species emissions factors for the monoterpene class.

BEIS3 Species Code	Biogenic Emissions Factors (g C·kg^{-2}·hr^{-1})														
	α-pinene	β-pinene	d3-carene	d-limonene	camphene	myrcene	α-terpinene	β-phellan-drene	sabinene	p-cymene	o-cimene	α-thujene	terpinolene	γ-terpinene	carbon monoxide
3	8	4	2	2	2	2	0	0	0	0	0	0	0	0	30
4	8	4	2	2	2	2	0	0	0	0	0	0	0	0	90
5	20	10	5	5	5	5	0	0	0	0	0	0	0	0	150
6	11	6	3	3	3	3	0	0	0	0	0	0	0	0	120
7	32	16	8	8	8	8	0	0	0	0	0	0	0	0	120
8	8	4	2	2	2	2	0	0	0	0	0	0	0	0	90
9	0	0	0	0	0	0	0	0	0	0	0	0	0	0	15
10	16	8	4	4	4	4	0	0	0	0	0	0	0	0	30
11	24	12	6	6	6	6	0	0	0	0	0	0	0	0	30
12	36	18	9	9	9	9	0	0	0	0	0	0	0	0	90
13	100	50	25	25	25	25	0	0	0	0	0	0	0	0	150
14	550	275	138	138	138	138	0	0	0	0	0	0	0	0	165
15	90	45	23	23	23	23	0	0	0	0	0	0	0	0	135
16	0	0	0	0	0	0	0	0	0	0	0	0	0	0	0
17	128	64	32	32	32	32	0	0	0	0	0	0	0	0	120
18	1	1	0	0	0	0	0	0	0	0	0	0	0	0	15
19	80	40	20	20	20	20	0	0	0	0	0	0	0	0	60
20	6	3	2	2	2	2	0	0	0	0	0	0	0	0	45
21	0	0	0	0	0	0	0	0	0	0	0	0	0	0	0
22	3	1	1	1	1	1	0	0	0	0	0	0	0	0	90
23	7	3	2	2	2	2	0	0	0	0	0	0	0	0	90
24	0	0	0	0	0	0	0	0	0	0	0	0	0	0	90
25	7	3	2	2	2	2	0	0	0	0	0	0	0	0	90
26	50	25	12	12	12	12	0	0	0	0	0	0	0	0	90
27	33	17	8	8	8	8	0	0	0	0	0	0	0	0	90
28	7	3	2	2	2	2	0	0	0	0	0	0	0	0	90
29	7	3	2	2	2	2	0	0	0	0	0	0	0	0	90
30	50	25	12	12	12	12	0	0	0	0	0	0	0	0	90
31	90	45	23	23	23	23	0	0	0	0	0	0	0	0	90
32	8	4	2	2	2	2	0	0	0	0	0	0	0	0	90
33	90	45	23	23	23	23	0	0	0	0	0	0	0	0	90
34	7	3	2	2	2	2	0	0	0	0	0	0	0	0	90
35	7	4	2	2	2	2	0	0	0	0	0	0	0	0	90
36	0	0	0	0	0	0	0	0	0	0	0	0	0	0	90
37	21	10	5	5	5	5	0	0	0	0	0	0	0	0	90
38	2	1	1	1	1	1	0	0	0	0	0	0	0	0	90
39	1623	132	0	63	0	33	0	0	0	0	0	0	0	0	210
40	13	7	3	3	3	3	0	0	0	0	0	0	0	0	113
41	4	15	0	7	0	0	0	0	0	1	6	1	0	0	113
42	13	7	3	3	3	3	0	0	0	0	0	0	0	0	113
43	7	3	1	0	0	7	0	15	0	0	0	0	0	0	113

BEIS3 Species Code	Biogenic Emissions Factors (g C·kg^{-2}·hr^{-1})														
	α-pinene	β-pinene	d3-carene	d-limonene	camphene	myrcene	α-terpinene	β-phellandrene	sabinene	p-cymene	o-cimene	α-thujene	terpinolene	γ-terpinene	carbon monoxide
44	13	7	3	3	3	3	0	0	0	0	0	0	0	0	113
45	63	24	12	48	1	3	16	0	1	24	0	1	0	0	113
46	19	0	0	19	14	0	0	0	0	14	0	0	0	0	113
47	13	7	3	3	3	3	0	0	0	0	0	0	0	0	113
48	13	7	3	3	3	3	0	0	0	0	0	0	0	0	113
49	9	4	0	0	0	2	1	0	12	1	0	0	0	4	113
50	13	7	3	3	3	3	0	0	0	0	0	0	0	0	113
51	13	7	3	3	3	3	0	0	0	0	0	0	0	0	113
52	13	7	3	3	3	3	0	0	0	0	0	0	0	0	113
53	42	170	0	52	0	0	0	0	0	0	0	0	0	0	450
54	284	54	11	103	130	10	0	0	54	68	0	75	0	4	450
55	13	7	3	3	3	3	0	0	0	0	0	0	0	0	113
56	12	5	0	6	0	11	0	0	0	0	0	0	0	0	113
57	14	0	0	10	0	8	0	0	0	0	0	0	0	0	113
58	514	4	43	24	0	25	0	0	0	0	0	0	0	0	113
59	107	3	205	142	41	0	0	0	0	25	0	0	7	0	113
60	1360	449	57	112	21	53	0	2	64	0	0	0	0	0	450
61	7	0	0	7	13	0	0	0	0	7	0	0	0	0	113
62	13	7	3	3	3	3	0	0	0	0	0	0	0	0	113
63	3	11	0	4	0	0	0	0	14	0	0	2	0	0	113
64	351	187	0	206	0	0	0	0	0	0	248	0	0	0	113
65	1072	1421	48	806	365	68	79	226	0	135	0	0	0	0	450
66	1588	794	397	397	397	397	0	0	0	0	0	0	0	0	450
67	878	552	40	1171	397	60	496	0	0	338	0	40	0	0	450
68	1588	794	397	397	397	397	0	0	0	0	0	0	0	0	450
69	2251	711	28	163	397	203	0	143	52	0	0	0	24	0	450
70	365	528	0	1211	95	397	0	1191	0	338	0	0	71	107	450
71	1588	794	397	397	397	397	0	0	0	0	0	0	0	0	450
72	1588	794	397	397	397	397	0	0	0	0	0	0	0	0	450
73	1588	794	397	397	397	397	0	0	0	0	0	0	0	0	450
74	1588	794	397	397	397	397	0	0	0	0	0	0	0	0	450
75	1588	794	397	397	397	397	0	0	0	0	0	0	0	0	450
76	1322	1390	0	246	238	167	0	79	397	0	0	0	115	16	450
77	13	7	3	3	3	3	0	0	0	0	0	0	0	0	113
78	1	0	0	0	0	1	0	0	0	0	64	0	0	0	113
79	13	7	3	3	3	3	0	0	0	0	0	0	0	0	113
80	18	7	1	20	34	2	0	0	0	27	0	15	0	0	210
81	128	38	177	102	2	37	0	0	16	0	0	1	30	1	113
82	26	13	7	7	7	7	0	0	0	0	0	0	0	0	113
83	149	122	115	48	48	0	0	0	0	48	0	0	0	0	113
84	53	26	13	13	13	13	0	0	0	0	0	0	0	0	450
85	123	0	247	0	0	0	0	0	0	0	0	0	0	0	210
86	13	7	3	3	3	3	0	0	0	0	0	0	0	0	113
87	13	7	3	3	3	3	0	0	0	0	0	0	0	0	113

BEIS3 Species Code	Biogenic Emissions Factors (g C·kg^{-2}·hr^{-1})														
	α-pinene	β-pinene	d3-carene	d-limonene	camphene	myrcene	α-terpinene	β-phellan-drene	sabinene	p-cymene	o-cimene	α-thujene	terpinolene	γ-terpinene	carbon monoxide
88	13	7	3	3	3	3	0	0	0	0	0	0	0	0	113
89	13	7	3	3	3	3	0	0	0	0	0	0	0	0	113
90	602	263	16	56	6	51	0	0	0	0	0	0	0	0	113
91	13	7	3	3	3	3	0	0	0	0	0	0	0	0	113
92	112	23	132	69	27	42	3	0	114	0	0	4	0	4	113
93	112	23	132	69	27	42	3	0	114	0	0	4	0	4	113
94	112	23	132	69	27	42	3	0	114	0	0	4	0	4	113
95	112	23	132	69	27	42	3	0	114	0	0	4	0	4	113
96	112	23	132	69	27	42	3	0	114	0	0	4	0	4	113
97	112	23	132	69	27	42	3	0	114	0	0	4	0	4	113
98	112	23	132	69	27	42	3	0	114	0	0	4	0	4	113
99	112	23	132	69	27	42	3	0	114	0	0	4	0	4	113
100	112	23	132	69	27	42	3	0	114	0	0	4	0	4	113
101	112	23	132	69	27	42	3	0	114	0	0	4	0	4	113
102	112	23	132	69	27	42	3	0	114	0	0	4	0	4	113
103	112	23	132	69	27	42	3	0	114	0	0	4	0	4	113
104	112	23	132	69	27	42	3	0	114	0	0	4	0	4	113
105	13	7	3	3	3	3	0	0	0	0	0	0	0	0	113
106	13	7	3	3	3	3	0	0	0	0	0	0	0	0	113
107	25	12	6	6	6	6	0	0	0	0	0	0	0	0	210
108	13	7	3	3	3	3	0	0	0	0	0	0	0	0	113
109	26	13	7	7	7	7	0	0	0	0	0	0	0	0	113
110	43	35	18	63	13	28	0	0	0	0	0	0	0	0	113
111	23	4	0	9	5	0	0	0	0	7	10	0	8	0	113
112	23	4	0	9	5	0	0	0	0	7	10	0	8	0	113
113	23	4	0	9	5	0	0	0	0	7	10	0	8	0	113
114	23	4	0	9	5	0	0	0	0	7	10	0	8	0	113
115	23	4	0	9	5	0	0	0	0	7	10	0	8	0	113
116	23	4	0	9	5	0	0	0	0	7	10	0	8	0	113
117	23	4	0	9	5	0	0	0	0	7	10	0	8	0	113
118	23	4	0	9	5	0	0	0	0	7	10	0	8	0	113
119	23	4	0	9	5	0	0	0	0	7	10	0	8	0	113
120	23	4	0	9	5	0	0	0	0	7	10	0	8	0	113
121	23	4	0	9	5	0	0	0	0	7	10	0	8	0	113
122	23	4	0	9	5	0	0	0	0	7	10	0	8	0	113
123	23	4	0	9	5	0	0	0	0	7	10	0	8	0	113
124	23	4	0	9	5	0	0	0	0	7	10	0	8	0	113
125	23	4	0	9	5	0	0	0	0	7	10	0	8	0	113
126	23	4	0	9	5	0	0	0	0	7	10	0	8	0	113
127	23	4	0	9	5	0	0	0	0	7	10	0	8	0	113
128	23	4	0	9	5	0	0	0	0	7	10	0	8	0	113
129	23	4	0	9	5	0	0	0	0	7	10	0	8	0	113
130	23	4	0	9	5	0	0	0	0	7	10	0	8	0	113
131	23	4	0	9	5	0	0	0	0	7	10	0	8	0	113

BEIS3 Species Code	Biogenic Emissions Factors (g C·kg^{-2}·hr^{-1})														
	α-pinene	β-pinene	d3-carene	d-limonene	camphene	myrcene	α-terpinene	β-phellan-drene	sabinene	p-cymene	o-cimene	α-thujene	terpinolene	γ-terpinene	carbon monoxide
132	23	4	0	9	5	0	0	0	0	7	10	0	8	0	113
133	23	4	0	9	5	0	0	0	0	7	10	0	8	0	113
134	23	4	0	9	5	0	0	0	0	7	10	0	8	0	113
135	23	4	0	9	5	0	0	0	0	7	10	0	8	0	113
136	23	4	0	9	5	0	0	0	0	7	10	0	8	0	113
137	23	4	0	9	5	0	0	0	0	7	10	0	8	0	113
138	23	4	0	9	5	0	0	0	0	7	10	0	8	0	113
139	23	4	0	9	5	0	0	0	0	7	10	0	8	0	113
140	23	4	0	9	5	0	0	0	0	7	10	0	8	0	113
141	23	4	0	9	5	0	0	0	0	7	10	0	8	0	113
142	23	4	0	9	5	0	0	0	0	7	10	0	8	0	113
143	23	4	0	9	5	0	0	0	0	7	10	0	8	0	113
144	23	4	0	9	5	0	0	0	0	7	10	0	8	0	113
145	23	4	0	9	5	0	0	0	0	7	10	0	8	0	113
146	23	4	0	9	5	0	0	0	0	7	10	0	8	0	113
147	23	4	0	9	5	0	0	0	0	7	10	0	8	0	113
148	23	4	0	9	5	0	0	0	0	7	10	0	8	0	113
149	23	4	0	9	5	0	0	0	0	7	10	0	8	0	113
150	23	4	0	9	5	0	0	0	0	7	10	0	8	0	113
151	23	4	0	9	5	0	0	0	0	7	10	0	8	0	113
152	23	4	0	9	5	0	0	0	0	7	10	0	8	0	113
153	23	4	0	9	5	0	0	0	0	7	10	0	8	0	113
154	23	4	0	9	5	0	0	0	0	7	10	0	8	0	113
155	13	7	3	3	3	3	0	0	0	0	0	0	0	0	113
156	13	7	3	3	3	3	0	0	0	0	0	0	0	0	113
157	13	7	3	3	3	3	0	0	0	0	0	0	0	0	113
158	17	16	0	0	0	0	0	0	0	0	0	0	0	0	113
159	1279	328	0	2	63	109	0	54	2	0	0	0	4	2	210
160	1801	0	0	52	0	0	0	0	0	0	0	0	0	0	210
161	402	617	765	26	0	33	2	0	7	0	0	0	0	0	210
162	741	371	185	185	185	185	0	0	0	0	0	0	0	0	210
163	402	617	765	26	0	33	2	0	7	0	0	0	0	0	210
164	1853	0	0	0	0	0	0	0	0	0	0	0	0	0	210
165	1745	0	107	0	0	0	0	0	0	0	0	0	0	0	210
166	537	282	50	359	37	141	0	178	232	17	4	0	17	4	210
167	1117	736	0	0	0	0	0	0	0	0	0	0	0	0	210
168	469	365	2	2	263	539	0	126	15	0	0	72	0	0	210
169	1829	15	0	9	0	0	0	0	0	0	0	0	0	0	210
170	563	463	193	111	135	233	2	32	80	2	2	0	33	0	210
171	826	122	0	430	126	300	0	28	56	9	6	0	4	0	210
172	702	397	69	291	24	198	0	145	6	0	20	0	4	0	210
173	1853	0	0	0	0	0	0	0	0	0	0	0	0	0	210
174	1075	447	19	128	15	156	4	0	0	9	0	0	2	0	210
175	408	367	93	335	100	180	82	195	26	30	4	0	30	6	210

BEIS3 Species Code	Biogenic Emissions Factors (g C·kg^{-2}·hr^{-1})														
	α-pinene	β-pinene	d3-carene	d-limonene	camphene	myrcene	α-terpinene	β-phellan-drene	sabinene	p-cymene	o-cimene	α-thujene	terpinolene	γ-terpinene	carbon monoxide
176	778	995	50	26	0	2	0	0	0	0	0	0	0	0	210
177	717	773	2	198	2	150	0	13	0	0	0	0	0	0	210
178	741	371	185	185	185	185	0	0	0	0	0	0	0	0	210
179	1820	0	0	33	0	0	0	0	0	0	0	0	0	0	210
180	1681	76	9	0	13	0	0	0	0	0	0	0	0	0	210
181	1362	334	158	0	0	0	0	0	0	0	0	0	0	0	210
182	311	387	0	1138	9	0	0	7	0	2	0	0	0	0	210
183	402	617	765	26	0	33	2	0	7	0	0	0	0	0	210
184	182	4	33	647	358	135	85	0	0	408	0	0	0	0	210
185	841	1001	0	2	6	0	0	2	0	2	0	0	0	0	210
186	384	397	565	145	7	174	35	141	4	0	0	0	2	0	210
187	1019	261	93	422	9	43	2	0	2	0	0	0	0	0	210
188	876	699	139	106	2	9	0	20	0	0	0	0	0	0	210
189	926	926	0	0	0	0	0	0	0	0	0	0	0	0	210
190	1538	315	0	0	0	0	0	0	0	0	0	0	0	0	210
191	741	371	185	185	185	185	0	0	0	0	0	0	0	0	210
192	1395	317	143	0	0	0	0	0	0	0	0	0	0	0	210
193	613	237	634	228	83	56	0	0	2	0	0	0	0	0	210
194	741	371	185	185	185	185	0	0	0	0	0	0	0	0	210
195	710	489	41	193	54	245	0	96	17	0	0	0	9	0	210
196	550	484	602	63	0	152	0	0	0	0	0	0	0	0	210
197	402	617	765	26	0	33	2	0	7	0	0	0	0	0	210
198	11	2	0	9	6	1	0	0	0	4	0	0	0	0	113
199	12	5	0	3	4	0	0	0	0	0	8	0	0	0	113
200	13	7	3	3	3	3	0	0	0	0	0	0	0	0	113
201	0	0	0	0	0	33	0	0	0	0	0	0	0	0	113
202	0	3	0	0	3	0	0	0	3	14	0	0	9	0	113
203	34	1	0	16	0	8	1	6	38	1	1	0	1	25	450
204	13	7	3	3	3	3	0	0	0	0	0	0	0	0	113
205	13	7	3	3	3	3	0	0	0	0	0	0	0	0	113
206	13	7	3	3	3	3	0	0	0	0	0	0	0	0	113
207	13	7	3	3	3	3	0	0	0	0	0	0	0	0	113
208	78	33	26	62	0	0	0	0	0	0	0	0	0	0	113
209	13	7	3	3	3	3	0	0	0	0	0	0	0	0	113
210	961	115	1116	608	917	83	4	12	4	135	0	0	8	8	450
211	1346	1096	349	778	226	107	4	32	24	4	0	0	4	4	450
212	1588	794	397	397	397	397	0	0	0	0	0	0	0	0	450
213	1457	532	230	322	488	345	119	206	0	266	0	0	4	0	450
214	1799	492	341	401	341	262	0	163	131	36	0	0	4	4	450
215	794	322	1040	222	1144	230	0	119	0	68	0	0	16	12	450
216	687	397	0	4	87	2049	0	746	0	0	0	0	0	0	450
217	1588	794	397	397	397	397	0	0	0	0	0	0	0	0	450
218	953	449	214	1052	719	334	4	218	16	0	0	0	8	4	450
219	451	68	162	160	6	37	15	31	44	18	0	1	0	0	113

BEIS3 Species Code	Biogenic Emissions Factors (g C·kg^{-2}·hr^{-1})														
	α-pinene	β-pinene	d3-carene	d-limonene	camphene	myrcene	α-terpinene	β-phellan-drene	sabinene	p-cymene	o-cimene	α-thujene	terpinolene	γ-terpinene	carbon monoxide
220	13	7	3	3	3	3	0	0	0	0	0	0	0	0	113
221	13	7	3	3	3	3	0	0	0	0	0	0	0	0	113
222	13	7	3	3	3	3	0	0	0	0	0	0	0	0	113
223	13	7	3	3	3	3	0	0	0	0	0	0	0	0	113
224	25	12	6	6	6	6	0	0	0	0	0	0	0	0	210
225	13	7	3	3	3	3	0	0	0	0	0	0	0	0	113
226	13	7	3	3	3	3	0	0	0	0	0	0	0	0	113
227	288	512	0	128	0	65	0	0	0	0	0	0	0	0	113
228	13	7	3	3	3	3	0	0	0	0	0	0	0	0	113
229	4	0	0	7	0	0	0	0	0	6	16	0	0	0	113
230	3	4	0	27	1	18	0	1	0	0	7	0	6	3	113
231	13	7	3	3	3	3	0	0	0	0	0	0	0	0	113
232	13	7	3	3	3	3	0	0	0	0	0	0	0	0	113

3
CHAPTER 3

BEIS3 DESCRIPTION AND REVIEW COMMENTS

Global Estimates Of Anthropogenic And Naturally Occurring Emissions

The BEIS family of models estimates emissions of BVOCs that are the result of biological activity from land-based vegetative species and BNO that is the result of microbial activity from certain soil types (Guenther et al., 2000, 1999, 1993, 1991; Geron et al., 1994; Lamb et al., 1993; Williams et al., 1992; Pierce and Waldruff, 1991; Pierce et al., 1990). Also, a future release of the third generation of the BEIS family of models, BEIS3, will also estimate biogenic carbon monoxide (BCO) emissions (Pierce, 2001a), which are the result of photochemical transformation from vegetative species (Khalil et al., 1999). That is, the version of BEIS3 that was used in this study (BEIS3 v.0.9) did not contain the BCO formulation. Therefore, though BCO is discussed here it was not considered in the uncertainty analysis. Other sources of biogenic and geogenic emissions are currently outside the framework of the BEIS family of models. This includes such emissions as methane from termites, wetlands, and biomass burning, as well as, carbon monoxide from biomass burning and soils.

Table 3-1 presents a comparative overview of the global natural sources and anthropogenic sources inventories for methane (CH_4), non-methane volatile organic compounds (NMVOC), CO, and NO_X for 1990. The purpose of Table 3-1 is to contrast the magnitudes of emissions from anthropogenic and naturally occurring sources. Further, Table 3-1 identifies the source categories for which BEIS3 estimates emissions. The identification of sources in Table 3-1 follows that of the IPCC (2000). Among the source categories that require further explanation are as follows:

- Natural Sources – Other, includes emissions from other geogenic sources such as volcanoes and other biogenic sources such as enteric fermentation, a digestive process under anaerobic conditions in the intestines of animals, from wildlife and emissions from wildlife waste; and
- Anthropogenic Sources – Other, includes emissions from residential, commercial, and other industrial processes as well as production of CO from VOC oxidation.

In Table 3-1, both the nominal emissions estimate and the possible range, in parentheses, of the emissions estimate are shown. If an entry has a question mark, either the nominal value or the range is unknown. The highlighted entries for NMVOC from vegetation and NO_X from soils indicate the biogenic sources for which BEIS3 is formulated to estimate emissions.

The methods that were used to estimate the NMVOC from vegetation are the same methods that are embedded in BEIS3. The methods account for 20% to 25% of the 1990 global NMVOC emissions. CO emissions have also been observed from plants and are believed to be the result of direct photochemical transformation on the plant leaf or in the plant matrix (Tarr et al., 1995). Though a future release of BEIS3 will be formulated to estimate CO from vegetative species, the BCO formulation is suspect. Pierce (2001b) reports that BEIS3 will employ a temperature-based formulation to estimate CO emissions from plants. However, Tarr et al. (1995) report that the processes controlling CO production from plants are directly correlated with light. Further, the methods used to estimate global CO emissions from vegetative species are different than those embedded in BEIS3 (Khalil and Rasmussen, 1990). Regardless, it appears that CO from plants accounts for 10% to 16% of the total global CO emissions load. Also, CO emissions from plants may be higher since Tarr et al. (1995) report that CO emissions rates from deadfall, which appear to be missing from the estimates from Khalil and Rasmussen (1991) and Khalil et al. (1999), are upwards of an order of magnitude higher than for growing and senescent vegetative species. Finally, there is no evidence to suggest that methane or NO_X is released from vegetative species as a result of biological activity.

Because different methods than those embedded in BEIS3 were used to inventory the 1990 global NO_X emissions from soils, it is unknown how global NO_X emissions from soils estimated by BEIS3 compare to those shown in Table 3-1. Regardless, NO_X emissions from soils are about 25% to 30% of the 1990 global NO_X emissions.

If all sources of biospheric NO_X, NMVOC, methane, and CO are included as biogenic sources, the fraction of carbon and nitrogen emissions from biogenic sources jump to well over 50% of the total global load. Given the importance that these pollutants have in atmospheric chemistry, it is prudent to accurately characterize their contributions to the total emissions load.

The emissions estimates presented in Table 3-1 are not necessarily equally distributed throughout the globe. For example, though global BVOC emissions are roughly equally divided between the northern and southern hemisphere, 51% and 49% respectively, 90% of the BVOC emissions in the southern hemisphere occur between the equator and 25°S latitude. In the northern hemisphere, 65% of the BVOC emissions occur between the equator and 25°N latitude, 27% between 25°N and 50°N latitudes, and 8% between 50°N and 80°N latitudes (Guenther et al., 1995). Mobile source CO emissions are even more disparate with approximately 90% produced in the northern hemisphere (Bradley et al., 1999).

Table 3-1.
Global emissions estimates of CH_4, NMVOC, CO, and NO_X for natural and anthropogenic sources for 1990. Emissions estimates are in terragrams carbon (Tg C) or terragrams nitrogen (Tg N). Question marks (?) indicate that either the nominal emissions estimate or the range, shown in parentheses, of the emissions estimate is unknown. Shaded boxes (i.e. NMVOC, CO, and NO_X) indicate the source sectors for which BEIS3 has been formulated to estimate emisstions.

Source	Pollutant (Tg C or N per year)				References
	CH_4	NMVOC	CO	NO_X	
Natural Sources					
Wetlands	110-115 (50-170)[1,2]				1. IPCC, 1994, 1995 2. Mathews, 2000
Termites	20 (10-50)[1, 2]				1. IPCC, 1994, 1995 2. Sanderson, 1995
Oceans	10-14 (5-50)[1,2,3]	5 (2-15)[4]	13-100 (6-190)[5,6,7]		1. IPCC, 1994, 1995 2. Fang et al., 1991 3. Lambert and Schmidt, 1995 4. Guenther et al., 1995 5. Seiler and Crutzen, 1990 6. Bates et al., 1995 7. Khalil and Rasmussen, 1990
Soils			30 (?-?)[1]	19 (4-21)[2,3]	1. Khalil et al., 1999 2. Yienger and Levy, 1995 3. Davidson and Kingerlee, 1997

Source	Pollutant (Tg C or N per year)				References
	CH_4	NMVOC	CO	NO_X	
Vegetation (including agricultural lands)		Isoprene: 503 (200-800) [1] Monoterpenes: 127 (50-500) [1] Other VOCs: 515 (20-1800) [1]	75-230 (20-400) [2,3]		1. Guenther et al., 1995 2. Khalil and Rasmussen, 1990 3. Khalil et al., 1999
Lightning				17 (2-25) [1,2]	1. Price et al., 1997a, 1997b 2. Pickering et al., 1997
Petroleum Seeps	? (8-65) [1]	1 (0.2-6) [2]			1. Hovland et al., 1993 2. Wilson et al., 1994
Fires		2360(?-?) [1] -- includes methane	35 (25-75) [2,3]	-- included in Biomass Burning	1. UNEP, 1999 2. Olivier et al., 1999 3. Seiler and Crutzen, 1990
Other	15 (10-40) [1]				1. IPCC, 1994, 1995
Anthropogenic Sources					
Natural Gas Production and Combustion	40 (25-50) [1]	7 (?-?) [2]		1 (0.5-2) [2,3]	1. IPCC, 1994, 1995 2. Olivier et al., 1999, 2000 3. Lee et al., 1997
Coal Mining	30 (15-45) [1]				1. IPCC, 1994, 1995

Source	Pollutant (Tg C or N per year)				References
	CH_4	NMVOC	CO	NO_X	
Petroleum Industry	15 (5-30)[1]	22 (?-?)[2]	<1 (?-?)[2]	<1 (?-?)[2]	1. IPCC, 1994, 1995 2. Olivier et al., 1999, 2000
Coal Combustion	? (1-30)[1]	<1 (?-?)[2]	1 (?-?)[2]	5 (2-7)[2,3]	1. IPCC, 1994, 1995 2. Olivier et al., 1999, 2000 3. Lee et al., 1997
Enteric Fermentation	80-85 (65-100)[1]				1. IPCC, 1994, 1995
Rice Paddies	60 (20-100)[1]				1. IPCC, 1994, 1995
Biomass Burning	40 (20-80)[1]	1540 (?-?)[2]	500 (300-700)[3,4]	8 (3-15)[5]	1. IPCC, 1994, 1995 2. UNEP, 1999 3. IPCC, 2000 4. Olivier et al., 1999, 2000 5. Lee et al., 1997
Landfills	40 (20-70)[1]				1. IPCC, 1994, 1995
Animal Waste Treatment And Decomposition	25 (20-30)[1]				1. IPCC, 1994, 1995
Domestic Sewage Treatment And Decomposition	25 (15-80)[1]				1. IPCC, 1994, 1995

Source	Pollutant (Tg C or N per year)				References
	CH_4	NMVOC	CO	NO_X	
On-road And Non-road Mobile Sources	<1 (?-?)[1]	34 (?-?)[1]	210-500 (200-600) [1,2,3]	5 (3-8)[4]	1. Olivier et al., 1999, 2000 2. Bradley et al., 1999 3. Khalil et al., 1999 4. Lee et al., 1997
Other	15 (?-?)[1]	64 (?-?)[1]	300-1100 (200-1500) [1,2,3]	10 (5-14)[1,4]	1. Olivier et al., 1999, 2000 2. IPCC, 2000 3. Khalil et al., 1999 4. Lee et al., 1997

BEIS3 Plant Species And Chemical Species

Appendix A lists the 230 species for which BEIS3 estimates emissions (Pierce, 2001a). These 230 plant species are believed to represent the vast majority of plant species, at least in the North America, that emit one or more chemical species which impact atmospheric chemistry from the urban scale to the global scale. However, at least one gap in our knowledge of biogenic emissions needs to be closed. For some plant species, emission factors for specific terpenes, sesquiterpenes, and oxygenated compounds need to be determined (Lamb et al., 1999). This is needed since in some cases, the emissions factors for some compounds from some plant species are based on taxonomical assignment from those plant species whose emissions factors are relatively well known (e.g. Benjamin et al., 1996).

Also listed in Appendix A are the BEIS3 species codes, leaf area indices, dry leaf biomass factors, wintertime adjustment factors, and biogenic emissions factors (Pierce, 2001a). These are inputs to the BEIS3 model.

Leaf area index (LAI) is defined as the total one-sided, or one half of the total all-sided, green leaf area per unit ground surface area (Chen and Black, 1992). LAI describes a fundamental property of the plant canopy in its interaction with the atmosphere, especially concerning radiation, energy, momentum and gas exchange (Monteith and Unsworth, 1990). Leaf area plays a key role in the absorption of radiation, in the deposition of photosynthates during the diurnal and seasonal cycles, and in the pathways and rates of biogeochemical cycling within the canopy-soil system (Bonan, 1995). Globally, LAI varies from less than one to above ten but also exhibits significant variation within biomes at regional, landscape, and local levels (Monteith and Unsworth, 1990). In the context of BEIS3, LAI is used to adjust the isoprene emissions for the effects of PAR penetrating through the leaf canopy.

Leaf biomass provides the energy that drives the growth of the tree stand and as such, is the subject of several models (Valentine, 1985; Makela, 1986). It is also possible to describe changes in leaf biomass using less formal techniques including expert knowledge, which is subject to verification using visual estimation or photogrametric techniques. The leaf biomass values that are listed in Appendix A reflect peak foliar density (i.e. these values are the maximum leaf biomass factors that occur during the growing season).

The wintertime adjustment factor indicates the fraction of the emissions factors to use when estimating biogenic emissions in the winter months (e.g. zero indicates that the plant species does not emit in the winter months; 0.5 indicates that the plant species emits at one-half the listed emissions factors in the winter months). It is unclear how this factor was determined, and is therefore likely to be highly uncertain.

The biogenic isoprene, monoterpenes, OVOCs, and NO emissions factors are the flux-rate that each species emits under standard environmental conditions (i.e. 30°C and 1000 $umol \cdot m^{-2} \cdot s^{-1}$ PAR for isoprene and 30°C for monoterpenes, OVOCs, and NO). The biogenic emissions factors are based primarily on enclosure flux measurements (Guenther et al, 2000). The enclosure flux methods include static branch chamber (e.g. Lamb et al., 1985), dynamic flow branch chamber

with and without environmental control (e.g. Dement et al., 1975; Arey et al., 1995), dynamic whole plant chamber with and without environmental control (e.g. Tingey, 1981; Pier, 1995), dynamic leaf cuvette with and without environmental control (e.g. Geron et al. 1997; Harley et al., 1996, 1997), and leaf cuvette (e.g. Harley et al., 1996).

Though the current release of BEIS3 is formulated to estimate emissions of isoprene, monoterpenes, OVOCs, and nitric oxide, Pierce (2001b) indicates that a future release of BEIS3 will allow for the estimation of the discrete chemical compounds that comprise the monoterpene and OVOC classes. Pierce (2001b) also indicates that a future release of BEIS3 will also allow for the estimation of BCO. Although BCO is released both as a biomass combustion by-product and as the result of less than well-understood direct photoproduction processes that occur on the plant tissues or within the plant matrix (Lamb et al., 1999; Tarr et al., 1995), BEIS3 will only be formulated to estimate BCO from the latter process (Pierce, 2001b). However, as indicated earlier, the BEIS3 BCO formulation is suspect since Tarr et al. (1995) report that BCO production is regulated by light, but Pierce (2001b) indicates that BEIS3 will control BCO production via a temperature-dependent mechanism. Appendix B lists the emissions factors for the discrete OVOC chemical compounds for each plant species listed in Appendix A. Appendix C lists the emissions factors for the discrete monoterpene chemical compounds and BCO for each plant species listed in Appendix A.

Though BEIS3 has been formulated to estimate BNO from soils, the BEIS3 formulation uses only the "agricultural soils" BNO model described by Williams et al., (1992). BEIS3 does not utilize the BNO formulations for grassland soils, forest soils, wetland soils, or "other agricultural soils" that are also discussed by Williams et al., (1992).

As identified in Table 3-1, BEIS3 is not formulated to estimate methane from any biogenic source sector including:

- Wetlands – under anaerobic conditions, methane is released due to the bacterial remineralization of labile organic matter (IPCC, 1995, 2000);
- Termites – in their digestive tracts, methane is produced during the breakdown of cellulose by symbiotic microorganisms (Seiler et al., 1984; Fraser et al., 1986); and
- Naturally occurring combustion of biomass – methane is released as a by-product of incomplete combustion (UNEP, 1999).

Under international protocol, the following biogenic source sectors are classified as anthropogenic due to the human management of the root plant or animal species and are not included in BEIS3 (IPCC, 1994, 1995, 2000):

- Enteric fermentation (commonly known as belching cows) – methane is produced in the intestines of domesticated species such as cattle and sheep as a result of digestive processes under anaerobic conditions (Johnson et al., 1994; Moss et al., 1994; Johnson and Johnson, 1995); and
- Rice paddies – same process that produces methane from wetlands (van der Gon et al., 1999, 2000).

Further, BEIS3 is not formulated to estimate emissions of NMVOC, CO and NO_X that are released during the combustion of biomass.

BEIS3 Model Formulation

Numerous peer-reviewed papers have been written on the BVOC and BNO model formulations that are embedded in BEIS3 including most recently Lamb et al. (1999) and Guenther et al. (1999, 2000). All three papers provide more detailed information concerning the most recent biogenic emissions models. However, there has been some confusion generated as a result of the Lamb et al. (1999) study which identifies the model formulations therein as representative of the BEIS3 model formulations that are used by Pierce (2001a). Pierce (2001a) uses an earlier form of the model formulations reported in Lamb et al. (1999) and Guenther et al. (2000), more specifically those reported in Guenther et al. (1993), and the deviations in the models used by Pierce (2001a) are identified here.

Isoprene

Early studies (e.g. Tingey et al., 1979) showed that short-term variation in isoprene emissions from vegetative species were influenced by leaf temperature and the amount of PAR reaching the leaves. Isoprene is emitted only during daylight hours from specific deciduous species, such as oak (e.g. Anderson et al., 2000), willow (e.g. Isebrands et al., 1999), aspen (e.g. Baldocchi et al., 1999), and poplar (e.g. Isebrands et al., 1999), and only from spruce (Kempf et al., 1996) among coniferous species. Though the biochemical pathway is well known (Sharkey et al., 1991; Fall and Wildermuth, 1998), the reasons why plants emit isoprene are not well understood. Sharkey and Singaas (1995) suggest that isoprene is emitted as a thermal stress relief mechanism, whereas Guenther et al. (1993, 2000) suggest that isoprene emissions are related to chloroplast production, which are necessary for chlorophyll storage. Regardless, it appears that the ability to model isoprene emissions from vegetative species is relatively good (Lamb et al., 1996; Guenther et al., 1996; Fuentes et al., 1996; Baldocchi et al., 1995)

Pierce (2001a) uses a slightly modified form of the Guenther et al. (1993) formulations to estimate isoprene emissions based on leaf temperature and PAR (Eq. 3-1):

$$E = \xi \cdot E_s \cdot C_L^A \cdot C_T \cdot A \qquad \textbf{(3-1)}$$

where E ($\mu g \cdot hr^{-1}$) is the emissions rate of isoprene; ξ is the seasonal adjustment coefficient (ξ is one for the spring, summer, and fall or the "wintertime adjustment factor" identified in Appendix A); E_s ($\mu g \cdot ha^{-1} \cdot hr^{-1}$) is the species-specific emissions flux at 30°C and 1000 $\mu mol \cdot m^{-2} \cdot s^{-1}$ PAR (the biogenic emissions factors identified in Appendices A, B, and C); C_L^A is the environmental correction factor that accounts for changes in PAR as attenuated by the leaf; C_T is the environmental correction factor that accounts for changes in leaf temperature; and A (ha) is the areal extent of the species

However, Guenther et al. (1995, 1999, 2000) have refined their model to estimate isoprene emissions (Eq. 3-2):

$$E = \varepsilon \cdot D_P \cdot D_f \cdot \gamma_P \cdot \gamma_T \cdot \gamma_A \cdot \rho \cdot A \quad \textbf{(3-2)}$$

where ε is a landscape average emission capacity ($\mu g \cdot g \cdot hr^{-1}$); D_P is the annual peak foliar density (i.e. biomass) ($g \cdot ha^{-1}$); D_f is the fraction of foliage present at a particular time of year; the emission activity factors γ_P, γ_T, and γ_A account for the influence of photosynthetic photon flux density (PPFD), temperature, and leaf age, respectively; and ρ is the canopy escape efficiency that represents the fraction of emissions released into the above-canopy atmosphere.

$\varepsilon \cdot D_P$ in the Guenther et al. (2000) formulation is equivalent to E_s in BEIS3 (the biomass factors, ε, and biogenic emissions factors, E_s, in Appendices A, B, and C where $D_P = E_s / \varepsilon$); γ_T is equivalent to C_T; and γ_P is equivalent to C_L^A. However, though the parameters are equivalent, the formulation of the parameters may be slightly different. This leaves the Guenther et al. (2000) terms D_f, γ_A, and ρ unaccounted for in the Pierce (2001a) BEIS3 formulation.

Fraction Of Foliage (D_f)

Guenther et al. (2000) introduce D_f to account for changes in biomass as the plant progresses through its growing season. Guenther et al. (2000) indicate that D_f is both a function of time of year and forest type. Though D_f is excluded from the BEIS3 formulation, Pierce (2001a) includes a simple approach for capturing the seasonal change in biomass with the introduction of the seasonal adjustment factor, ξ. During the spring, summer, and fall, Pierce (2001a) assumes that the seasonal adjustment factor, ξ, is one. This treats the plant as if it exists under conditions of peak foliar density at all time during the spring, summer, and fall. During the winter, Pierce (2001a) assumes that for most plants, there is no biomass (i.e. ξ=0.0), and for a few plants, the biomass is one-half of (i.e. ξ=0.5) or equal to (i.e. ξ=1.0) to the peak foliar density. However, this is a very limited approximation of the seasonally changing biomass.

Though Guenther et al. (2000) indicate that D_f is both a function of time of year and forest type, GLOBEIS (Environ, 2001), a biogenic emissions model based on the work of Guenther et al. (1999), uses a lookup table based on geographic location to define D_f. It is unclear which approach (i.e. Guenther et al. [2000] or Environ [2001]) is better suited to model D_f, but either could be adapted for use in BEIS3. Because the assumption in the BEIS3 formulation is that plants emit as if they are at peak foliar density during the spring, summer and fall, from a qualitative perspective, the exclusion of D_f from the BEIS3 formulation likely results in higher predicted isoprene emissions. Yet the magnitude of this overestimate is unknown since no study has been conducted to examine this issue.

Leaf Age (γ_A)

The biogenic emissions estimation algorithm that is used by Pierce (2001a) (Eq. 1) accounts only for the environmental conditions that a leaf has been exposed to in the past hour. The modified algorithm (Eq. 3-2) accounts for the influence of the environmental conditions that a leaf has been exposed to in the past several weeks (γ_A). γ_A accounts for the findings of Guenther et al. (1991) and Monson et al. (1994) that showed disparate isoprene emissions rates between young and old leaves. Results from Monson et al. (1994), Geron et al. (1997), and Goldstein et al. (1998) suggest that isoprene emissions begin 650 growing degree-days after leaf-out. Therefore,

the onset of isoprene emissions can occur several days to several weeks after budbreak. Peak seasonal isoprene emissions occur after 1050 growing degree-days, oscillating with the rise and fall of temperature and PAR, and continue for on the order of 65 days (Goldstein et al., 1998). Thereafter, isoprene emissions decline to zero when temperatures fall below some minimum value or leaf death occurs (Goldstein et al., 1998).

Monson et al. (1994), Geron et al. (1997), Goldstein et al. (1998) and Lamb et al. (1999) use, or allude to, the term "heating degree-day." Technically, this is incorrect. The better term is "growing degree-day." Growing degree-day is defined as the amount of accumulated heat required for a plant to reach a certain stage of development (e.g. Griffith et al., 1997a, 1997b). This relationship holds true for most organisms if their growth and development is regulated by temperature (e.g., weeds, insects, pathogens) (e.g. Griffith et al., 1997a, 1997b). The basic concept is that development will only occur if the temperature exceeds some minimum developmental threshold, or base temperature (T_b). The base temperature is determined experimentally and is different for each plant (e.g. Griffith et al., 1997a, 1997b). However, in the case of isoprene emissions from plants, it appears that the community has agreed to a base temperature of 65°F for all plant species (Lamb et al. 1999). The number of growing degree-days is the day-to-day accumulated difference between the average temperature for the day (T_a $=[T_{max}+T_{min}]/2$ where T_{max} is the maximum observed temperature and T_{min} is the minimum observed temperature for a day) and T_b for T_a greater than T_b. For days where T_a is less than T_b, no growing degree-days are accumulated. The use of the minimum and maximum temperature for a given day to compute the average daily temperature for use in estimating the "growing degree-day" appears to be historical. The concept of "growing degree-day" was meant to be an aide to the agricultural community for use in determining when to plant crops. Because it was thought that hourly temperatures would not be routinely available to farmers, it appears that the simpler measure of average daily temperature (i.e. $=[T_{max}+T_{min}]/2$) would be a more accessible quantity to compute. The growing degree-days are accumulated starting from January 1 and continue through the end of the year.

Guenther et al. (1999) suggest that the effects of leaf age can be modeled as a function of D_f(Eq. 3-3).

$$\gamma_A = a_1 \cdot \frac{\left|D_f^i - D_f^{i-1}\right|}{MAX(D_f^i, D_f^{i-1})} + a_2 \cdot \left(1 - \frac{\left|D_f^i - D_f^{i-1}\right|}{MAX(D_f^i, D_f^{i-1})}\right) \qquad \textbf{(3-3)}$$

where $a_1 = 0.33$ and is the average of the emissions activity of young and old leaves; $a_2 = 0.95$ and is the fraction of mature foliage present during the month of peak foliar density; and D_f^i and D_f^{i-1} are the fraction of peak foliar densities present for the current month and the previous month respectively. Guenther et al. (1999) expect the coefficients a_1 and a_2 to change with landscape type but have no data to develop such relationships. The model is based on the assumption that increasing D_f indicates the presence of a greater proportion of younger leaves and decreasing D_f indicates the greater proportion of older leaves. Given that D_f ranges from zero to one, the maximum value for γ_A in Eq. 3-3 is 0.95 and occurs during periods of peak foliar density. Because the assumption in the BEIS3 formulation is that plants emit as if they are at

peak foliar density, from a qualitative perspective, the exclusion of γ_A from the BEIS3 formulation results in slightly higher predicted isoprene emissions. Though periods other than those of peak foliar density occur, the magnitude of this overprediction is not known since no study has been conducted to examine this issue.

Canopy Escape Efficiency (ρ)

ρ is used to account for discrepancies between observed emissions rates at the leaf-level and measured above-canopy flux rates with the former typically being higher. Guenther et al. (1999) rigorously model ρ as a function of canopy ventilation rate and isoprene deposition rate based on the work of Jacob and Bakwin (1991). They assume that the canopy ventilation rate is proportional to the mean wind speed within the canopy. They base the isoprene deposition rate on observations of microbial consumption of isoprene in soils reported by Cleveland and Yavitt (1997). In contrast, Guenther et al. (2000) assign a default value of 0.95 to ρ due to a lack of BVOC deposition or canopy loss data. Regardless, in both Guenther et al. (1999) and Guenther et al. (2000), they conclude that their isoprene model performance (i.e. comparison of observed to predicted isoprene emissions) is acceptable. Because there is no information in the literature that contrasts these two approaches against the same data set, it is unclear which approach is a better physical description. However, exclusion of ρ from the BEIS3 formulation results in an overestimate of predicted isoprene emissions, but the magnitude of the overestimate is unknown since no study has been conducted to examine this issue. Incorporation of a constant, such as that used by Guenther et al (2000), into the BEIS3 framework is relatively straightforward.

Light Correction Factor (C_L and γ_P)

Pierce (2001a) follows the formulation of Guenther et al. (1993) to estimate the light correction factor in BEIS3 (Eq. 3-4).

$$\gamma_P = C_L = \frac{\alpha \cdot c_{L1} \cdot L}{\sqrt{1 + \alpha^2 \cdot L^2}} \qquad \textbf{(3-4)}$$

where $\alpha = 0.0027$ and $c_{L1} = 1.066$ are empirical coefficients; and L is the PAR flux rate ($\mu mol \cdot m^{-2} \cdot s^{-1}$). Guenther et al. (1993) explain the derivation of the terms in Eq. 3-4. The response of the light correction factor is shown in Figure 4-1 and is based on $\alpha = 0.0027$ and $c_{L1} = 1.06$, as reported in Guenther et al., (1993). As shown in Figure 4-1, the light correction factor exhibits a nearly linear response through very low-light conditions, approximately 0 to 500 $umol \cdot m^{-2} \cdot s^{-1}$. From approximately 500 to 1000 $\mu mol \cdot m^{-2} \cdot s^{-1}$, conditions of low to moderate light, Eq. 3-4 sub-linearly transitions to an almost constant value and remains so through the solar spectra of interest. The structure of Eq. 3-4 is similar to that used to model the dependence of photosynthesis on light (e.g. Harley and Tenhunen, 1991). Also, Figure 3-1 shows the solar constant in terms of PAR. That is, the solar constant is approximately 1370 $W \cdot m^{-2}$ (Duffie and Beckman, 1980). Roughly 45% to 50% of the total incoming solar radiation falls in the range of PAR, 400nm to 700nm (Chou 1990, 1992). Finally, conversion of PAR from energy terms to photon flux terms is done by applying a conversion factor of 4.6 (Pierce and Geron, 1996), which itself is subject to uncertainty. PAR can be expressed in energy terms (i.e. $W \cdot m^{-2}$) and in photon terms (i.e., $\mu mol \cdot m^{-2} \cdot s^{-1}$). In energy terms, PAR is expressed as PAR irradiance, which is

the total energy in the PAR range (400 nm to 700 nm). When measured in photon terms, PAR is also called Photosynthetic Photon Flux Density (PPFD), which is a measure of the number of photons in the 400 nm to 700 nm waveband that are incident per unit time on a unit surface. When expressed in photon terms, all the photons are considered equal, independent of their energy. The quantity of photons is measured in moles of photons (1 mole of photons = $6.022 \cdot 10^{23}$ photons). Since a photon carries energy that is inversely proportional to its wavelength, it is necessary to integrate the PPFD across the PAR waveband to accurately compute PAR in energy terms. PAR in terms of photon terms is used due to the dependence of photosynthesis and related processes on specific wavelengths of light in the 400 nm to 700 nm spectra and not on the total energy available in the spectra.

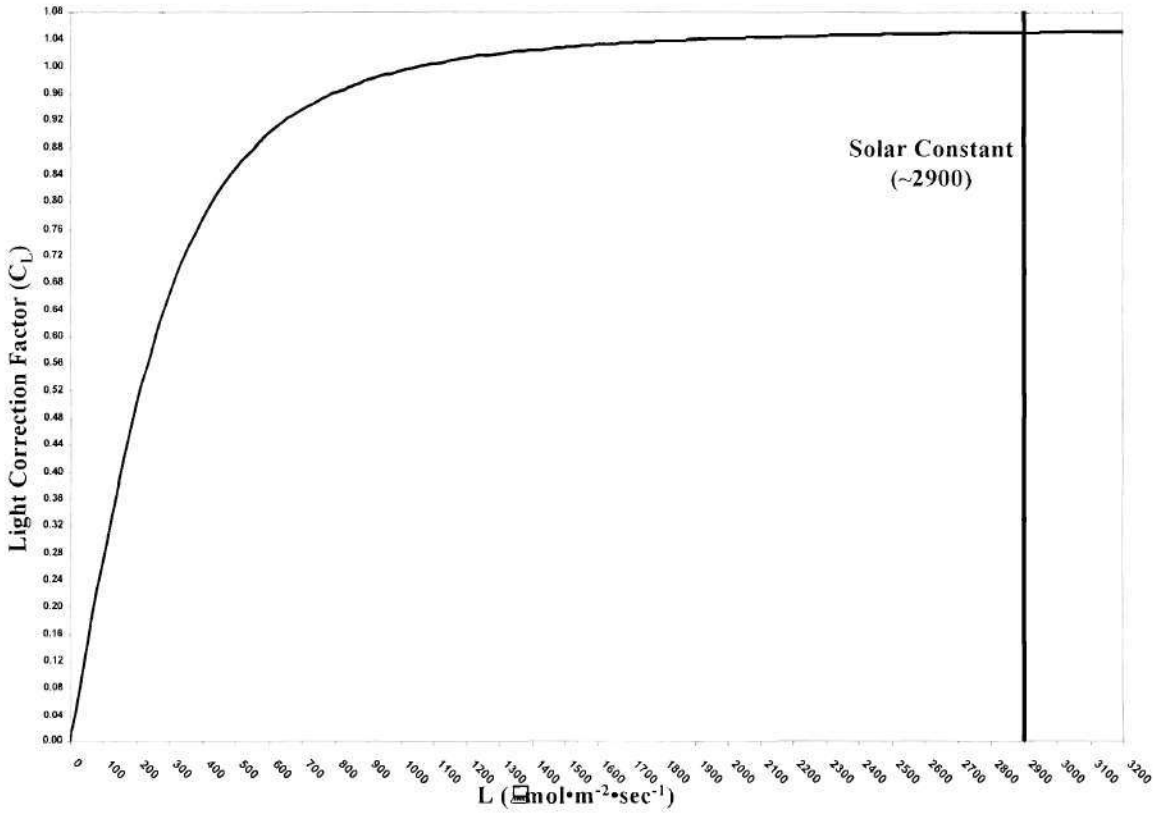

Figure 3-1.
Isoprene light correction factor as a function of PAR defined by Equation 3-4. The solar constant in the PAR spectrum (~2900 μmol·m^{-2}·s^{-1}) is also identified.

Though Pierce (2001a) treats α and c_{L1} as did Guenther et al. (1993, 1995), Harley et al. (1996, 1997) have shown that the empirical coefficients α and c_{L1} vary with past PAR levels experienced by the leaf. Therefore, Guenther et al. (1999) updated the formulation of α (Eq. 3-5) and c_{L1} (Eq. 3-6) to account for variations in these coefficients as a function of LAI.

$$\alpha = 0.001 + 0.00085 \cdot LAI \quad \textbf{(3-5)}$$

$$c_{L1} = 1.42 \cdot \exp(-0.31 \cdot LAI) \quad \textbf{(3-6)}$$

Incorporation of these additional extensions results in a light correction factor of about one for PAR of 1000 $\mu mol \cdot m^{-2} \cdot s^{-1}$ and LAI depth of less that 0.5 (i.e. near the top of the canopy). For a leaf in the lower canopy (i.e. LAI depth greater than five) and PAR of 1000 $\mu mol \cdot m^{-2} \cdot s^{-1}$, the light correction factor is less than 0.30 (Guenther et al., 1999). Because these extensions are missing from the Pierce (2001a) formulation, BEIS3 is likely to slightly overestimate isoprene emissions. The magnitude of this overestimate, however, is unknown since no study has been conducted to examine this issue. Incorporation of these extensions into BEIS3 is relatively straightforward.

Temperature Correction Factor (C_T and γ_T)

Pierce (2001a) follows the formulation of Guenther et al. (1993) to estimate the temperature correction factor in BEIS3 (Eq. 3-7).

$$C_T = \frac{\exp\left(\frac{c_{T1} \cdot (T - T_S)}{R \cdot T_S \cdot T}\right)}{1 + \exp\left(\frac{c_{T2} \cdot (T - T_M)}{R \cdot T_S \cdot T}\right)} \qquad \textbf{(3-7)}$$

where $c_{T1} = 95000$ $J \cdot mol^{-1}$, $c_{T2} = 230000$ $J \cdot mol^{-1}$, and $T_M = 314$ are empirical coefficients; R is the ideal gas constant (8.314 $J \cdot K^{-1} \cdot mol^{-1}$); T_S is the normalizing temperature (303 K); and T is the leaf temperature which is taken to be the ambient temperature (K). Guenther et al. (1993) explain the derivation of the terms in Eq. 3-7. The response of the temperature correction factor is shown in Figure 3-2. The temperature correction factor is relatively small for temperatures below about 16°C but rapidly increases thereafter peaking about 39°C and then rapidly declining. The form of Eq. 3-7 has been used to simulate the temperature response of enzymatic activity (e.g. Johnson et al., 1942; Sharpe and DeMichelle, 1977).

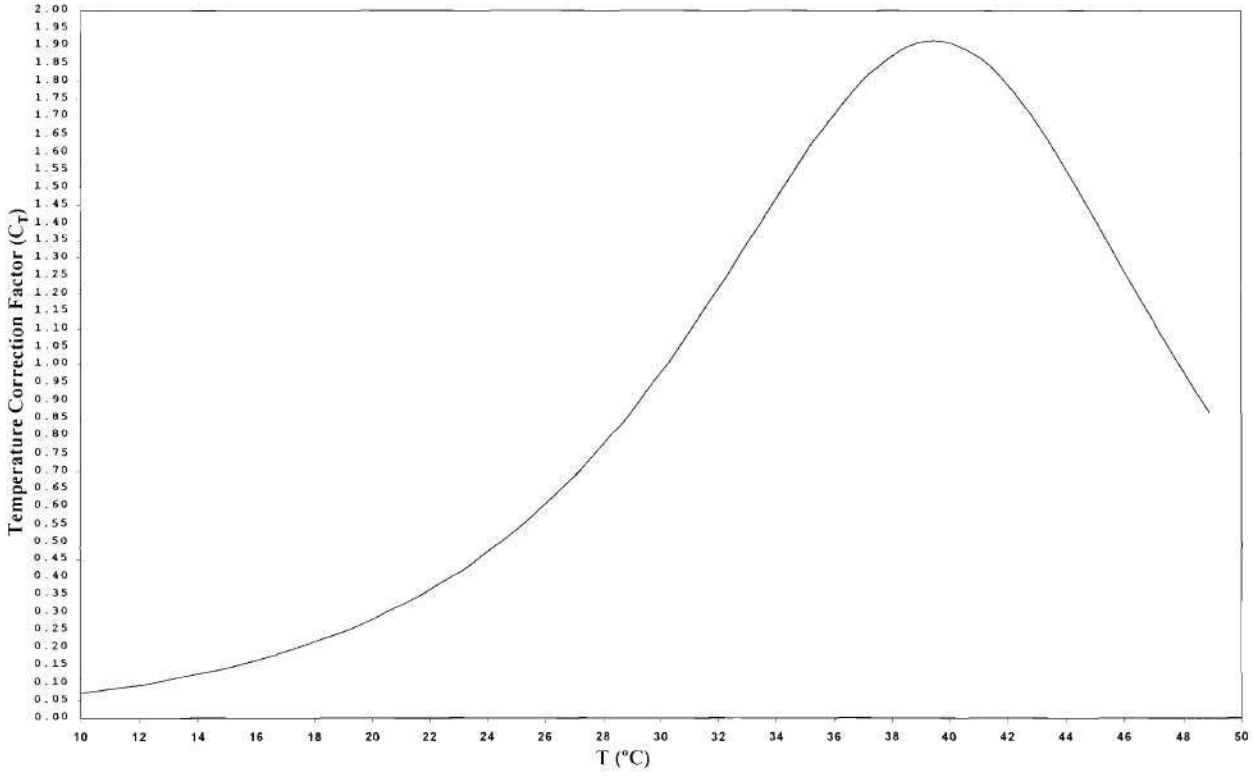

Figure 3-2.
Isoprene temperature correction factor as a function of ambient temperature defined by Equation 3-7.

Guenther et al. (1999) updated the temperature correction formulation to account for findings by Sharkey et al. (1999) that the temperature correction factor is dependent on temperatures during the past several days (Eq. 3-8).

$$\gamma_T = \frac{E_{opt} \cdot c_{T2} \cdot \exp\left(\frac{c_{T1}}{R}\left[\frac{1}{T_{opt}} - \frac{1}{T}\right]\right)}{\left(c_{T2} - c_{T1}\right)\left(1 - \exp\left(\frac{c_{T2}}{R}\left[\frac{1}{T_{opt}} - \frac{1}{T}\right]\right)\right)} \qquad \textbf{(3-8)}$$

where $E_{opt} = 1.9 \cdot \exp(0.125[T_d - 301])$ and $T_{opt} = 312.5 + 0.5(T_d - 301)$ are empirical coefficients; and T_d is the mean temperature of the last fifteen days (K). Guenther et al (1999) show that for values of $E_{opt} = 1.9$ and $T_{opt} = 312.5$, Eq. 3-8 is almost identical to Eq. 3-7. Also, though Guenther et al. (1999) suggest a lapse period of fifteen days, Sharkey et al. (1999) and Lamb et al. (1999) suggest that this period may be from eighteen hours to several weeks. It is unclear what the overall effect on the BEIS3 isoprene emissions estimates is due to the exclusion of the updated Guenther et al. (2000) temperature correction factor since the mean temperature of the prior fifteen days can vary considerable depending on the time of year. Further, incorporation of the revised formulation into the BEIS3 framework may be difficult given the requirement for fairly extensive prior knowledge of temperatures.

Canopy Adjusted PAR (C_L^A)

In BEIS3, C_L^A is computed via a canopy model that accounts for the effects of PAR as it penetrates the leaf canopy (Pierce, 2001a). The canopy model in BEIS3, which is a function of LAI and is based on a leaf energy balance, is a modified form of that used in BEIS (Pierce and Waldruff, 1991) and better accounts for visible and near-infrared scattered, direct, and diffuse radiation on both sunlit and shaded leaves. C_L^A differs from γ_P in that the PAR used in C_L^A is adjusted via a leaf energy balance as PAR migrates through the canopy. The application of γ_P assumes that whatever the PAR is at the top of the canopy is the PAR that is experienced by all leaves within the canopy. Pierce (2001a) computes the canopy adjusted PAR for the sunlit and shaded leaves based on the work of Campbell and Norman (1998) (Eq. 3-9).

$$C_L^A = L_S^f \cdot C_L\left(L = PAR_S\right) + L_D^f \cdot C_L\left(L = PAR_D\right) \quad \textbf{(3-9)}$$

where L_S^f is the fraction of sunlit leaves defined by Eq. 3-10; L_D^f is the fraction of shaded leaves defined by Eq. 3-11; PAR_D is the amount of PAR on the shaded leaves defined by Eq. 3-16 ($\mu mol \cdot m^{-2} \cdot s^{-1}$); PAR_S is the amount of PAR on the sunlit leaves defined by Eq. 3-17 ($\mu mol \cdot m^{-2} \cdot s^{-1}$); and C_L is the light correction factor defined by Eq. 3-4.

$$L_S^f = \frac{1 - \exp(-K \cdot LAI)}{K \cdot LAI} \quad \textbf{(3-10)}$$

$$L_D^f = 1 - L_S^f \quad \textbf{(3-11)}$$

where K is the direct beam solar radiation extinction coefficient defined by Eq. 3-12.

$$K = \frac{\sqrt{1 + [\tan(\theta)]^2}}{2} \quad \textbf{(3-12)}$$

where θ is the solar zenith angle. Pierce (2001a) computes the solar zenith angle from Eq. 3-13 (Duffie and Beckman, 1980).

$$\theta = a\cos\left(\delta_s \cdot \sin\left(\frac{\pi\phi}{180}\right) + \sqrt{1.0 - \delta_s^2} \cdot \cos\left(\frac{\pi\phi}{180}\right) \cdot \cos\left(\frac{15\pi}{180}\left| t + \frac{\lambda}{15} - 0.123470\sin\left(t_r\right) + 0.004289\cos\left(t_r\right) - 0.153809\sin\left(t_r + t_r\right) - 0.060783\sin\left(t_r + t_r\right) - 12\right|\right)\right) \quad \textbf{(3-13)}$$

where ϕ is the latitude (°); λ is the longitude (°); t is local time converted to Greenwich Mean Time (hours); t_r is the terrestrial rotation angle (rad) defined by Eq. 3-14; and δ_s is a parameter of the earth's declination to the solar plane defined by Eq. 3-15.

$$t_r = \frac{\pi \Omega t}{180} \quad \textbf{(3-14)}$$

$$\delta_s = \sin\left(\frac{\pi\delta}{180}\right)\cdot\sin\left(t_r + \frac{\pi}{180}\left[\begin{array}{rr} 279.9348 + 1.914827\sin(t_r) & -0.079525\cos(t_r)+ \\ 0.019938\sin(t_r + t_r) & -0.00162\cos(t_r + t_r)\end{array}\right]\right) \quad \textbf{(3-15)}$$

where Ω is the fraction of complete rotation per day (360/365.242); and δ is the earth's declination to the solar plane (23.443833°). Please note that though the formulation of Eq. 3-15 takes into account the time of day, it does not take into account the day of the year. Instead Eq. 3-15 treats radiation reaching the earth as if every day were the summer solstice in the northern hemisphere. To account for day of year, the first term in Eq. 3-15 should read $\sin\left(\frac{\pi\delta}{180}\sin\left[\frac{\pi}{180}\left(360\frac{284+n}{365}\right)\right]\right)$ (Duffie, 1980) where n is the julian day of the year (i.e. 1 to 365). By excluding the effect of the day of the year, BEIS3 will overestimate the amount of radiation reaching the canopy resulting in an overestimate of the isoprene emissions. Though the overestimate will be small during much of the summer, it will be noticeably large during winter days.

The PAR for shaded leaves is computed via Eq. 3-16, and the PAR for sunlit leaves is computed via Eq. 3-17.

$$PAR_D = \frac{PAR_d\left[1-\exp(-0.61\cdot LAI)\right]}{0.61\cdot LAI} + \frac{PAR_b\left[\exp(-0.894\cdot LAI)-\exp(-K\cdot LAI)\right]}{2} \quad \textbf{(3-16)}$$

$$PAR_S = K\cdot\left(PAR_b + PAR_d\right)\cdot PAR_D \quad \textbf{(3-17)}$$

where PAR_d is the amount of PAR from diffuse visible solar radiation defined by Eq. 3-18 ($\mu mol\cdot m^{-2}\cdot s^{-1}$); and PAR_b is the amount of PAR from direct beam, visible radiation defined by Eq. 3-19 ($\mu mol\cdot m^{-2}\cdot s^{-1}$).

$$PAR_b = I_r\cdot I_c^v\cdot I_b^v\cdot f \quad \textbf{(3-18)}$$

$$PAR_d = I_r\cdot I_c^v\cdot I_d^v\cdot f \quad \textbf{(3-19)}$$

where I_r is the ratio of the observed, or modeled, solar radiation to the clear sky total solar radiation defined by Eq. 3-26; I_b^v is the fraction of visible solar radiation that is from direct beam solar radiation defined by Eq. 3-20; I_d^v is the fraction of visible solar radiation that is from diffuse beam solar radiation defined by Eq. 3-21; I_c^v is the clear sky total visible solar radiation defined by Eq. 3-22 ($W\cdot m^{-2}$); and $f = 4.6$ is an empirical factor that converts solar radiation in terms of energy (i.e. $W\cdot m^{-2}$) to solar radiation in terms of photon flux (i.e. $\mu mol\cdot m^{-2}\cdot s^{-1}$).

$$I_b^v = \begin{cases} 0.009550 \dfrac{I_{cb}^v}{I_c^v} & for\ I_r \le 0.21 \\ \left(1.0 - \left(\dfrac{0.9 - I_r}{0.7}\right)^{2/3}\right) \dfrac{I_{cb}^v}{I_c^v} & for\ 0.21 < I_r < 0.89 \\ 0.941124 \dfrac{I_{cb}^v}{I_c^v} & for\ I_r \ge 0.89 \end{cases} \quad \textbf{(3-20)}$$

$$I_d^v = 1 - I_b^v \quad \textbf{(3-21)}$$

$$I_c^v = I_{cb}^v + I_{cd}^v \quad \textbf{(3-22)}$$

where I_{cb}^v is the clear sky, direct beam visible solar radiation defined by Eq. 3-23 ($W \cdot m^{-2}$); and I_{cd}^v is the clear sky, diffuse visible solar radiation defined by Eq. 3-24 ($W \cdot m^{-2}$).

$$I_{cb}^v = 600 \cdot \exp(-0.185m) \cdot \cos(\theta) \quad \textbf{(3-23)}$$

$$I_{cd}^v = 0.42 \cdot (600 - I_{cb}^v) \cdot \cos(\theta) \quad \textbf{(3-24)}$$

where m is the atmospheric optical thickness defined by Eq. 3-25.

$$m = \frac{P}{P_o \cdot \cos(\theta)} \quad \textbf{(3-25)}$$

where P is the observed pressure (mb); and P_o is standard pressure (1013.25 mb).

$$I_r = \frac{I}{I_c} \quad \textbf{(3-26)}$$

where I is the observed, or modeled incoming solar radiation; and I_c is the clear sky total solar radiation defined by Eq. 3-27 ($W \cdot m^{-2}$)

$$I_c = I_{cb}^i + I_{cd}^i + I_{cb}^v + I_{cd}^v \quad \textbf{(3-27)}$$

where I_{cb}^i is the clear sky, direct beam near-infrared solar radiation defined by Eq. 3-28 ($W \cdot m^{-2}$); and I_{cd}^i is the clear sky, diffuse near-infrared solar radiation defined by Eq. 3-29 ($W \cdot m^{-2}$).

$$I_{cb}^i = (720 \cdot \exp(-0.06m) - \omega) \cdot \cos(\theta) \quad \textbf{(3-28)}$$

$$I_{cd}^i = 0.65 \cdot (720 - \omega - I_{cb}^i) \cdot \cos(\theta) \quad \textbf{(3-29)}$$

where ω is absorption by water of solar radiation in the near-infrared spectrum defined by Eq. 3-30 ($W \cdot m^{-2}$).

$$\omega = 101.64 \cdot (2m)^{0.3} \quad \textbf{(3-30)}$$

Though Pierce (2001a) accounts for canopy attenuation of PAR, there is still some debate in the literature about how best to account for canopy effects not only for PAR but also for temperature (Lamb et al. [1999 – Chapter 2] summarizes the issues surrounding the debate). It is well known that discrepancies exist between the typically higher measured leaf-level isoprene emissions and lower measured above-canopy isoprene emissions. Even with the application of isoprene canopy escape efficiency, ρ, coupled with a canopy attenuation model (Goudriaan and van Laar, 1994), in a modified version of the GLOBEIS (Environ, 2001), that is more rigorous than that used by Pierce (2001a), Guenther et al. (1999) did not seem to necessarily improve isoprene model performance. Therefore, it seems that our knowledge of canopy effects is still incomplete and requires further investigation so that these effects can be better modeled.

Monoterpenes

Early studies show that short-term variation in terpenoid emissions from vegetative species was influenced by leaf temperature and relative humidity (e.g. Dement et al., 1975) as well as foliar moisture (Lamb et al., 1985; Schade et al., 1999) and to some degree, solar radiation (Steinbrecher et al., 1988). However, unlike isoprene emissions, no seasonal effects have been clearly established for monoterpene emissions (Lamb et al., 1999). Also, though the dependence of monoterpene emissions on solar radiation has been established, no quantitative description of this dependency appears to exist (Guenther et al., 1993). On the other hand, Schade et al. (1999) propose a model to account for humidity effects on monoterpene though this model has not been incorporated into BEIS3. Monoterpene emissions occur from coniferous species (Guenther et al., 1994) and some deciduous species (Keiser, 1997). However, the specific terpenoid species are not necessarily well characterized (Lamb et al., 1999). In fact, almost all studies report monoterpene emissions in terms of a small number of predominant compounds, typically α-pinene, β-pinene, limonene, and Δ^3-carene, along with a larger number of terpenes present only in trace amounts. Hence, many terpenoid species have been identified from plant species, but their biogenic emissions capacities for the chemical species are not well known (Lamb et al., 1999). The biochemical pathway for monoterpene production in needles is relatively well understood (Croteau, 1987), and it appears to be used in both tissue defense and chloroplast production (Guenther et al., 2000). Due to their temperature dependence, terpene emissions from vegetation follow a diurnal pattern with low emissions at night, increasing emissions during the day to a mid-afternoon maximum, and returning to low emissions rates in the late evening (Lamb et al., 1999). Further, because of the storage pools that exist in the needles, wounding of the needle, either due to mechanical stress or herbivory, can lead to large increases in the monoterpene emission rate (Lamb et al., 1999). Again, unlike isoprene, there have been few canopy-scale flux studies of terpene emissions suitable for use in model performance evaluation. Therefore, it is difficult to determine how well the BEIS family of models performs with respect to observed monoterpene emissions rates.

Pierce (2001a) follows the recommendation of Guenther et al. (1993) to estimate monoterpene emissions (Eq. 3-31).

$$E = \xi \cdot E_s \cdot A \cdot C_T \quad \textbf{(3-31)}$$

C_T is estimated based on leaf temperature, which is taken to be ambient temperature (Eq. 3-32).

$$C_T = \exp(\beta[T - T_S]) \quad \textbf{(3-32)}$$

where $\beta = 0.09\ K^{-1}$ is the empirical coefficient that establishes the temperature dependence of the emissions rate. The response of the temperature correction factor is shown in Figure 3-3. Unlike the isoprene temperature correction factor, the monoterpene and OVOC temperature correction factor does not exhibit a "break over" point where emissions are predicted to decline with increasing temperature. Instead, monoterpene and OVOC emissions are predicted to monotonically increase with increasing temperature until plant death at which time emissions rapidly drop to zero. Guenther et al. (1993) report that some variation exists in β, which may be due to such factors as leaf-to-leaf and seasonal emissions rate variability, different vapor pressure and solubilities for the monoterpenes, different chemical storage and emissions pathways, and experimental error. The form of Equation 3-32 appears to be based purely on a statistical fit of the measured emissions rate data (i.e. it appears to have little or no basis to any biological process).

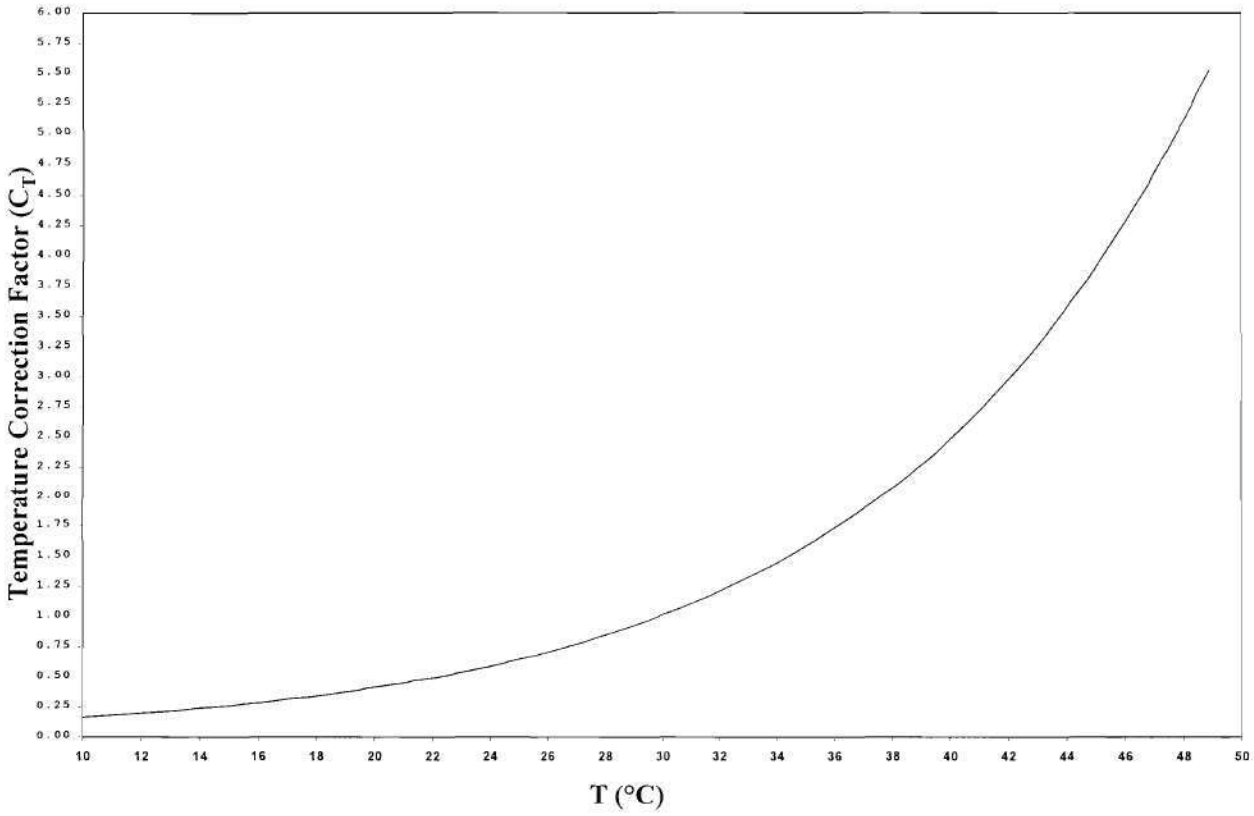

Figure 3-3.
Monoterpene and OVOC temperature correction factor as a function of ambient temperature defined by Equation 3-32.

Much like the isoprene formulation, BEIS3 does not account for the effects of leaf age (γ_A) and seasonal changes in foliar density (D_f) on monoterpene emissions estimates. Guenther et al.

(2000) suggest that it is appropriate to add these terms to the monoterpene formulation, and given the BEIS3 framework, these changes are relatively easy to implement. Further, the BEIS3 monterpene formulation does not account for solar radiation (γ_P) and canopy escape efficiency (ρ) though there is no recent evidence to support such dependencies nor is there evidence to support the attenuation of monoterpene emissions from the leaf canopy similar to what is done for isoprene. Also, as stated earlier, the effects of short-term changes in humidity on monoterpene emissions are not accommodated in BEIS3 (Schade et al., 1999). Finally, Guenther et al. (2000) model the monoterpenes that are related to chloroplast production using the isoprene formulation. Because BEIS3 excludes these environmental factors, BEIS3 is likely to overestimate monoterpene emissions. It is unclear, however, what the magnitude of the emissions change is for those monoterpenes modeled using the isoprene formulation since no study reports this comparison.

Oxygenated And Other Biogenic VOCs

It is well known that a wide variety of oxygenated and other BVOCs, which are collectively named OVOC, are emitted from vegetation including 2-methyl-3-buten-2-ol (MBO), a variety of hexene compounds, aldehydes, alcohols, ketones, and organic acids (e.g. Kesselmeier et al., 1997; Kirstine et al., 1998; MacDonald and Fall, 1993; Winer et al., 1992; Gabriel et al., 1999). While MBO is released from pines via a chloroplast mechanism (Guenther et al., 1999) and has similar environmental dependencies to isoprene (Goldan et al., 1993; Harley et al., 1998), most of the OVOCs appear to be emitted as defense mechanisms (Lamb et al., 1999). The hexene compounds have antibiotic properties (Croft et al., 1993) and are released as a result of plant damage through mechanical stress (de Gouw et al., 1999), infection, or herbivory (Lamb et al., 1999). However, Lamb et al. (1999) imply that though these emissions can be quite large, quantitative methods to estimate OVOC emissions from such plant damage is limited and requires further work before they can be included in regional inventory development efforts. In situations where plant damage is not apparent, other OVOCs are emitted as well, sometimes in large quantities, but typically in lower quantities when compared to visibly damaged plants.

Pierce (2001a) uses the monoterpene formulation (Eq. 3-31) to estimate BVOC emissions. Except for MBO, this approach is the same as that used by Guenther et al. (1999, 2000) with the caveats that accompany the monoterpene formulation noted in the previous section. For MBO, Guenther et al. (2000) use the isoprene formulation to estimate emissions of this species. It is unclear what direction the predicted magnitude of the MBO emissions estimate will take using the isoprene formulation in-lieu of the monoterpene formulation since no studies have reported such a comparison.

Biogenic Nitric Oxide

BNO is emitted as a result of microbial nitrification-denitrification activities in soil and is enhanced through such practices as nitrogen-based fertilizer application (Williams et al, 1992), stubble burning (Levine, 1990), and soil tilling (Civerolo and Dickerson, 1998). Soil NO emissions are dependent on both long-term and short-term environmental conditions. Potter et al. (1996) include the following as long-term conditions that impact soil NO emissions: soil texture, organic matter content, soil pH, and nitrate levels; and the following as short-term conditions:

soil temperature and water-filled pore space. The primary means for developing NO emission factors from soils has been through measurements with static or dynamic chambers (Williams et al., 1992; Thornton et al. 1997); however, Parrish et al. (1987) express concern over the results derived from such techniques since it is unclear whether the chamber measurements represent a true NO_X (NO + NO_2) flux from the soil to the atmosphere, and there exist concerns about extrapolating the flux results from small field studies to regional-scale fluxes. Soil NO emissions factors range over two orders magnitudes or more (Williams et al., 1992; Yienger and Levy, 1995; Davidson and Kingerlee, 1997). In general, wetlands and tundra have very low soil NO emissions, forests have moderate soil NO emissions, and agricultural and grasslands have the highest soil NO emission rates.

Pierce (2001a) uses the empirical model of Williams et al. (1992) to model NO emissions from soils (Eq. 3-32).

$$E = E_s \cdot A \cdot C_T \tag{3-33}$$

C_T is estimated based on soil temperature (Eq. 3-34).

$$C_T = \exp(T_3[T_{soil} - 30]) \tag{3-34}$$

where $T_3 = 0.071°C^{-1}$ is an empirical parameter that relates soil temperature to BNO emissions; and T_{soil} is the soil temperature (°C) as determined by Eq. 3-35.

$$T_{soil} = T_1(T - 273.15) + T_2 \tag{3-35}$$

where $T_1 = 0.72$ and $T_2 = 5.8°C$ are empirical parameters that relate soil temperature to ambient temperature. The response of the temperature correction factor is shown in Figure 3-4. As with the monoterpene and OVOC temperature correction factor, the BNO temperature correction factor also exhibits an increasing monotonic structure with increasing temperature. BNO emissions are based on the soil temperature (Williams et al., 1992). Because soil temperatures are not readily available in most air quality modeling studies, Williams et al. (1992) based the soil temperature on land use classification. Williams et al. (1992) applied a linear least squares fit between ambient and soil temperatures for agricultural, grassland, wetland, and forest areas.

In BEIS3, Pierce (2001a) uses only the agricultural-corn formulation to model soil temperature for all species. Pierce (2001a) does not use the grasslands, forests, wetlands, or agricultural-other soil temperature models of Williams et al. (1992) in the BEIS3 formulation. Table 3-2 shows the soil model parameters for each land use category identified by Williams et al. (1992). Pierce (2001b) states that the use of only the agricultural soils model results in only a small deviation from the results produced when the other soils models are rigorously applied. Though this is likely true when the emissions are considered on a domain wide basis, use of the different soils models may result in widely varying BNO emissions estimates at a more local scale. This, in turn, may have greater consequences for air quality model predictions at the local scale. However, no studies have been conducted to determine what the impact of using the various BNO soils models are on emissions estimates or predicted air quality at local or regional scales.

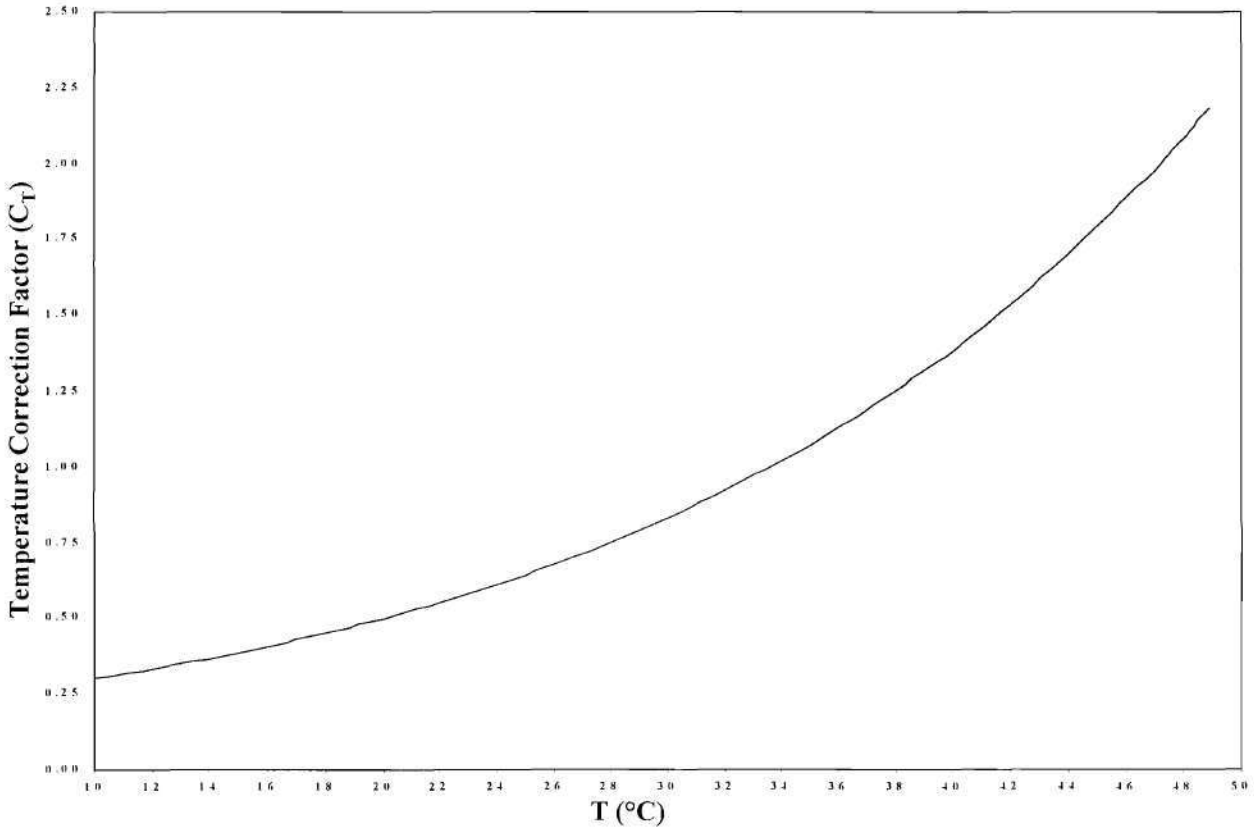

Figure 3-4.
Nitric oxide temperature correction factor as a function of ambient temperature defined by Equation 3-34.

Table 3-2.
Biogenic NO soil model parameters from Williams et al. (1992).

Soil Model	Soil Model Parameters (Eq. 33)	
	T_1	T_2
Agricultural-corn	0.72	5.8
Agricultural-other	1.03	2.9
Grasslands	0.66	8.8
Forests	0.84	3.6

4
CHAPTER 4

SAMPLING APPROACH

There are two types of BEIS3 information that were sampled in the current study: model parameters and model data inputs. The model parameters refer to the variables that are specific to the BEIS3 formulation. The model parameters are temporally and spatially invariant. The model data inputs refer to the variables that are required to drive the BEIS3 formulation in order for BEIS3 to estimate the biogenic emissions. The meteorological-specific model data inputs vary in both time and space, whereas, the plant species-specific model data inputs are temporally and spatially invariant.

Table 4-1 summarizes the BEIS3 model parameters and model data inputs that were treated as uncertain. The model parameters are identified as the "BVOC Model Parameters" and the "BNO Model Parameters." The model data inputs are identified as the "Biogenic Emissions Factors," the "Leaf Area Index," the "Ambient Temperature," and the "Photosynthetically Active Radiation." Each parameter is listed with its mean value, its uncertainty range, the type of distribution from which samples were drawn, an indicator as to the parameter's variability, and the pollutants that the parameter affects. Also, Table 4-1 indicates the references from which the uncertainty values were derived.

Table 4-1
Summary of uncertain BEIS3 parameters.

Parameter	Mean	Uncertainty	Distribution	Variability[4]	Pollutants[5]
BVOC Model Parameters (Guenther, 1995, 1997)					
α	0.0027	0.0015 (1 σ)	Lognormal	SI, TI, PI	I
C_{L1}	1.06	0.2 (1 σ)	Normal	SI, TI, PI	I
C_{T1}	95,000	20,000 (1 σ)	Lognormal	SI, TI, PI	I
C_{T2}	230,000	150,000 (1 σ)	Lognormal	SI, TI, PI	I
T_M	314	3 (1 σ)	Normal	SI, TI, PI	I
β	0.09	0.02 (1 σ)	Lognormal	SI, TI, PI	T, O
BNO Model Parameters (Williams et al., 1992; Williams, 1997)					

Parameter	Mean	Uncertainty	Distribution	Variability[4]	Pollutants[5]
T_3	0.071	0.007 (1 σ)	Normal	SI, TI, PI	N
T_2	5.8	2.9 (1 σ)	Lognormal	SI, TI, P[6]	N
T_1	0.72	0.36 (1 σ)	Lognormal	SI, TI, P[6]	N
Biogenic Emissions Factors (Guenther, 1995, 1997; Pierce, 1996)					
E_S	(1)	±50% (95% CI)	Normal	SI, TI, P	I, T, O, N
Leaf Area Index (Pierce, 2001a)					
LAI (summer)	(2)	±25% (95% CI)	Normal	SI, T, P	I
LAI (spring/fall)	(2)	±2 units (95% CI)	Normal	SI, T, P	I
Ambient Temperature (Tesche, 2001)					
T	(3)	1.9 (1 σ)	Normal	S, T, PI	I, T, O, N
Photosynthetically Active Radiation (Pierce, 2001b)					
L	(3)	±25% (95% CI)	Normal	S, T, PI	I

(1) Mean value is plant species-specific and pollutant-specific.
(2) Mean value is plant species-specific.
(3) Mean value is taken from spatially and temporally varying meteorological inputs.
(4) SI is spatially invariant; TI is temporally invariant; S is spatially variant; T is temporally variant; PI is plant-species invariant; and P is plant-species variant.
(5) I is isoprene; T is monoterpenes; O is OVOCs; and N is NO_X.
(6) Though these parameters are plant species-specific, only the agricultural parameters defined by Williams et al. (1992) are used in the BEIS3 formulation since Pierce (2001c) states that the use of only the agricultural model results in only a small deviation from the results produced when the other BNO models are rigorously applied.

Because no specific distributions were specified in the attendant references of Table 4-1, it was necessary to determine the types of distributions from which the samples were to be drawn. Morgan and Henrion (1990) suggest that a normal distribution can be used to represent the uncertainty in data as long as the coefficient of variation is less than 0.2. However, when the coefficient of variation is greater than 0.2, more care must be taken when drawing random samples from a normal distribution since there is a higher probability of sampling a negative value, which is inappropriate for the subject analysis. In cases where the coefficient of variation is greater than 0.2, say as a factor of two or more, or where quantities are constrained to being positive, Morgan and Henrion (1990) suggest using a lognormal distribution to represent the uncertainty in the data. For the current study, if the coefficient of variation was greater than 0.2, a lognormal distribution of the parameter was assumed. Otherwise, a normal distribution of the parameter was assumed. Though in the case of the normal distribution, if a negative sample was drawn, the sample was discarded and a new sample was drawn.

The Simple Random Sampling (SRS) technique (Morgan and Henrion, 1990) was used to draw one thousand samples from the assigned distributions of each model parameter that is listed in Table 4-1. The sampling software that was developed by Iman and Shortencarier (1984) was used to perform the sampling. Though the sampling software can accommodate correlation among variables, insufficient data were available to compute the correlation matrix. Therefore, in this analysis, the model parameters were treated independently for sampling. The consequences of using this approach are discussed in Chapter 5.

The ambient temperature uncertainty was based on a summary of the model performance evaluations for twenty-nine meteorological modeling studies (Tesche, 2001). The twenty-nine studies covered a variety of 12 km domains over the eastern United States. The mean bias across all studies is zero with an average gross error of 1.9°C. The gross error was used as the overall uncertainty in the temperatures for the episodes that were selected for use in this study.

5
CHAPTER 5

RESULTS

One thousand Monte Carlo simulations were run using BEIS3 for 11-15 July 1995 and 4-9 September 1995. The BEIS3 model parameters and model data inputs that were perturbed were discussed previously. For each episode, the following sections discuss the results of the uncertainty analysis. To drive the analysis, the following plots were developed for both episodes:

- Mean daily, gridded temperatures;
- Mean daily, gridded PAR values;
- CDFs of daily emissions estimates by pollutant;
- Mean daily, gridded emissions estimates by pollutant;
- Gridded coefficient of variation of the daily emissions by pollutant;
- Gridded standard deviation of the daily emissions by pollutant; and
- Gridded correlation coefficients of the pollutant-specific parameters to daily emissions estimates.

11-15 July 1995

Meteorology

Figure 5-1a shows the mean daily, gridded temperature field, and Figure 5-1b shows the mean daily, gridded PAR field that result from the random sampling. As can be observed from Figure 5-1a, much of the eastern United States experienced warm weather with temperatures in excess of 25.5°C. The notable exception was that on the first two days of the episode, the upper Midwest United States, Canada, and the greater Northeast United States experienced cooler weather with temperatures below 21.0°C and in some cases as low as 11°C. This trend persisted, in particular, over Lake Superior for the duration of the episode. Through the first three days of the episode, PAR values were basically saturated (i.e. in excess of 90 $W \cdot m^{-2}$ for the mean daily PAR value) throughout much of the land-based domain. Though on the last two days of the episode, PAR values dropped precipitously indicating the development of clouds.

Analysis Of Total Uncertainty

Figure 5-2 show the Cumulative Distribution Functions (CDFs) of the daily emissions estimates for each pollutant. A CDF gives the probability, P, that the random variable X will be less than or

equal to a particular value of x (i.e. $F(x) = P[X \leq x] = \int_{-\infty}^{x} f(x)dx$). Also, the 95% Confidence Interval (CI) is shown on each plot. The CDFs were constructed by summing the daily BEIS3 emissions estimates by pollutant and by sample set. The resulting daily emissions estimates were then rank ordered and plotted. *Lognormal* and *normal* distributions (e.g. Morgan and Henrion, 1990; Evans et al., 2000) were fitted to the daily emissions estimates, and the distribution that exhibited the best chi-square statistic (e.g. Kreyszig, 1979; DeGroot, 1989; Press et al., 1992) was chosen to represent the distribution in the emissions. Table 5-1 summarizes the basic statistics of each pollutant distribution. The fundamental concept that is revealed by Figure 5-2 and Table 5-1 is that as a result of the BEIS3 uncertainty analysis, the uncertainty ranges in the BEIS3 daily emissions estimates are as follows:

- Isoprene emissions estimates have an almost one order of magnitude uncertainty in the 95% CI;
- NO_X emissions estimates have over an one order of magnitude uncertainty in the 95% CI; and
- OVOC and monoterpene emissions estimates are tightly distributed within about $\pm$15% of the mean in the 95% CI.

Table 5-1
Summary of the uncertainty in the daily BEIS3 emissions estimates for 11-15 July 1995.

Date	Pollutant	Median (tons/day)	Standard Deviation (tons/day)	95% CI (tons/day)	Fitted Distribution Parameters			Figure
					Type	μ	σ	
11 July	Isoprene	103,857	55,360	29,723-244,043	Lognormal	11.964	0.32555	5-2a
	Monoterpene	25,671	2,487	20,797-30,544	Normal	25,671	2,487	5-2f
	OVOC	33,202	2,261	28,971-37,833	Lognormal	10.796	4.6256	5-2k
	NOX	4,560	6,481	2,028-22,804	Lognormal	7.9857	1.0078	5-2p
12 July	Isoprene	119,247	64,004	34,177-281,781	Lognormal	12.092	0.33033	5-2b
	Monoterpene	27,349	2,431	22,583-32,116	Normal	27,349	2,431	5-2g
	OVOC	36,346	2,090	32,249-40,442	Normal	36,346	2,090	5-2l
	NOX	4,724	7,037	2,057-24,452	Lognormal	8.0342	1.0209	5-2q
13 July	Isoprene	125,837	68,006	35,875-298,881	Lognormal	12.141	0.33386	5-2c
	Monoterpene	28,148	2,402	24,439-32,857	Normal	28,148	2,402	5-2h
	OVOC	37,972	2,072	34,065-42,185	Lognormal	10.892	3.8523	5-2m

Date	Pollutant	Median (tons/day)	Standard Deviation (tons/day)	95% CI (tons/day)	Fitted Distribution Parameters			Figure
					Type	μ	σ	
	NOX	4,809	7,313	2,072-25,272	Lognormal	8.0584	1.0264	5-2r
14 July	Isoprene	105,946	60,290	29,231-261,791	Lognormal	11.926	0.36162	5-2d
	Monoterpene	27,287	2,432	22,522-32,053	Normal	27,287	2,432	5-2i
	OVOC	36,072	2,214	31,733-40,412	Normal	36,072	2,214	5-2n
	NOX	4,701	6,931	2,054-24,152	Lognormal	8.0273	1.0177	5-2s
15 July	Isoprene	94,377	53,888	26,032-233,850	Lognormal	11.806	0.36394	5-2e
	Monoterpene	26,442	2,463	21,836-31,488	Lognormal	10.878	4.6415	5-2j
	OVOC	33,113	2,410	28,475-37,922	Lognormal	11.774	1.8564	5-2o
	NOX	4,432	6,033	2,009-21,480	Lognormal	7.9461	0.99542	5-2t

Figure 5-3 shows the plots of mean daily isoprene emissions (Figure 5-3a), coefficient of variation of the daily isoprene emissions (Figure 5-3b), and standard deviation of the daily isoprene emissions (Figure 5-3c). Consistent with previous findings, maximum isoprene emissions occur in the southern United States (e.g. Guenther et al., 1994). Though in the latter part of the episode, high isoprene emissions are also predicted over parts of the northeastern states. This appears to be due to increasing temperature, Figure 5-1a, and PAR, Figure 5-1b, over the same area. The high coefficients of variation (CV), those in excess of about 0.6, that are predicted over much of the northern part of the domain for the duration of the episode are due to low predicted isoprene emissions estimates coupled with high standard deviations. Similar patterns of high CVs occur over much of Florida for most of the episode. High CVs are also observed over Texas and Louisiana in the latter part of the episode when both temperature and PAR decrease, which results in lower predicted isoprene emissions.

Figure 5-4 shows plots of mean daily monoterpene emissions (Figure 5-4a), coefficient of variation of the daily monoterpene emissions (Figure 5-4b), and standard deviation of the daily monoterpene emissions (Figure 5-4c). Again, consistent with previous findings, maximum monoterpene emissions occur in the coniferous forests of the southern United States and upper New England (e.g. Guenther et al., 1994). High monoterpene emissions are also predicted in the coniferous forests of upper Minnesota and upper Wisconsin throughout much of the episode. The monoterpene CVs are generally low with no CV exceeding 0.42. This is consistent with the earlier finding that the uncertainty in the monoterpene emissions is relatively low compared to the uncertainties that exist in the isoprene emissions estimates.

Figure 5-5 shows plots of mean daily OVOC emissions (Figure 5-5a), coefficient of variation of the daily OVOC emissions (Figure 5-5b), and standard deviation of the daily OVOC emissions (Figure 5-5c). Unlike the predicted monoterpene emissions, OVOC emissions are more uniformly distributed throughout the domain. This is because OVOC emissions are suspected to be ubiquitous to plant species, in general, for purposes of plant tissue defense (Lamb et al., 1999). As with the monoterpene CVs, the OVOC CVs are generally low with no CV exceeding 0.42. Again, this is consistent with the earlier finding that the uncertainty in the OVOC emissions is relatively low compared to the uncertainties that exist in the isoprene emissions estimates.

Figure 5-6 shows plots of mean daily NO_X emissions (Figure 5-6a), coefficient of variation of the daily NO_X emissions (Figure 5-6b), and standard deviation of the daily NO_X emissions (Figure 5-6c). The highest NO_X emissions are predicted to be in farm belt of the United States. Because large uncertainties exist in NO_X emissions, Figures 5-2p through 5-2t, large CVs, in excess of 1.0, are found. In the case of NO_X, an extreme tail in the distribution dominates the large uncertainties. The NO_X CVs are less than 1.0 only where temperatures are predicted to be low (i.e. the Northeast United States and Canada on the first two days of the episode).

Analysis Of Correlations

Pairwise Pearson linear correlation coefficients (Weiss, 1997) were computed for each of the sampled parameters to its respective emissions estimates. The parameters that affect isoprene emissions are the following:

- C_T, the environmental correction factor that accounts for changes in leaf temperature (Eq. 3-7), which is a nonlinear combination of c_{T1}, c_{T2}, T_M, and T;
- c_{T1}, an empirical coefficient that impacts C_T;
- c_{T2}, an empirical coefficient that impacts C_T;
- T_M, an empirical coefficient that impacts C_T;
- T, the ambient temperature that is used to compute C_T;
- C_L^A, the environmental correction factor that accounts for changes in PAR (Eq. 3-9), which is a nonlinear combination of α, c_{L1}, L, and LAI;
- α, an empirical coefficient that impacts C_L^A;
- c_{L1}, an empirical coefficient that impacts C_L^A;
- L, the PAR that is used to compute C_L^A;
- LAI, the leaf area index that is used to compute C_L^A (Eq. 3-10) and
- E_S, the biogenic emissions factor for isoprene.

The parameters that affect OVOC and monoterpene emissions are the following:

- C_T, the environmental correction factor that accounts for changes in leaf temperature (Eq. 3-32), which is a nonlinear combination of T and β;
- T, the ambient temperature that is used to compute C_T;
- β, the empirical coefficient that establishes the temperature dependence of the emissions rate; and
- E_S, the biogenic emissions factor for OVOC or monoterpenes.

The parameters that affect biogenic NO_X emissions are the following:

- C_T, the environmental correction factor that accounts for changes in soil temperature (Eq. 3-34), which is a nonlinear combination of T_1, T_2, T_3, and T;
- T_1, an empirical parameter that relates soil temperature to ambient temperature;
- T_2, an empirical parameter that relates soil temperature to ambient temperature;
- T_3, an empirical parameter that relates soil temperature to BNO emissions;
- T, the ambient temperature that is used to compute C_T; and
- E_S, the biogenic emissions factor for NO_X.

Figure 5-7 shows plots of the correlation coefficients for BEIS3 isoprene emissions estimates and the parameters that impact isoprene emissions estimates. The terms used in Figure 5-7: C_T, c_{T1}, c_{T2}, T_M, T, C_L^A, α, c_{L1}, L, LAI, and E_S, are consistent with the terms used previously to describe the BEIS3 model formulation for isoprene. Correlation coefficients were computed for each model parameter or model data input that was perturbed to the isoprene emissions estimates. Figure 5-7a shows the correlation of C_T to isoprene emissions estimates. C_T is a nonlinear combination of c_{T1}, c_{T2}, T_M, and T. Throughout much of the domain, C_T shows a relatively weak correlation to the isoprene emissions estimates. A breakdown of the correlation of c_{T1} (Figure 5-7b), c_{T2} (Figure 5-7c), T_M (Figure 5-7d), and T (Figure 5-7e) to the isoprene emissions estimates shows that all variables have relatively weak correlations. However, it is interesting to note that c_{T1} and c_{T2} have both positive and negative correlations, and that the mean daily temperature has very low correlation to isoprene emissions estimates.

In contrast, the model parameters that impact the PAR attenuation of isoprene emissions estimates terms: C_L^A, α, and c_{L1} with C_L^A being a nonlinear combination of α and c_{L1}, are all strongly correlated to the isoprene emissions estimates throughout the domain with correlation coefficients in excess of 0.7. Though like mean daily temperature, the model data input PAR (Figure 5-7i) is weakly correlated to the isoprene emissions estimates. Further, the model data input LAI (Figure 5-7j) is also weakly, but negatively, correlated to isoprene emissions. This makes sense since increasing LAI effectively reduces the amount of PAR penetrating the leaf canopy, which in turn reduces the effective isoprene emission rate. Finally, the area weighted isoprene emissions factor (Figure 5-7k) is also weakly correlated to the isoprene emissions estimates. In summary, in order to reduce the overall uncertainty in the isoprene emissions estimates requires, it appears that we need to develop a better understanding of the parameters internal to BEIS3 that impact how isoprene emissions are estimated. That is, focusing on

developing better model data inputs: isoprene emissions factors (E_S), temperature (T), PAR (L), and LAI, will not necessarily be the best means to reduce the overall uncertainty that exists in the isoprene emissions estimates.

Figure 5-8 shows plots of the correlation coefficients for BEIS3 monoterpene and OVOC emissions estimates and related parameters. The terms used in Figure 5-8: C_T, T, β, and E_S, are consistent with the terms used previously to describe the BEIS3 model formulation for monoterpenes and OVOCs. Correlation coefficients were computed for each model parameter or model data input that was perturbed to the monoterpene and OVOC emissions estimates. Figure 5-8a shows the correlation of C_T to monoterpene emissions estimates. C_T is a nonlinear combination of β and T. The correlation of C_T to the monoterpene emissions estimates exhibits two distinctive traits: strong correlation throughout much of the Midwest and Northeast United States and Canada (i.e. coefficients in excess of 0.7) and weak correlation for the rest of the domain. The correlation of β (Figure 5-7b) also exhibits two distinctive traits. Throughout the Midwest and Northeast United States and Canada, β has strong negative correlation whereas in the rest of the domain, the correlation is weak both in the positive and negative directions. In general, mean daily temperature (Figure 5-7c) shows relatively weak correlation to the monoterpene emissions estimates. On the other hand, the area weighted monoterpene emissions factor (Figure 5-7d) shows strong correlation to the monoterpene emissions estimates throughout the domain with the exception of the Northeast United States and upper Midwest where the correlation is weak. The magnitudes and spatial distributions of the correlations of C_T, T, β, and E_S to OVOC emissions estimates (Figures 5-5e through 5-5h) follows patterns that are similar to those of the monoterpene emissions estimates. In summary, it appears that in order to reduce the overall uncertainty in the monoterpene and OVOC emissions estimates requires that we develop a better understanding of both the parameters that impact how monoterpene and OVOC emissions are estimated and the monoterpene and OVOC emissions factors (E_S). It appears that developing better estimates of temperature (T) will not necessarily be the best means to reduce the overall uncertainty that exists in the monoterpene and OVOC emissions estimates.

Figure 5-9 shows plots of the correlation coefficients for BEIS3 NO_X emissions estimates and related parameters. The terms used in Figure 5-9: C_T, T_1, T_2, T_3, T, and E_S, are consistent with the terms used previously to describe the BEIS3 model formulation for NO_X. Correlation coefficients were computed for each model parameter or model data input that was perturbed to the NO_X emissions estimates. Figure 5-9a shows the correlation of C_T to NO_X emissions estimates. C_T is a nonlinear combination of T_1, T_2, T_3, and T. Throughout the entire domain, C_T shows a strong correlation to the NO_X emissions estimates. A breakdown of the correlation shows that T_1 (Figure 5-9b) is the most important contributor to the correlation of C_T to the NO_X emissions estimates with T_2 (Figure 5-9c), T_3 (Figure 5-9d), and the mean daily temperature (Figure 5-9e) showing weak correlation. Further, the area weighted NO_X emissions factor (Figure 5-9f) is weakly correlated to the NO_X emissions estimates. In summary, in order to reduce the overall uncertainty in the NO_X emissions estimates, it appears that we need to develop a better understanding of the parameters internal to BEIS3 that impact how NO_X emissions are estimated. That is, focusing on developing better model data inputs (i.e. NO_X emissions factors [E_S] and better temperature values [T]) will not necessarily be the best means to reduce the overall uncertainty that exists in the NO_X emissions estimates.

At first glance through the isoprene emissions estimates to PAR and temperature correlation coefficients, the reader might conclude that isoprene emissions are not influenced by PAR or temperature. Yet it must be restated that BEIS3 isoprene emissions are still sensitive to changes in PAR and temperature, when only a nominal BEIS3 run is made (i.e. a standard BEIS3 run not considering the uncertainties in the model parameters and data inputs). That is, in a nominal BEIS3 run, all the model data parameters remain fixed. Then, a simple sensitivity run where temperature or PAR is perturbed will reveal that BEIS3 isoprene emissions estimates are influenced by changes to these values, particularly temperature. Then the question is "why particularly temperature?" This is because isoprene emissions are very insensitive to increasing PAR after PAR reaches its saturation point, which is about 1000 $\mu mol \cdot m^{-2} \cdot s^{-1}$ (Figure 3-1). On cloudless days, PAR reaches the saturation point typically within one hour of sunrise, and PAR drops rapidly to zero during the hour of sunset. Recall that when PAR is zero, the plant species does not emit isoprene. This basically means that once the sun is up, temperature becomes more of the driving force as to the magnitude of the emissions if other uncertainties are not considered.

Similarly, the reader might conclude that the OVOC, NO_X, and monoterpene emissions are not influenced by temperature after reviewing the OVOC, NO_X, and monoterpene emissions estimates to temperature correlation coefficients. Here again, BEIS3 OVOC, NO_X, and monoterpene emissions are sensitive to changes in temperature, when only a nominal BEIS3 run is made. Like the simple isoprene sensitivity run just mentioned, a similar sensitivity run will reveal that BEIS3 OVOC, NO_X, and monoterpene emissions estimates are influenced by temperature changes.

However, when the uncertainties across the model parameters (e.g. α, c_{L1}, c_{T2}) and the data inputs (e.g. T, E_s) are considered, there is a precipitous drop in the correlation of the BVOC and BNO emissions to the meteorological variables for the following reasons:

- The uncertainties in the temperature are small when compared to the uncertainties in the BEIS3 model parameters. That is, the uncertainty in temperature is $\pm$1.9K at one standard deviation. This equates to about $\pm$1% of the nominal temperature value. On the other hand, the uncertainty in many of the BEIS3 model parameters is $\pm$50% at one standard deviation.
- The temperature varies greatest during the night when PAR is zero. Recall that when PAR is zero, there are no isoprene emissions. Though when we correlate the widely varying nighttime temperatures to zero isoprene emissions, it effectively reduces the overall isoprene emissions to temperature correlation.
- Similarly, the BEIS3 model parameters for monoterpenes, OVOCs, and NOX have much larger uncertainty values compared to temperature. Hence, the variation in the emissions is more highly correlated to the variation in the model parameters.
- For all pollutants, the variation in the emissions factors is smaller than the variation in the BEIS3 model parameters. The variation in the emissions factors is treated as $\pm$50% in the 95% confidence interval, which equates to about $\pm$23% at one standard deviation. Therefore, the emissions to emissions factor correlation is expected to be smaller than the correlation of emissions to the BEIS3 model parameters. Though, because the variation in the emissions factors is greater than the variation in the temperature or PAR, the emissions factors are more strongly correlated to the emissions than are the meteorological parameters.

Also, it is wise to restate an assumption about computing pair-wise correlation coefficients. That is, pair-wise correlation assumes that the system is linear. For BEIS3, the system is not linear, which further confounds the interpretation of the correlation coefficients.

04-09 September 1995

Meteorology

Figure 5-10a shows the mean daily, gridded temperature field, and Figure 5-10b shows the mean daily, gridded PAR field that result from the random sampling. As can be observed from Figure 5-10a, much of the eastern United States experienced typical fall conditions with temperatures in the low twenties and high teens at the start of the episode with the exception of Oklahoma and Texas where temperatures were much warmer. As the episode progresses, there is a notable cooling trend throughout much of the Midwest and Northeast United States as an Arctic front pushes through from the north-northwest. Though the South remained relatively warm for the duration of the episode with temperatures in the mid- to upper-twenties. Only the first day of the episode exhibited PAR values that were basically saturated (i.e. in excess of 90 $W \cdot m^{-2}$ for the mean daily PAR value) throughout much of the land-based domain. As the episode progressed, PAR values progressively dropped as the frontal system moved into the domain where even the Southern United States experienced less than saturated values over much of its domain.

Analysis Of Total Uncertainty

CDFs were generated in manner similar to those generated for the 11-15 July 1995 episode. Table 5-2 summarizes the basic statistics of each pollutant distribution for the period 04-09 September 1995. The fundamental concept that is revealed by Table 5-2 is that as a result of the BEIS3 uncertainty analysis, the uncertainty ranges in the BEIS3 daily emissions estimates for the September 1995 episode are as follows:

- Isoprene emissions estimates have roughly a factor of nine uncertainty in the 95% CI;
- NO_X emissions estimates have roughly a factor of eight uncertainty in the 95% CI; and
- OVOC and monoterpene emissions estimates are relatively tightly distributed within about $\pm$25% of the mean in the 95% CI.

Contrasted to the 11-15 July 1995 period, the uncertainty bounds are just a bit greater for the 04-09 September 1995 episode.

Table 5-2
Summary of the uncertainty in the daily BEIS3 emissions estimates for 04-09 September 1995.

Date	Pollutant	Median (tons/day)	Standard Deviation (tons/day)	95% CI (tons/day)	Fitted Distribution Parameters		
					Type	μ	σ
04	Isoprene	55,599	30,294	16,150-133,188	Lognormal	11.293	0.34512

Date	Pollutant	Median (tons/day)	Standard Deviation (tons/day)	95% CI (tons/day)	Fitted Distribution Parameters		
					Type	μ	σ
Sep	Monoterpene	18,232	2,360	13,742-22,990	Lognormal	11.282	2.9691
	OVOC	25,174	2,654	19,972-30,376	Normal	25,174	2,654
	NOX	4,107	4,867	1,926-18,036	Lognormal	7.8581	0.94592
05 Sep	Isoprene	53,065	29,292	15,363-128,442	Lognormal	11.231	0.35347
	Monoterpene	17,539	2,418	12,923-22,401	Lognormal	11.418	2.6566
	OVOC	24,815	2,777	19,373-30,257	Normal	24,815	2,777
	NOX	4,118	4,862	1,929-18,038	Lognormal	7.8619	0.94404
06 Sep	Isoprene	55,027	29,594	16,112-130,520	Lognormal	11.294	0.33810
	Monoterpene	17,589	2,395	12,895-22,282	Normal	17,589	2,395
	OVOC	24,207	2,785	18,865-29,780	Lognormal	11.762	2.1708
	NOX	4,052	4,663	1,915-17,428	Lognormal	7.8413	0.93573
07 Sep	Isoprene	39,975	23,112	11,383-100,354	Lognormal	10.902	0.38139
	Monoterpene	16,516	2,380	11,851-21,180	Normal	16,516	2,380
	OVOC	20,806	2,860	15,388-26,597	Lognormal	11.337	3.4074
	NOX	3,536	3,398	1,801-13,367	Lognormal	7.6528	0.88507
08 Sep	Isoprene	19,024	14,936	4,819-60,932	Lognormal	9.9753	0.55200
	Monoterpene	19,677	2,310	15,205-24,258	Lognormal	12.130	0.01246
	OVOC	21,667	2,664	16,445-26,889	Normal	21,667	2,664
	NOX	3,440	3,213	1,782-12,743	Lognormal	7.6098	0.87993
09 Sep	Isoprene	32,805	19,511	9,228-84,205	Lognormal	10.682	0.39766
	Monoterpene	15,738	2,337	11,335-20,495	Lognormal	10.989	3.9418
	OVOC	17,487	2,861	12,197-23,406	Lognormal	10.815	5.7344
	NOX	3,102	2,423	1,702-10,152	Lognormal	7.4652	0.82497

Figure 5-11 shows the plots of mean daily isoprene emissions (Figure 5-11a), coefficient of variation of the daily isoprene emissions (Figure 5-11b), and standard deviation of the daily isoprene emissions (Figure 5-11c). Again, consistent with previous findings, maximum isoprene

emissions occur in the southern United States (e.g. Guenther et al., 1994). Higher isoprene emissions predominate in the early part of the episode since cooler temperatures and lower PAR values result in the latter part of the episode as a cold front moves into the domain. For the first three days of the episode, the CVs (Figure 5-11b) remain relatively low over much of the domain with the exception of the greater northern part of the domain. The high CVs over the greater northern part of the domain are due to very low isoprene emissions estimates coupled with high standard deviations (Figure 5-11c). During the last three days of the episode, high CVs appear as temperature and PAR values drop due to the introduction of the cold front, which results in lower isoprene emissions estimates and higher standard deviations in the same.

Figure 5-12 shows plots of mean daily monoterpene emissions (Figure 5-12a), coefficient of variation of the daily monoterpene emissions (Figure 5-12b), and standard deviation of the daily monoterpene emissions (Figure 5-12c). Again, consistent with previous findings, maximum monoterpene emissions occur in the coniferous forests of the southern United States and upper New England (e.g. Guenther et al., 1994). High monoterpene emissions are also predicted in the coniferous forests of upper Minnesota and upper Wisconsin throughout much of the episode. Higher monoterpene emissions are predicted in the earlier part of the episodes when temperatures are highest and drop substantially as the cold front moves through in the latter part of the episode. The monoterpene CVs are generally low with no CV exceeding 0.48. This is consistent with the earlier finding that the uncertainty in the monoterpene emissions is relatively low compared to the uncertainties that exist in the isoprene emissions estimates.

Figure 5-13 shows plots of mean daily OVOC emissions (Figure 5-13a), coefficient of variation of the daily OVOC emissions (Figure 5-13b), and standard deviation of the daily OVOC emissions (Figure 5-13c). Again, OVOC emissions are more uniformly distributed throughout the domain than are the monoterpene emissions. As with the monoterpene emissions estimates, the OVOC emissions are predicted to be higher in the early part of the episode. However, the OVOC emissions estimates drop much faster than do the monoterpene emissions estimates in the latter part of the episode due to declining temperatures. Also, the OVOC CVs are generally low with no CV exceeding 0.48. This again is consistent with the earlier finding that the uncertainty in the OVOC emissions is relatively low compared to the uncertainties that exist in the isoprene emissions estimates.

Figure 5-14 shows plots of mean daily NO_X emissions (Figure 5-14a), coefficient of variation of the daily NO_X emissions (Figure 5-14b), and standard deviation of the daily NO_X emissions (Figure 5-14c). The highest NO_X emissions are predicted to be in farm belt of the United States. Like the OVOC emissions estimates, the NO_X emissions drop precipitously in the latter part of the episode as the cold front moves into the domain. Because large uncertainties exist in NO_X emissions, large CVs, in excess of 1.0, are found. The NO_X CVs are less than 1.0 only where temperatures are predicted to be low.

Analysis Of Correlations

Figure 5-15 shows plots of the correlation coefficients for BEIS3 isoprene emissions estimates and related parameters. The terms used in Figure 5-15: C_T, c_{T1}, c_{T2}, T_M, T, C_L^A, α, c_{L1}, L, LAI, and E_S, are consistent with the terms used previously to describe the BEIS3 model formulation for

isoprene. Figure 5-15a shows the correlation of C_T to isoprene emissions estimates, and it is relatively weak throughout the domain. Consistent with findings for the 11-15 July 1995 episode, a breakdown of the C_T correlation into c_{T1} (Figure 5-15b), c_{T2} (Figure 5-15c), T_M (Figure 5-15d), and T (Figure 5-15e) shows that all variables have relatively weak correlations.

Also consistent with findings for the 11-15 July 1995 episode, the model parameters that impact the PAR attenuation of isoprene emissions estimates terms: C_L^A, α, and c_{L1}, are all strongly correlated to the isoprene emissions estimates throughout the domain. Here again it is seen that (1) the model data input PAR (Figure 5-15i) is weakly correlated to the isoprene emissions estimates, (2) the model data input LAI (Figure 5-15j) is weakly, but negatively, correlated to isoprene emissions, and (3) the area weighted isoprene emissions factor (Figure 5-15k) is weakly correlated to the isoprene emissions estimates.

Figure 5-16 shows plots of the correlation coefficients for BEIS3 monoterpene and OVOC emissions estimates and related parameters. The terms used in Figure 5-16: C_T, T, β, and E_S, are consistent with the terms used previously to describe the BEIS3 model formulation for monoterpenes and OVOCs. Figure 5-16a shows the correlation of C_T to monoterpene emissions estimates. Again, the correlation of C_T to the monoterpene emissions estimates exhibits two distinctive traits. But unlike the 11-15 July 1995 episode, the strong correlation dips much further into the south and western parts of the domain. As with the 11-15 July 1995 episode, the correlation of β (Figure 5-16b) also exhibits two distinctive traits but with deeper penetration of the strong negative correlation into the southern and western parts of the domain. The mean daily temperature (Figure 5-16c) shows relatively weak correlation to the monoterpene emissions estimates throughout the domain. On the other hand, the area weighted monoterpene emissions factor (Figure 5-16d) shows strong correlation to the monoterpene emissions estimates throughout the domain with the exception of the Northeast United States and upper Midwest where the correlation is weak. The magnitudes and spatial distributions of the correlations of C_T, T, β, and E_S to OVOC emissions estimates (Figures 5-16e through 5-16h) follows patterns that are similar to those of the monoterpene emissions estimates.

Figure 5-17 shows plots of the correlation coefficients for BEIS3 NO_X emissions estimates and related parameters. The terms used in Figure 5-17: C_T, T_1, T_2, T_3, T, and E_S, are consistent with the terms used previously to describe the BEIS3 model formulation for NO_X. Figure 5-17a shows the correlation of C_T to NO_X emissions estimates. Consistent with findings for the 11-15 July 1995 episode, C_T shows a strong correlation to the NO_X emissions estimates throughout the domain. The most important contributor to the overall correlation of C_T to the NO_X emissions estimates is again T_1 (Figure 5-17b). T_2 (Figure 5-17c), T_3 (Figure 5-17d), and the mean daily temperature (Figure 5-17e) all show weak correlation to the NO_X emissions estimates. The area weighted NO_X emissions factor (Figure 5-17f) is, as with the 11-15 July 1995 episode, weakly correlated to the NO_X emissions estimates.

24-29 May 1995

Meteorology

Figure 5-18a shows the mean daily, gridded temperature field, and Figure 5-18b shows the mean daily, gridded PAR field that result from the random sampling. As can be observed from Figure 5-18a, the temperatures are much cooler than either the July or September episodes with maximum daily average temperatures of about 28°C occurring in the Deep South. The spatial distribution of temperatures indicates that a stationary cold front existed covering the greater Northeast United States through the Midwest and into the panhandles of Oklahoma and Texas. The stationary cold front persisted for the duration of the episode. Temperatures remained relatively unchanged throughout the episode as well. The PAR field shows that much of the United States south and east of the stationary cold front were basically PAR saturated at least through the first four or five days of the episode. On the other hand, PAR values indicate the presence of clouds moving through the domain north and west of the stationary cold front as the episode progresses.

Analysis Of Total Uncertainty

CDFs were generated in manner similar to those generated for the 11-15 July 1995 episode. Table 5-3 summarizes the basic statistics of each pollutant distribution for the period 24-29 May 1995. The fundamental concept that is revealed by Table 5-3 is that as a result of the BEIS3 uncertainty analysis, the uncertainty ranges in the BEIS3 daily emissions estimates for the May 1995 episode are as follows:

- Isoprene emissions estimates have roughly a factor of nine uncertainty in the 95% CI;
- NO_X emissions estimates have roughly a factor of six uncertainty in the 95% CI; and
- OVOC and monoterpene emissions estimates are relatively tightly distributed within about +30% of the mean in the 95% CI.

The uncertainty bounds for the May episode are comparable to the uncertainty bounds for the September episode though the NO_X distribution in May is a bit tighter than that of September. The tighter distribution in the NO_X emissions is directly attributable to the very low temperatures over the region of the United States where biogenic NO_X is typically highest, namely the Midwest.

Table 5-3
Summary of the uncertainty in the daily BEIS3 emissions estimates for 24-29 May 1995.

Date	Pollutant	Median (tons/day)	Standard Deviation (tons/day)	95% CI (tons/day)	Fitted Distribution Parameters		
					Type	μ	σ
24	Isoprene	51,294	27,968	14,733-122,813	Lognormal	11.223	0.34236

Date	Pollutant	Median (tons/day)	Standard Deviation (tons/day)	95% CI (tons/day)	Fitted Distribution Parameters		
					Type	μ	σ
May	Monoterpene	16,889	2,642	11,711-22,068	Normal	16,889	2,642
	OVOC	18,558	2,957	12,982-24,570	Lognormal	11.248	3.8498
	NOX	3,027	2,560	1,706-10,440	Lognormal	7.3832	0.87972
25 May	Isoprene	45,516	26,458	12,724-114,589	Lognormal	11.042	0.38010
	Monoterpene	16,850	2,656	11,998-22,406	Lognormal	10.553	6.9112
	OVOC	17,942	3,008	12,046-23,838	Normal	17,942	3,008
	NOX	2,956	2,353	1,694-9,782	Lognormal	7.3448	0.86133
26 May	Isoprene	46,878	27,049	13,152-117,341	Lognormal	11.077	0.37595
	Monoterpene	17,817	2,668	12,937-23,385	Lognormal	10.594	6.6690
	OVOC	18,895	3,038	12,942-24,849	Normal	18,895	3,038
	NOX	3,074	2,559	1,726-10,791	Lognormal	7.4068	0.87007
27 May	Isoprene	47,088	27,124	13,241-117,725	Lognormal	11.082	0.37538
	Monoterpene	17,566	2,673	12,674-23,178	Lognormal	10.587	0.06723
	OVOC	19,184	3,051	13,390-25,348	Lognormal	11.476	3.1627
	NOX	3,164	2,742	1,748-11,102	Lognormal	7.4520	0.87961
28 May	Isoprene	41,316	25,011	11,355-107,404	Lognormal	10.912	0.40362
	Monoterpene	17,257	2,692	11,982-22,532	Normal	17,257	2,692
	OVOC	19,280	3,061	13,447-25,443	Lognormal	11.599	2.8073
	NOX	3,208	2,853	1,757-11,460	Lognormal	7.4736	0.88676
29 May	Isoprene	35,485	22,827	9,489-96,787	Lognormal	10.717	0.43772
	Monoterpene	16,600	2,747	11,534-22,298	Lognormal	10.731	0.05986
	OVOC	18,528	3,168	12,319-24,736	Normal	18,528	3,168
	NOX	3,127	2,612	1,743-10,702	Lognormal	7.4347	0.86718

Figure 5-19 shows the plots of mean daily isoprene emissions (Figure 5-19a), coefficient of variation of the daily isoprene emissions (Figure 5-19b), and standard deviation of the daily

isoprene emissions (Figure 5-19c). Consistent with previous findings, maximum isoprene emissions occur in the southern United States (e.g. Guenther et al., 1994). For the duration of the episode, the CVs (Figure 5-19b) remain relatively low over much of the domain to the south and east of the cold front. The relatively high CVs over the greater northern part of the domain are due to very low isoprene emissions estimates coupled with high standard deviations (Figure 5-19c). Further, the relatively high CVs appear to also be associated with the areas of very low PAR (Figure 5-18b).

Figure 5-20 shows plots of mean daily monoterpene emissions (Figure 5-20a), coefficient of variation of the daily monoterpene emissions (Figure 5-20b), and standard deviation of the daily monoterpene emissions (Figure 5-20c). Consistent with previous findings, the highest monoterpene emissions occur in the coniferous forests of the southern United States, upper New England, upper Minnesota, and upper Wisconsin throughout much of the episode. Because of the persistence of the stationary cold front, the monoterpene emissions that are predicted by BEIS3 remain relatively unchanged through the duration of the episode. The monoterpene CVs (Figure 5-20b) are generally low ahead of the stationary cold front. However, behind the stationary cold front, the monoterpene CVs do get moderately high.

Figure 5-21 shows plots of mean daily OVOC emissions (Figure 5-21a), coefficient of variation of the daily OVOC emissions (Figure 5-21b), and standard deviation of the daily OVOC emissions (Figure 5-21c). Consistent with previous findings, OVOC emissions are more uniformly distributed throughout the domain than are the monoterpene emissions. As with the monoterpene emissions estimates, the OVOC emissions are predicted to be about the same through the duration of the episode. Also, the OVOC CVs (Figure 5-21b) parallel the CVs of the monoterpene emissions.

Figure 5-22 shows plots of mean daily NO_X emissions (Figure 5-22a), coefficient of variation of the daily NO_X emissions (Figure 5-22b), and standard deviation of the daily NO_X emissions (Figure 5-22c). Unlike the previous episodes, the highest NO_X emissions are predicted to be in the southwestern most part of the domain. This is most likely due to the very low temperatures that are experienced over the Midwest United States during the episode. Like the previous emissions estimates for the episode, the NO_X emissions estimates remain relatively unchanged due the persistence of the cold front. Because large uncertainties exist in NO_X emissions, large CVs, in excess of 1.0, are found. Though, unlike the monoterpene and OVOC CVs for the episode, the NO_X CVs are lower behind (i.e. to the north and west) of the stationary cold front.

Analysis Of Correlations

Figure 5-23 shows plots of the correlation coefficients for BEIS3 isoprene emissions estimates and related parameters. The terms used in Figure 5-15: C_T, c_{T1}, c_{T2}, T_M, T, C_L^A, α, c_{L1}, L, LAI, and E_S, are consistent with the terms used previously to describe the BEIS3 model formulation for isoprene. Figure 5-23a shows the correlation of C_T to isoprene emissions estimates. It is relatively weak in areas where the temperature is high (i.e. to the east and south of the stationary cold front). Though the correlation of C_T to isoprene emissions estimates in areas where temperatures are low, for example, behind the stationary cold front, does increase, the correlation coefficient is rarely greater than 0.5. Consistent with findings for the July and September

episodes, a breakdown of the C_T correlation into c_{T1} (Figure 5-23b), c_{T2} (Figure 5-23c), T_M (Figure 5-23d), and T (Figure 5-23e) shows that all variables have relatively weak correlations. However, it is interesting to note that the correlations of c_{T1} (Figure 5-23b) and c_{T2} (Figure 5-23c) to BEIS3 isoprene emissions exhibit almost exclusively negative values, which was not seen in the July or September episode. Closer examination of the three episodes reveals that c_{T1} and c_{T2} become negatively correlated to isoprene emissions estimates when the temperature drops below the range of about 18°C to 20°C. This is interesting since this is also a transition point for the isoprene temperature correction factor as demonstrated in Figure 3-2. It is within this range of temperatures that isoprene temperature correction factor, C_T, begins to increase rapidly with increasing temperature.

Consistent with findings for the July and September 1995 episode, the model parameters that impact the PAR attenuation of the isoprene emissions estimates terms: C_L^A, α, and c_{L1}, are all strongly correlated to the isoprene emissions estimates throughout much of the domain. Again, it is seen that (1) the model data input PAR (Figure 5-23i) is weakly correlated to the isoprene emissions estimates, (2) the model data input LAI (Figure 5-23j) is weakly, but negatively, correlated to isoprene emissions, and (3) the area weighted isoprene emissions factor (Figure 5-23k) is weakly correlated to the isoprene emissions estimates.

Figure 5-24 shows plots of the correlation coefficients for BEIS3 monoterpene and OVOC emissions estimates and related parameters. The terms used in Figure 5-24: C_T, T, β, and E_S, are consistent with the terms used previously to describe the BEIS3 model formulation for monoterpenes and OVOCs. Figure 5-24a shows the correlation of C_T to monoterpene emissions estimates. For much of the domain, C_T is moderately to strongly correlated to the monoterpene emissions estimates. Though, unlike the July and September 1995 episodes, the correlation of β (Figure 5-24b) exhibits strong negative correlation over much of the domain. The mean daily temperature (Figure 5-24c) shows relatively weak correlation to the monoterpene emissions estimates throughout the domain. On the other hand, the area weighted monoterpene emissions factor (Figure 5-24d) shows strong correlation to the monoterpene emissions estimates ahead of the stationary cold front. Behind the stationary cold front, the correlation of temperature to monoterpene emissions is weak. The magnitudes and spatial distributions of the correlations of C_T, T, β, and E_S to OVOC emissions estimates (Figures 5-24e through 5-24h) follows patterns that are similar to those of the monoterpene emissions estimates for the episode.

Figure 5-25 shows plots of the correlation coefficients for BEIS3 NO_X emissions estimates and related parameters. The terms used in Figure 5-25: C_T, T_1, T_2, T_3, T, and E_S, are consistent with the terms used previously to describe the BEIS3 model formulation for NO_X. Figure 5-25a shows the correlation of C_T to NO_X emissions estimates. Consistent with findings for the July and September 1995 episodes, C_T shows a strong correlation to the NO_X emissions estimates throughout the domain. The most important contributor to the overall correlation of C_T to the NO_X emissions estimates is T_1 (Figure 5-25b). T_2 (Figure 5-25c), T_3 (Figure 5-25d), and the mean daily temperature (Figure 5-25e) all show weak correlation to the NO_X emissions estimates. The area weighted NO_X emissions factor (Figure 5-25f) is, as with the July and September 1995 episodes, weakly correlated to the NO_X emissions estimates.

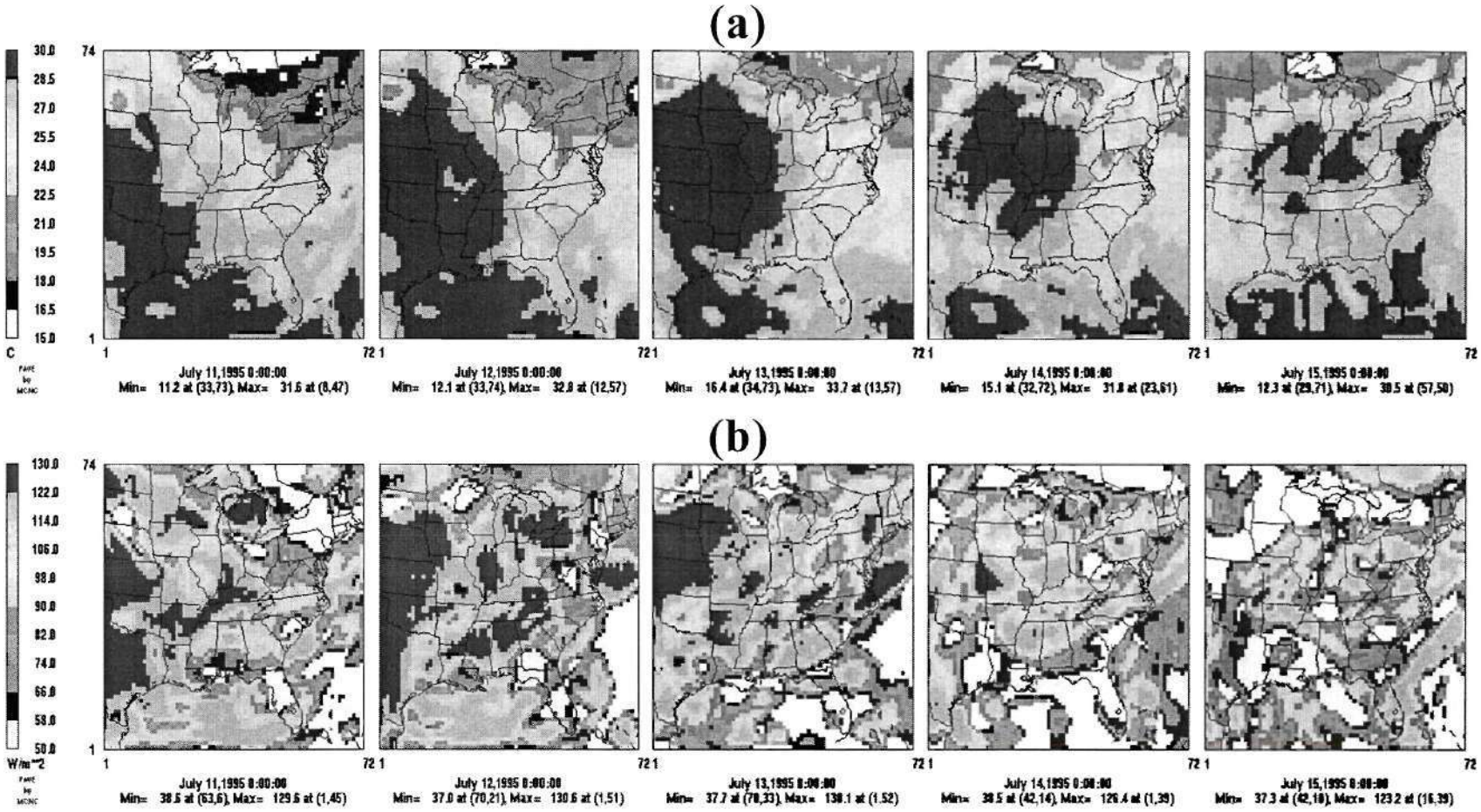

Figure 5-1.
Temperature and PAR values for 11-15 July 1995. (a) mean daily temperature (°C). (b) mean daily PAR ($W \cdot m^{-2}$).

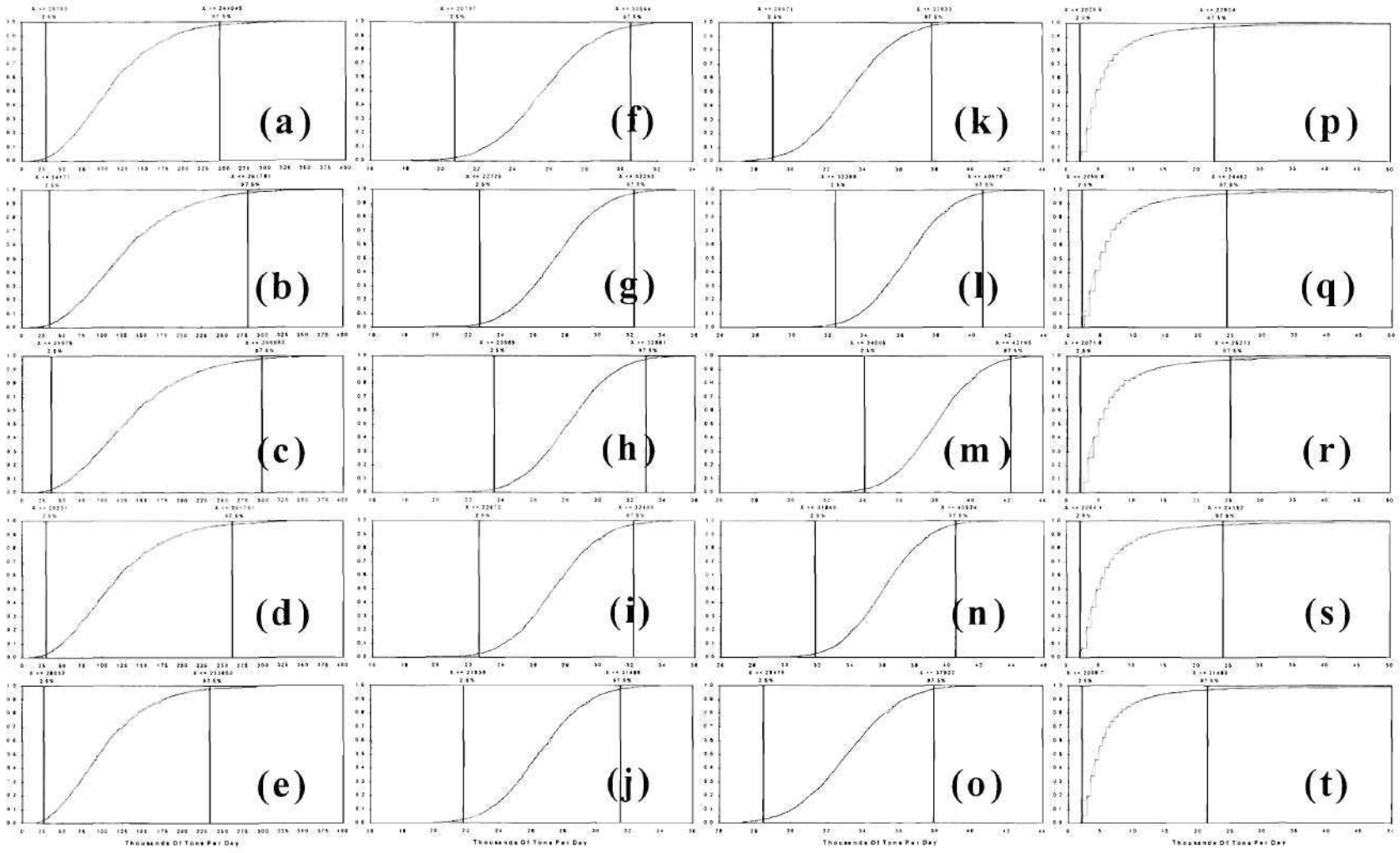

Figure 5-2.
CDFs of daily emissions estimates. (a)-(e) isoprene, 11-15 July 1995; (f)-(j) monoterpenes, 11-15 July 1995; (k)-(o) OVOCs, 11-15 July 1995; and (p)-(t) NO_X, 11-15 July 1995. The vertical gray lines on each plot indicate the 95% confidence interval of the emissions estimates. The blue lines of each plot are the BEIS3 predictions, and the red lines of each plot are the result of the fit of the distribution. y-axis ranges from 0.0 to 1.0 and x-axis is in thousands of tons per day.

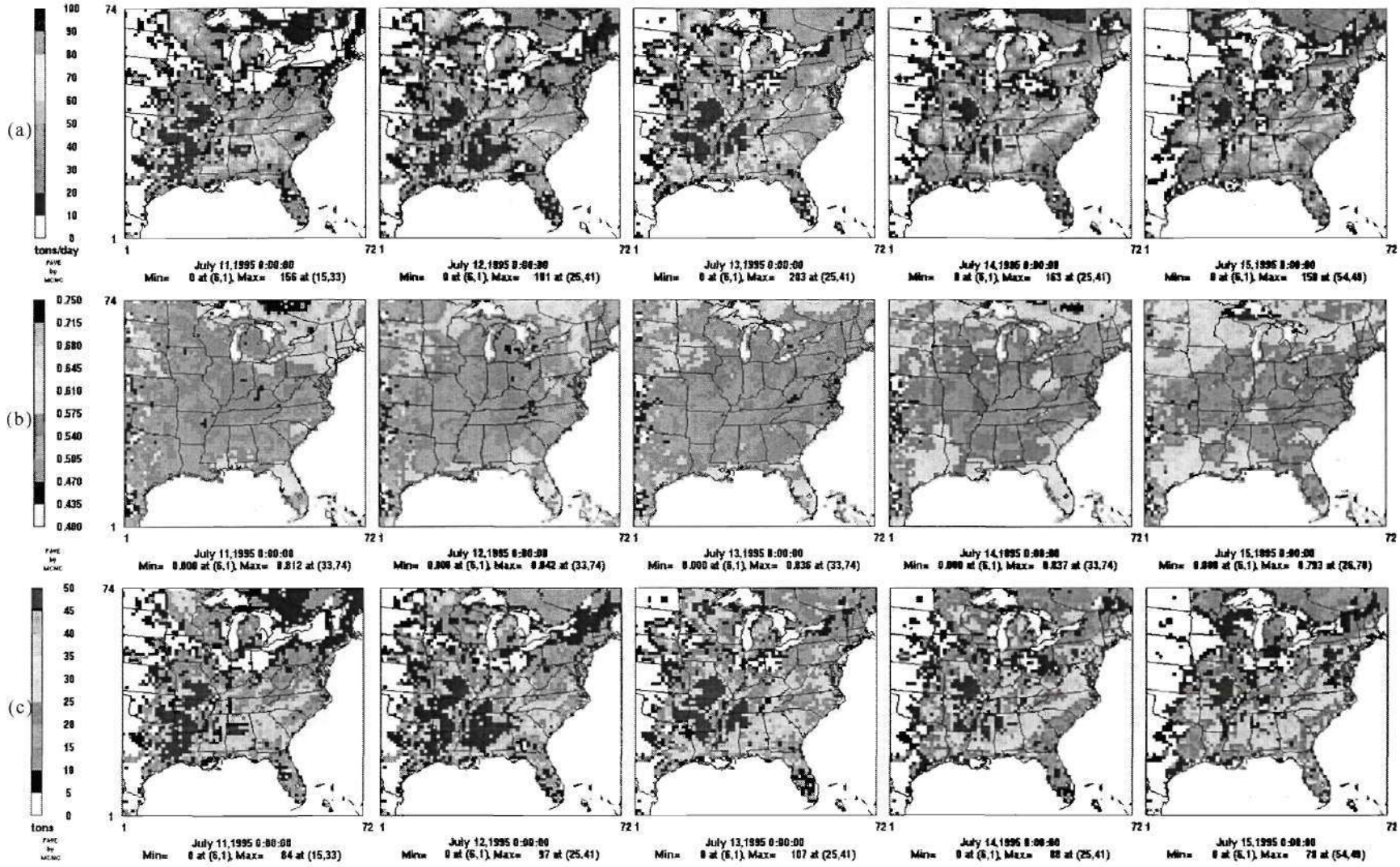

Figure 5-3.
Summary of BEIS3 isoprene emissions for 11-15 July 1995. (a) mean daily emissions (tons/day). (b) coefficient of variation in daily emissions. (c) standard deviation of daily emissions (tons).

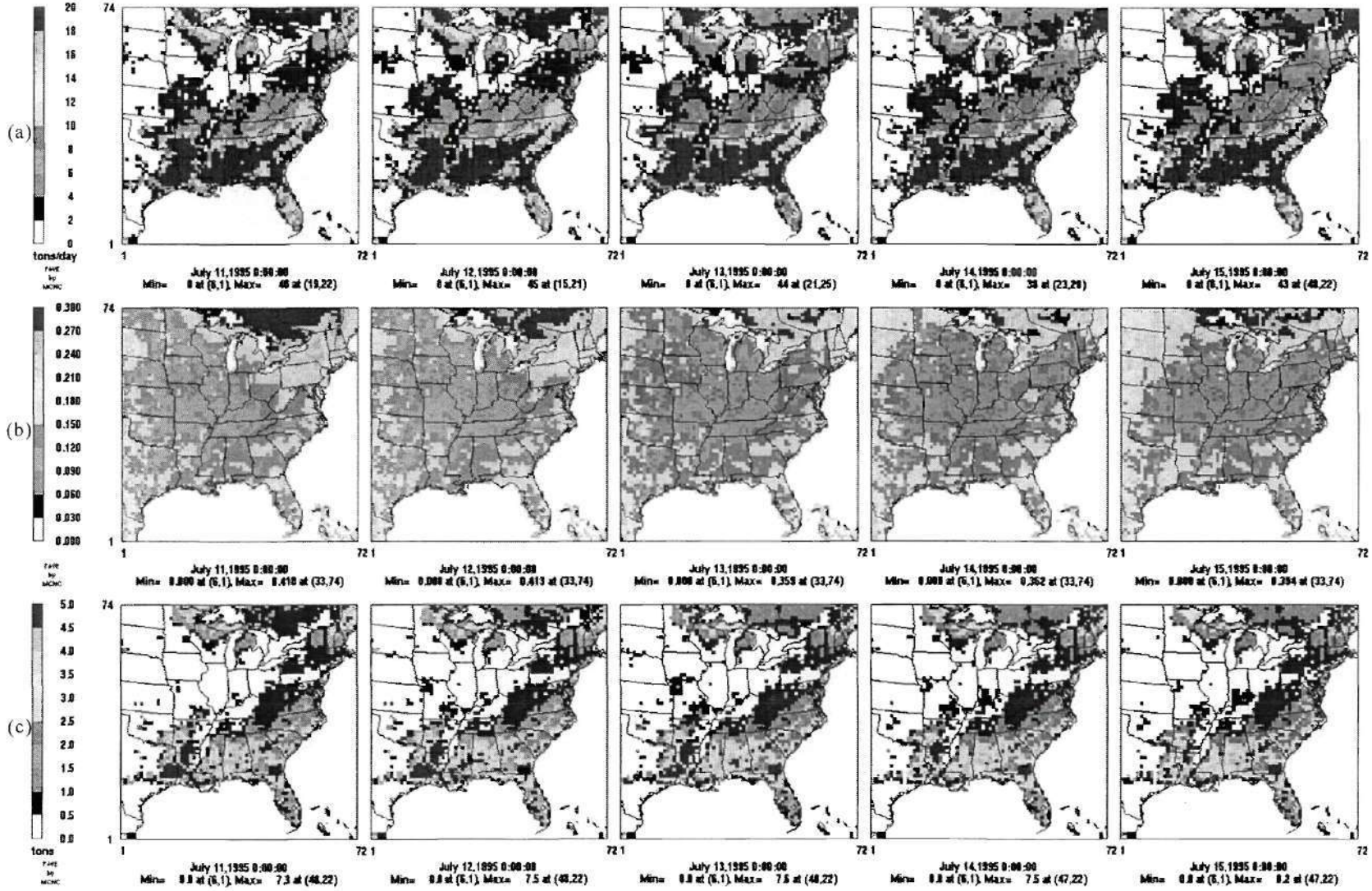

Figure 5-4.
Summary of BEIS3 monoterpene emissions for 11-15 July 1995. (a) mean daily emissions (tons/day). (b) coefficient of variation in daily emissions. (c) standard deviation of daily emissions (tons).

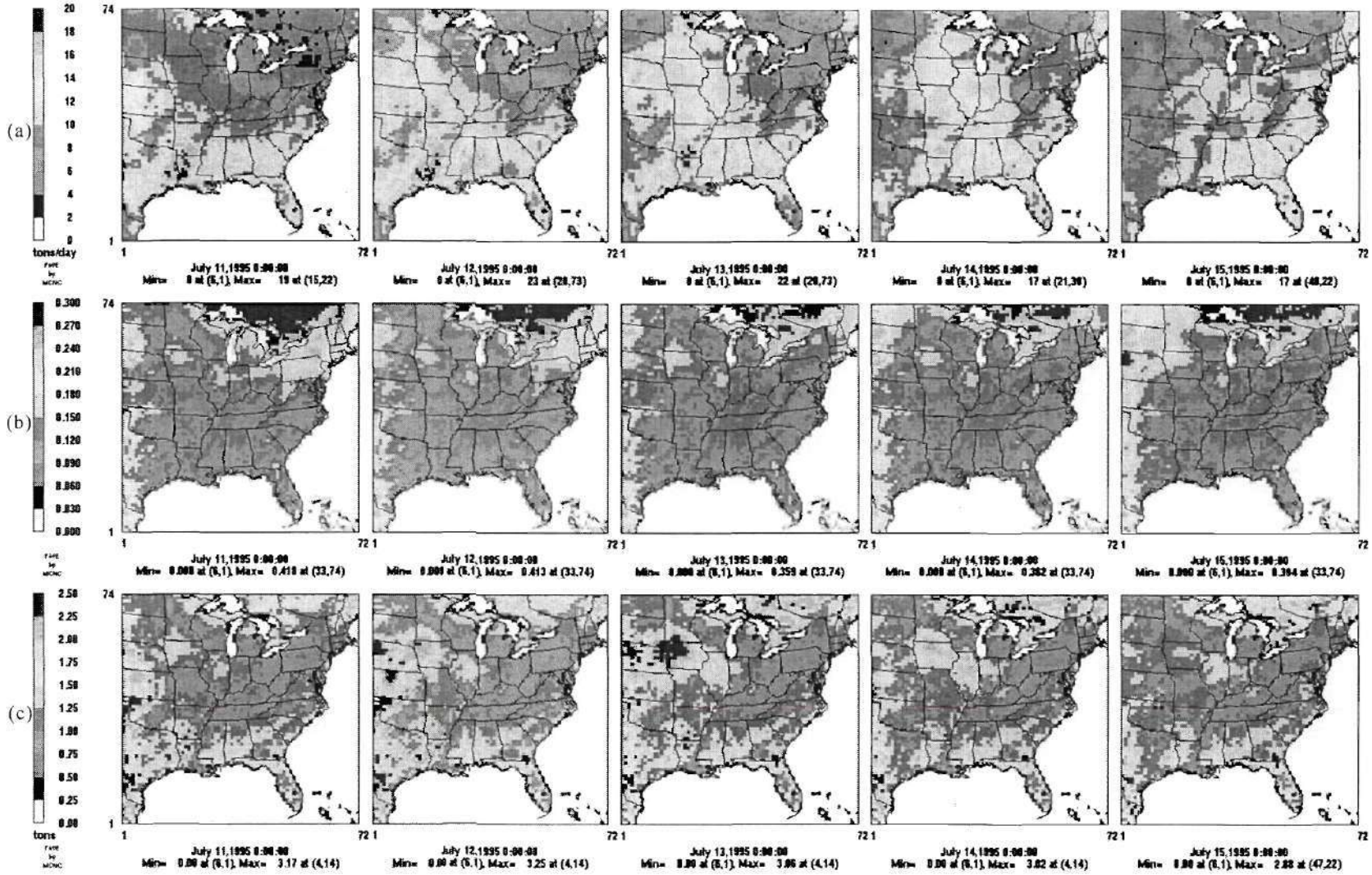

Figure 5-5.
Summary of BEIS3 OVOC emissions for 11-15 July 1995. (a) mean daily emissions (tons/day). (b) coefficient of variation in daily emissions. (c) standard deviation of daily emissions (tons).

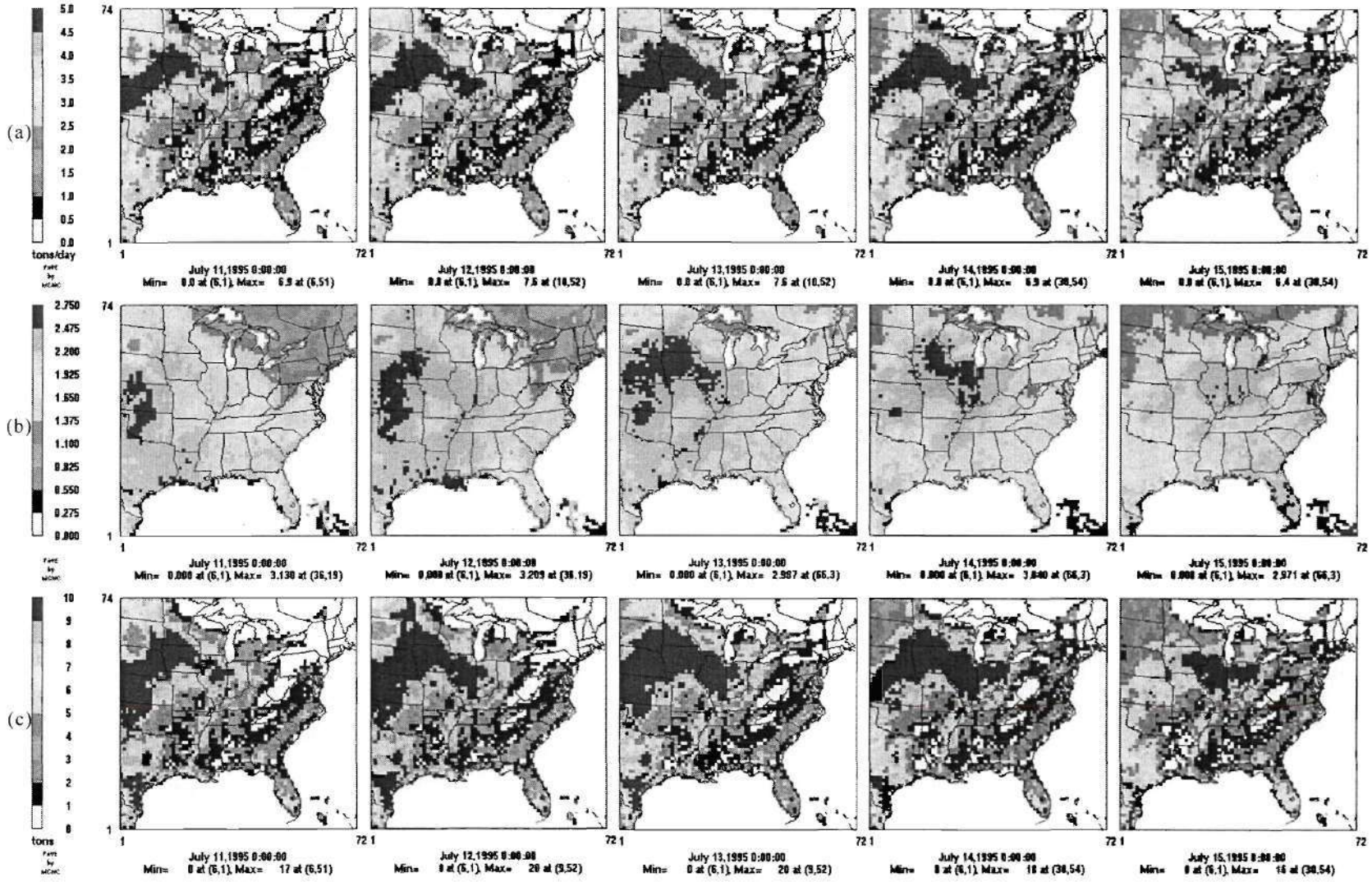

Figure 5-6.
Summary of BEIS3 NO_X emissions for 11-15 July 1995. (a) mean daily emissions (tons/day). (b) coefficient of variation in daily emissions. (c) standard deviation of daily emissions (tons).

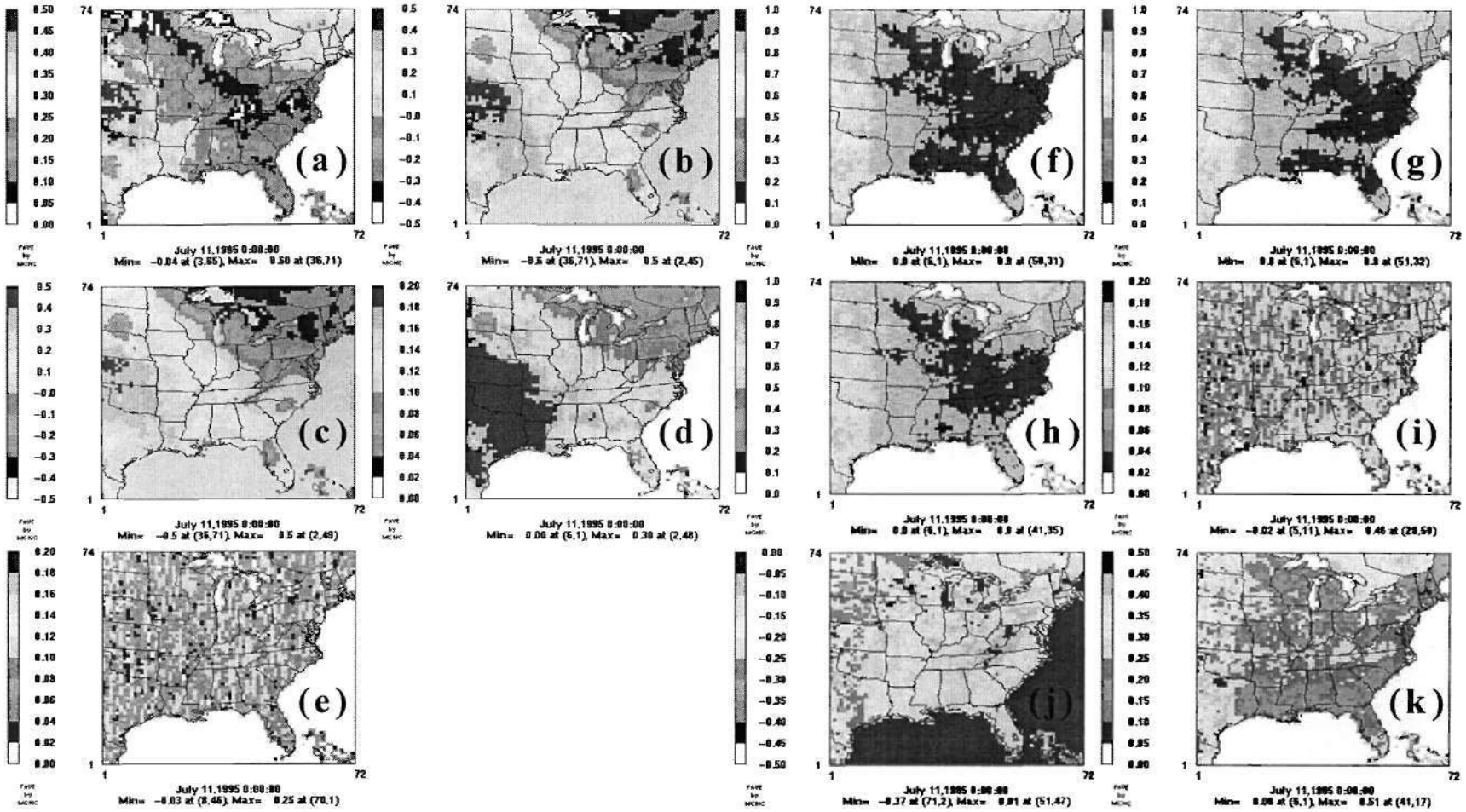

Figure 5-7.
Correlation coefficients of BEIS3 isoprene model parameters and model data inputs to BEIS3 isoprene emissions estimates for 11 July 1995. (a) C_T to BEIS3 isoprene emissions estimates; (b) c_{T1} to BEIS3 isoprene emissions estimates; (c) c_{T2} to BEIS3 isoprene emissions estimates; (d) T_M to BEIS3 isoprene emissions estimates; (e) T to BEIS3 isoprene emissions estimates; (f) C_L to BEIS3 isoprene emissions estimates; (g) α to BEIS3 isoprene emissions estimates; (h) c_{L1} to BEIS3 isoprene emissions estimates; (i) L to BEIS3 isoprene emissions estimates; (j) LAI to BEIS3 isoprene emissions estimates; and (k) E_S to BEIS3 isoprene emissions estimates.

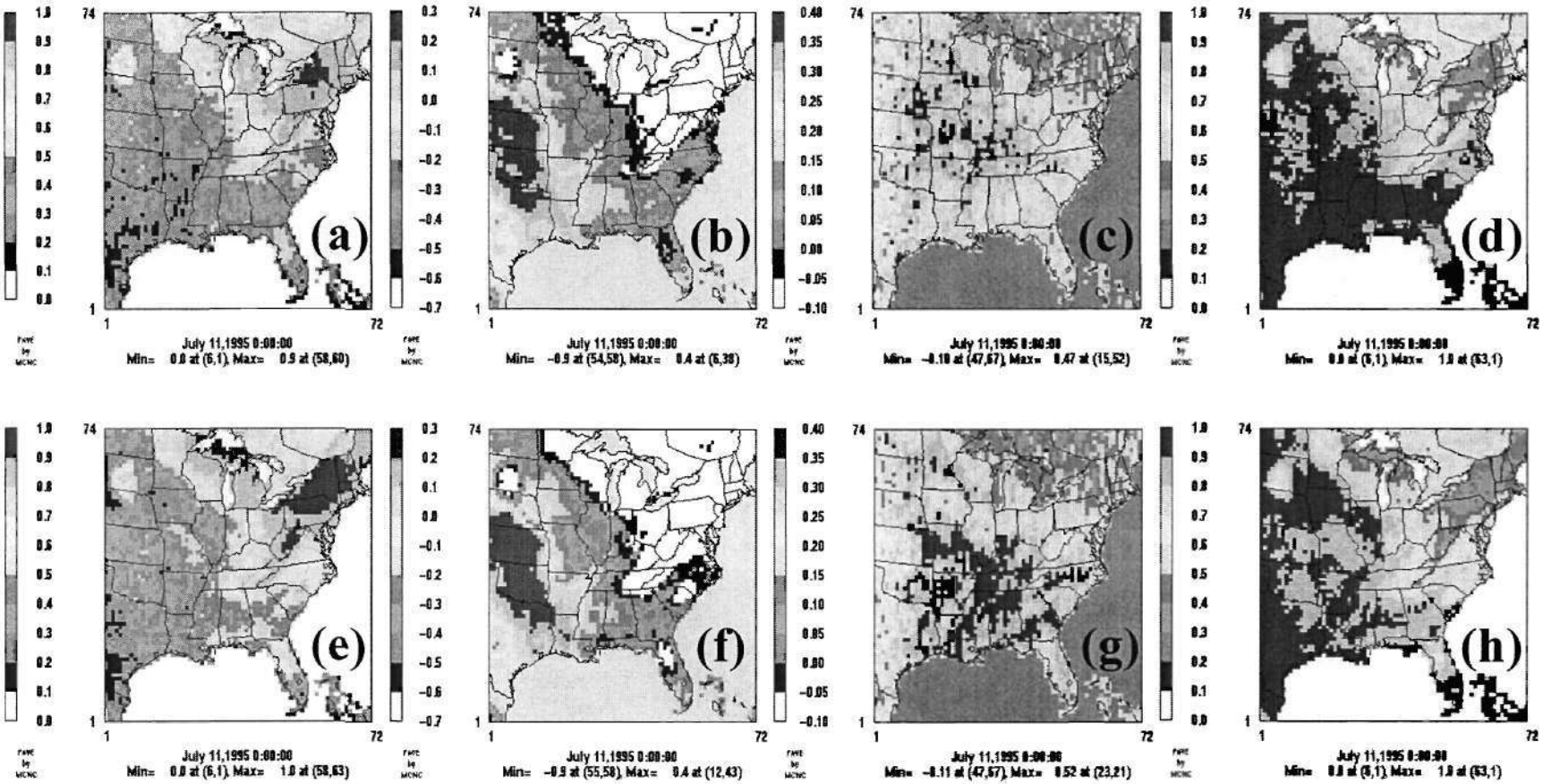

Figure 5-8.
Correlation coefficients of BEIS3 monoterpene and OVOC model parameters and model data inputs to BEIS3 monoterpene and OVOC emissions estimates for 11 July 1995. (a) C_T to BEIS3 monoterpene emissions estimates; (b) β to BEIS3 monoterpene emissions estimates; (c) T to BEIS3 monoterpene emissions estimates; (d) E_S to BEIS3 monoterpene emissions estimates; (e) C_T to BEIS3 OVOC emissions estimates; (f) β to BEIS3 OVOC emissions estimates; (g) T to BEIS3 OVOC emissions estimates; and (h) E_S to BEIS3 OVOC emissions estimates.

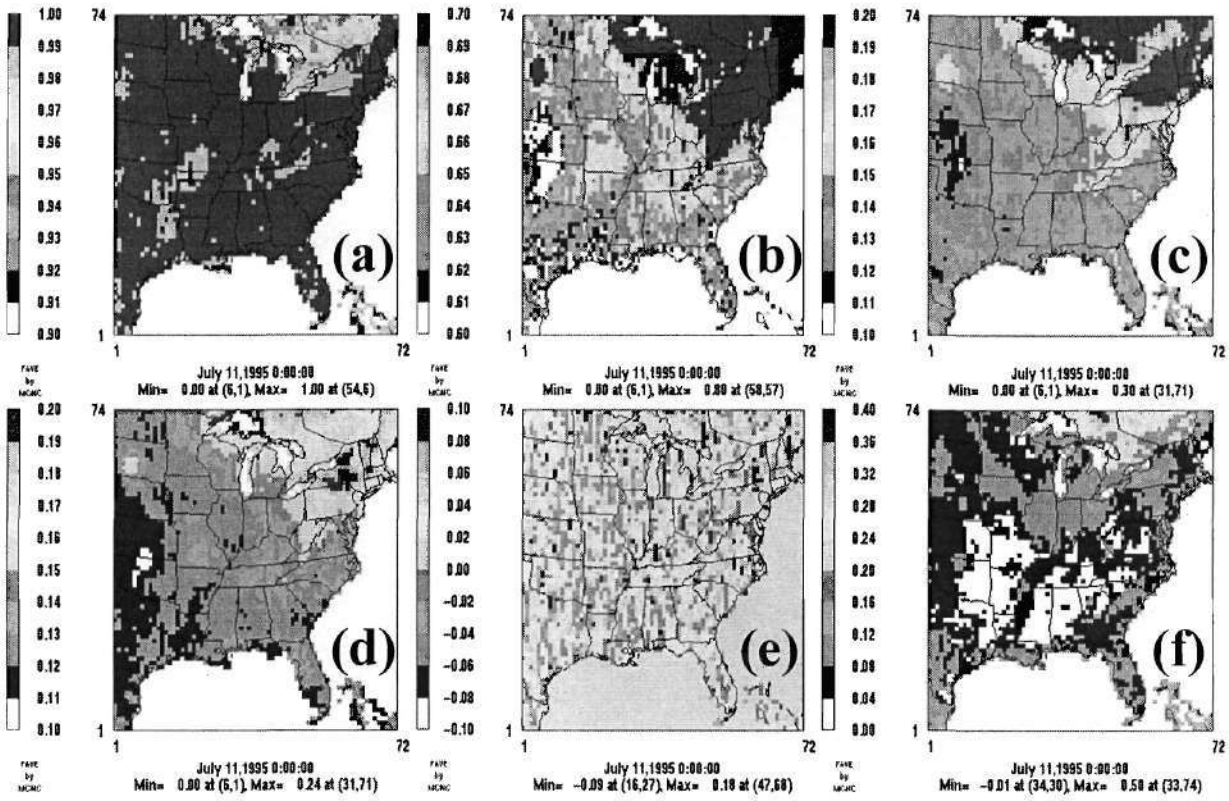

Figure 5-9.
Correlation coefficients of BEIS3 NO_X model parameters and model data inputs to BEIS3 NO_X emissions estimates for 11 July 1995. (a) C_T to BEIS3 NO_X emissions estimates; (b) T_1 to BEIS3 NO_X emissions estimates; (c) T_2 to BEIS3 NO_X emissions estimates; (d) T_3 to BEIS3 NO_X emissions estimates; (e) T to BEIS3 NO_X emissions estimates; and (f) E_S to BEIS3 NO_X emissions estimates.

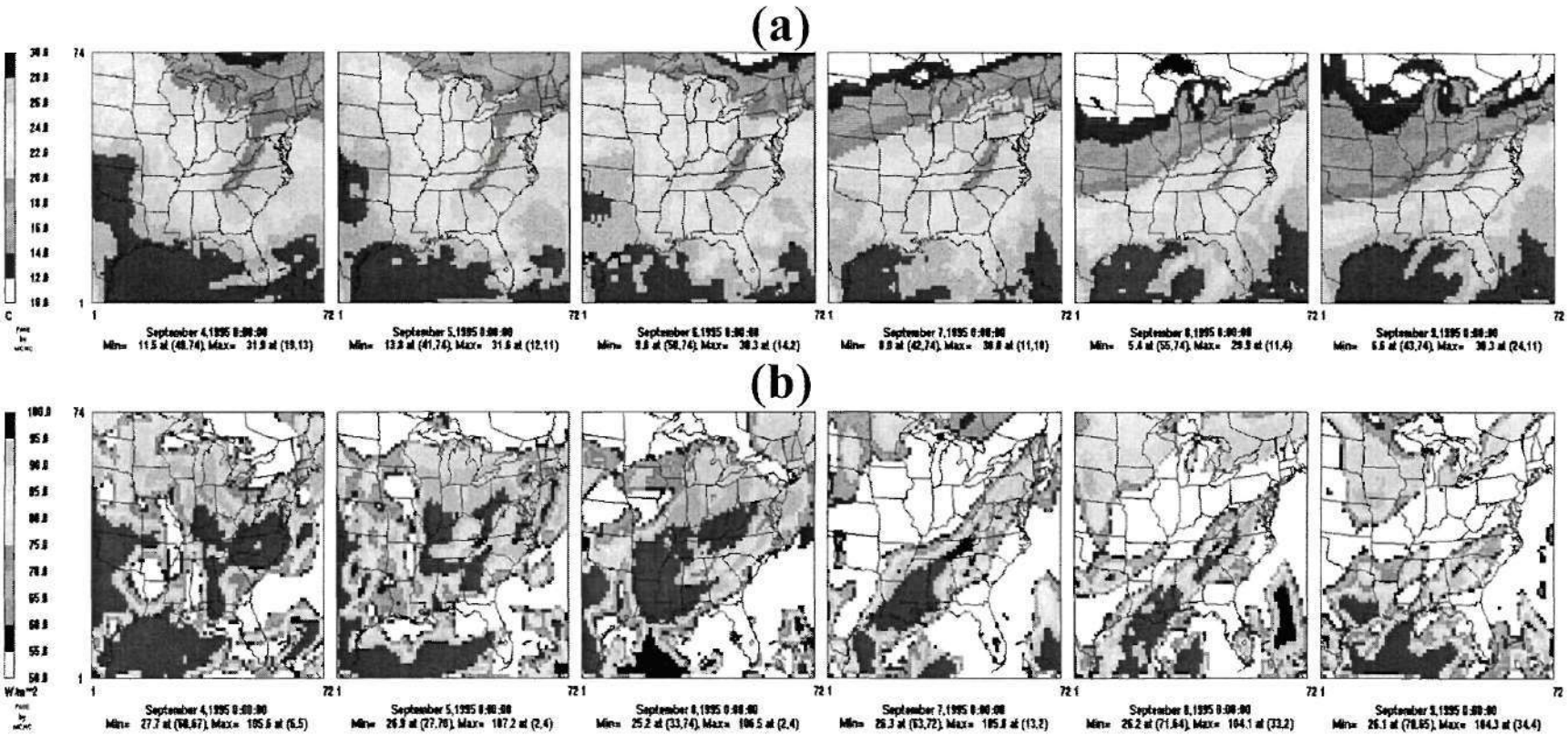

Figure 5-10.
Temperature and PAR values for 04-09 September 1995. (a) mean daily temperature (°C). (b) mean daily PAR ($W \cdot m^{-2}$).

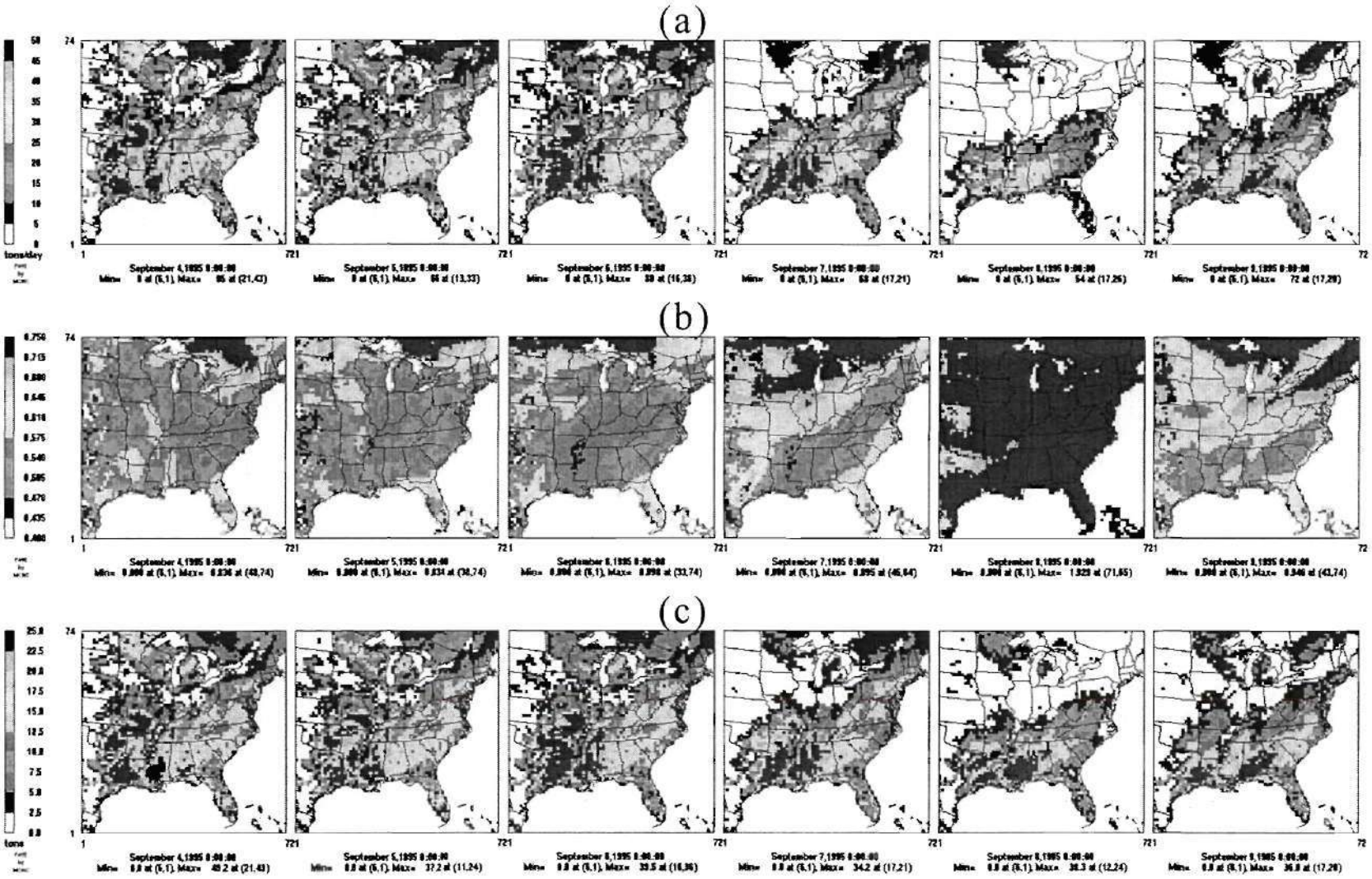

Figure 5-11.
Summary of BEIS3 isoprene emissions for 04-09 September 1995. (a) mean daily emissions (tons/day). (b) coefficient of variation in daily emissions. (c) standard deviation of daily emissions (tons).

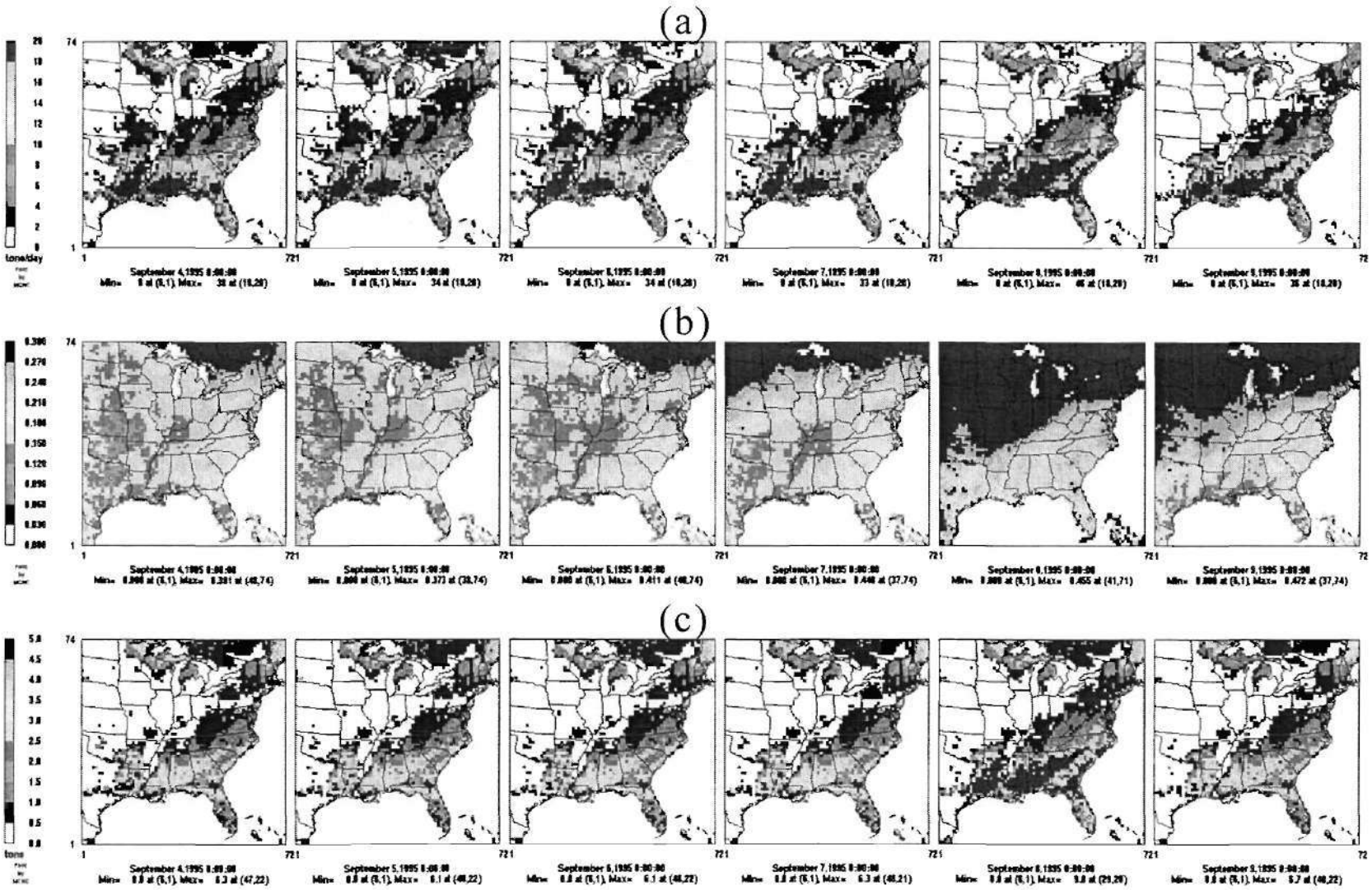

Figure 5-12.
Summary of BEIS3 monoterpene emissions for 04-09 September 1995. (a) mean daily emissions (tons/day). (b) coefficient of variation in daily emissions. (c) standard deviation of daily emissions (tons).

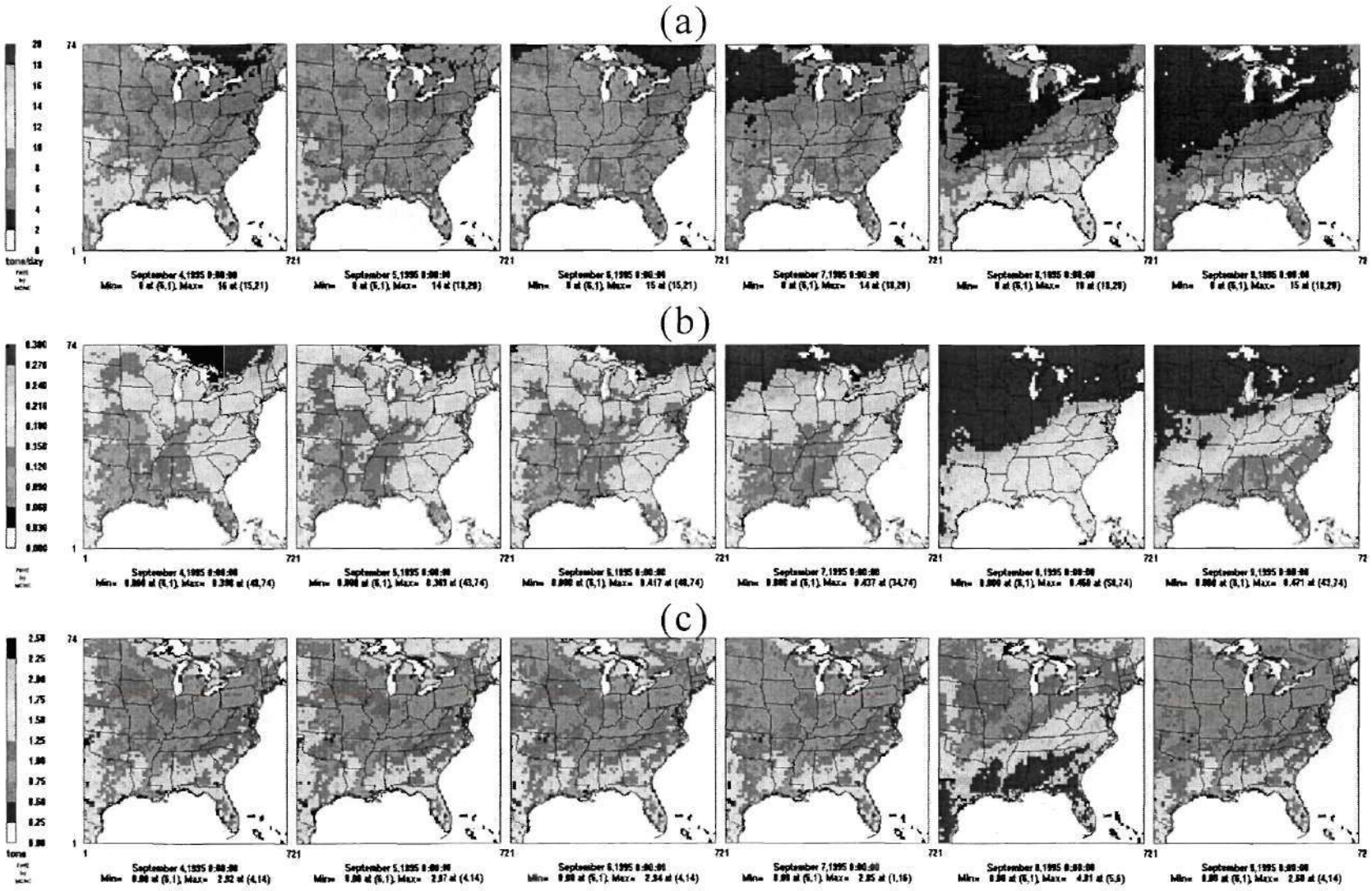

Figure 5-13.
Summary of BEIS3 OVOC emissions for 04-09 September 1995. (a) mean daily emissions (tons/day). (b) coefficient of variation in daily emissions. (c) standard deviation of daily emissions (tons).

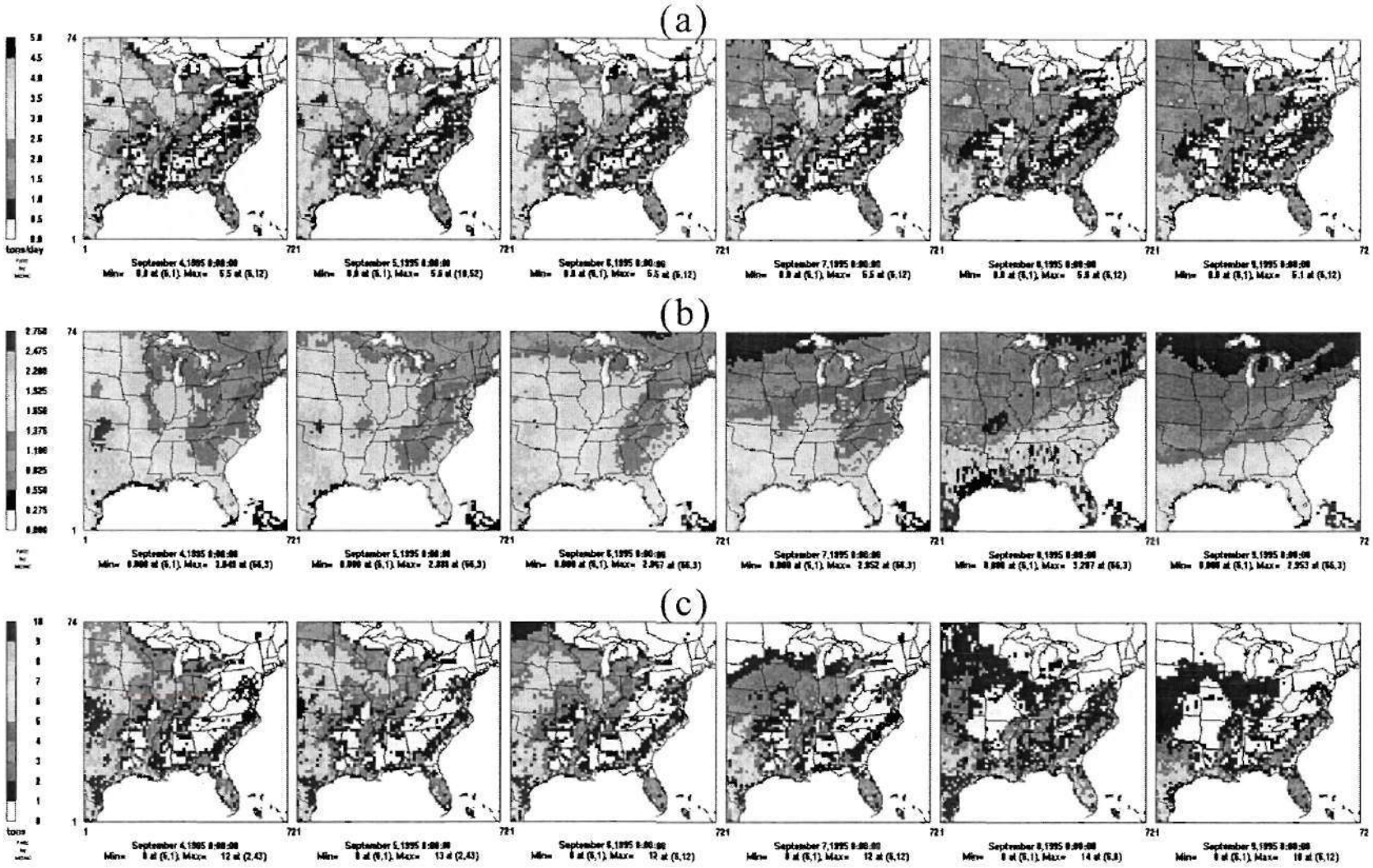

Figure 5-14.
Summary of BEIS3 NO_X emissions for 04-09 September 1995. (a) mean daily emissions (tons/day). (b) coefficient of variation in daily emissions. (c) standard deviation of daily emissions (tons).

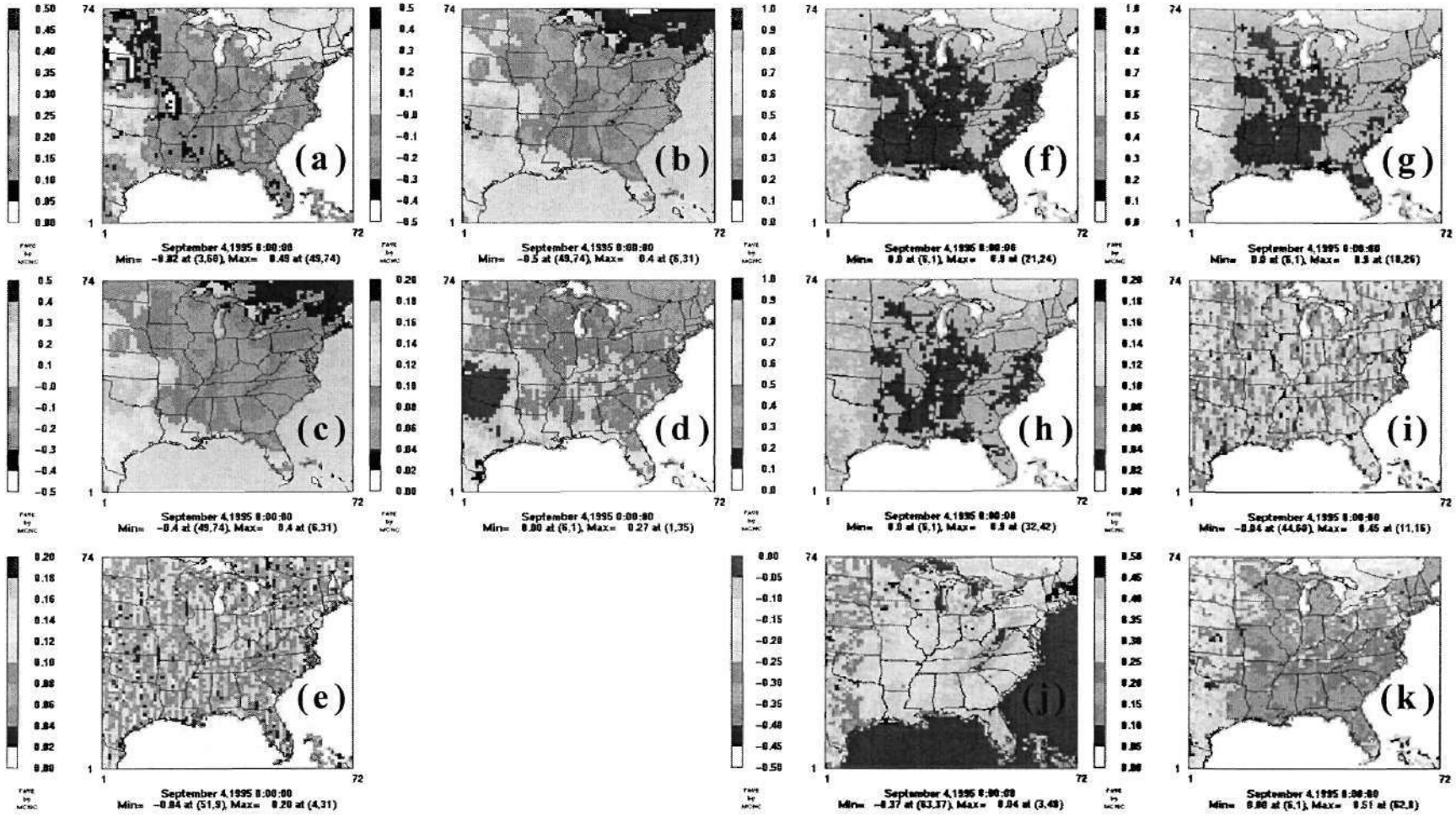

Figure 5-15.
Correlation coefficients of BEIS3 isoprene model parameters and model data inputs to BEIS3 isoprene emissions estimates for 04 September 1995. (a) C_T to BEIS3 isoprene emissions estimates; (b) c_{T1} to BEIS3 isoprene emissions estimates; (c) c_{T2} to BEIS3 isoprene emissions estimates; (d) T_M to BEIS3 isoprene emissions estimates; (e) T to BEIS3 isoprene emissions estimates; (f) C_L to BEIS3 isoprene emissions estimates; (g) α to BEIS3 isoprene emissions estimates; (h) c_{L1} to BEIS3 isoprene emissions estimates; (i) L to BEIS3 isoprene emissions estimates; (j) LAI to BEIS3 isoprene emissions estimates; and (k) E_S to BEIS3 isoprene emissions estimates.

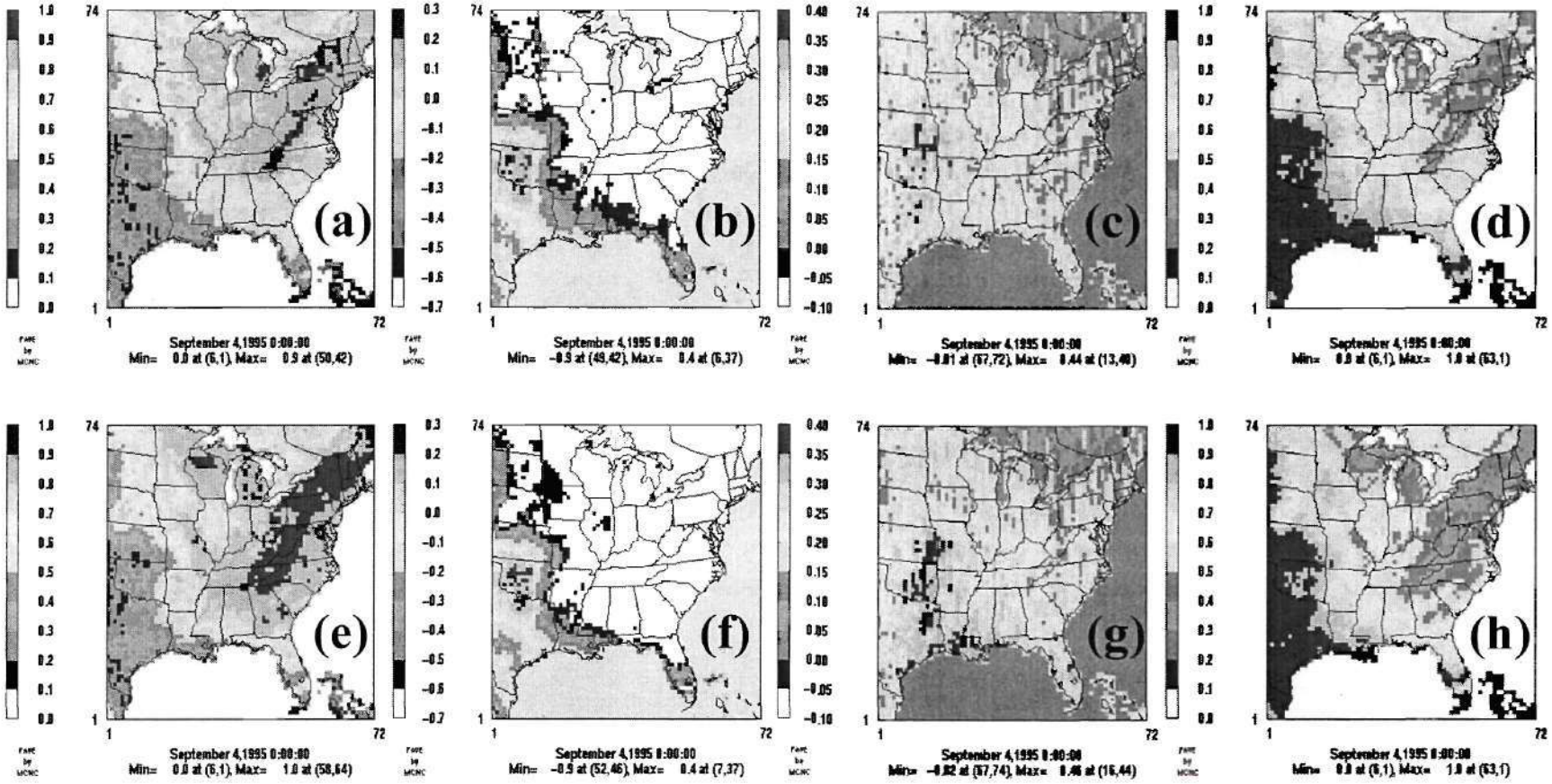

Figure 5-16.
Correlation coefficients of BEIS3 monoterpene and OVOC model parameters and model data inputs to BEIS3 monoterpene and OVOC emissions estimates for 04 September 1995. (a) C_T to BEIS3 monoterpene emissions estimates; (b) β to BEIS3 monoterpene emissions estimates; (c) T to BEIS3 monoterpene emissions estimates; (d) E_S to BEIS3 monoterpene emissions estimates; (e) C_T to BEIS3 OVOC emissions estimates; (f) β to BEIS3 OVOC emissions estimates; (g) T to BEIS3 OVOC emissions estimates; and (h) E_S to BEIS3 OVOC emissions estimates.

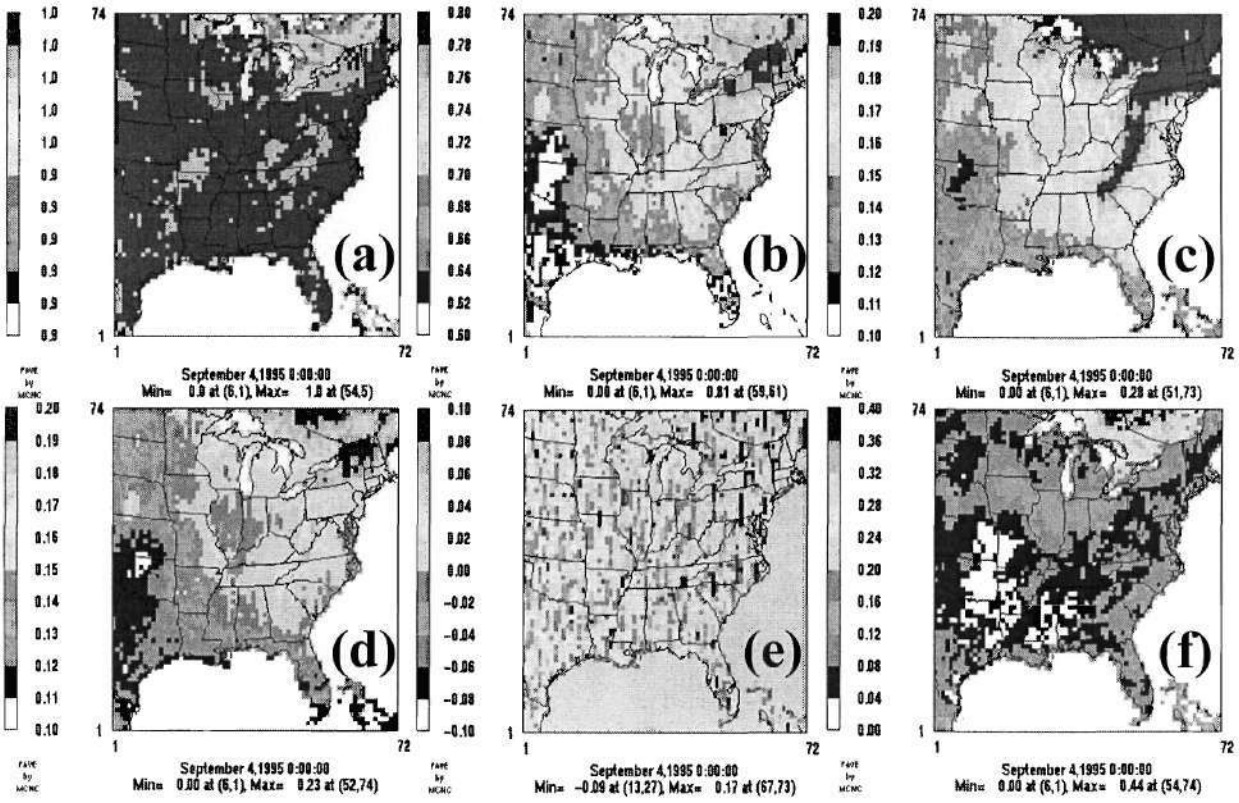

Figure 5-17.
Correlation coefficients of BEIS3 NO_X model parameters and model data inputs to BEIS3 NO_X emissions estimates for 04 September 1995. (a) C_T to BEIS3 NO_X emissions estimates; (b) T_1 to BEIS3 NO_X emissions estimates; (c) T_2 to BEIS3 NO_X emissions estimates; (d) T_3 to BEIS3 NO_X emissions estimates; (e) T to BEIS3 NO_X emissions estimates; and (f) E_S to BEIS3 NO_X emissions estimates.

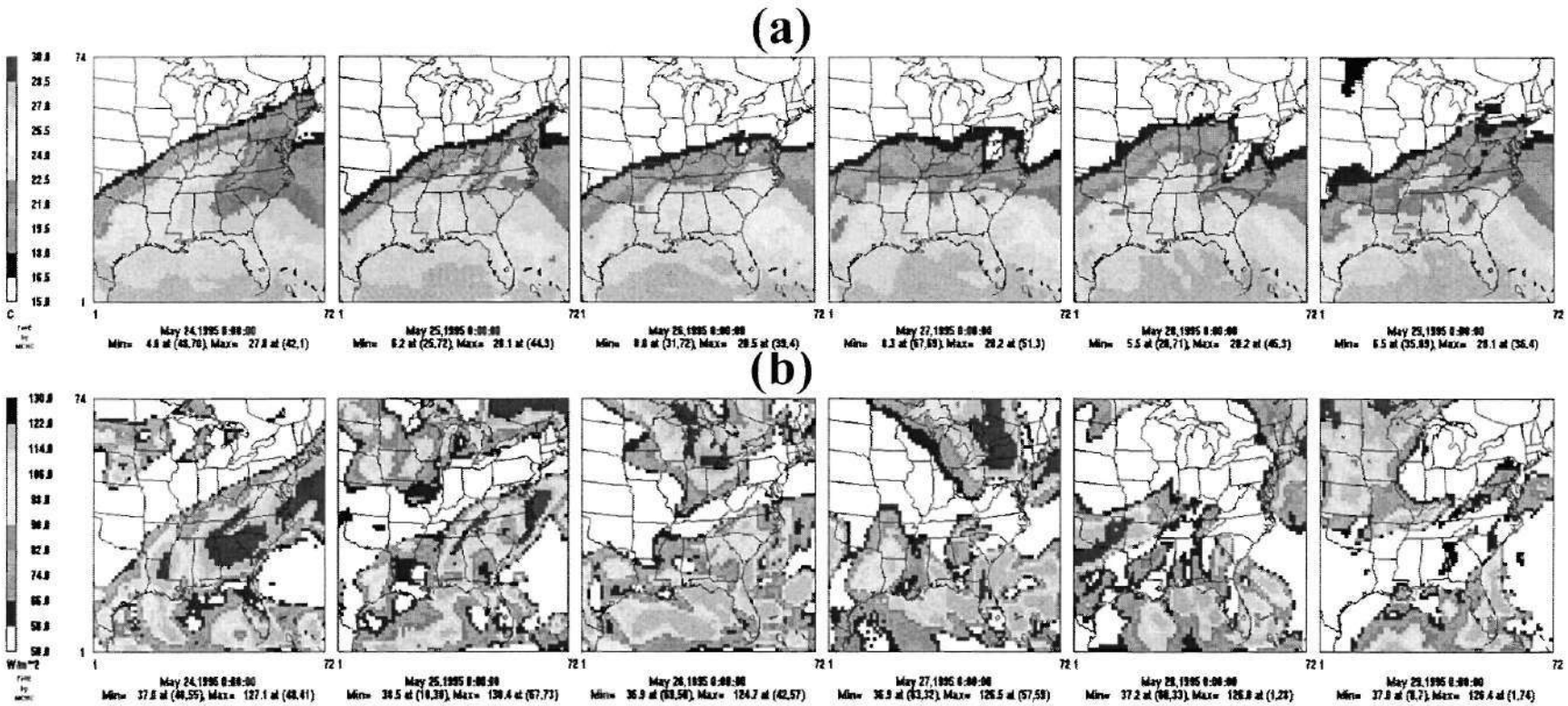

Figure 5-18.
Temperature and PAR values for 24-29 May 1995. (a) mean daily temperature (ºC). (b) mean daily PAR (W·m-2).

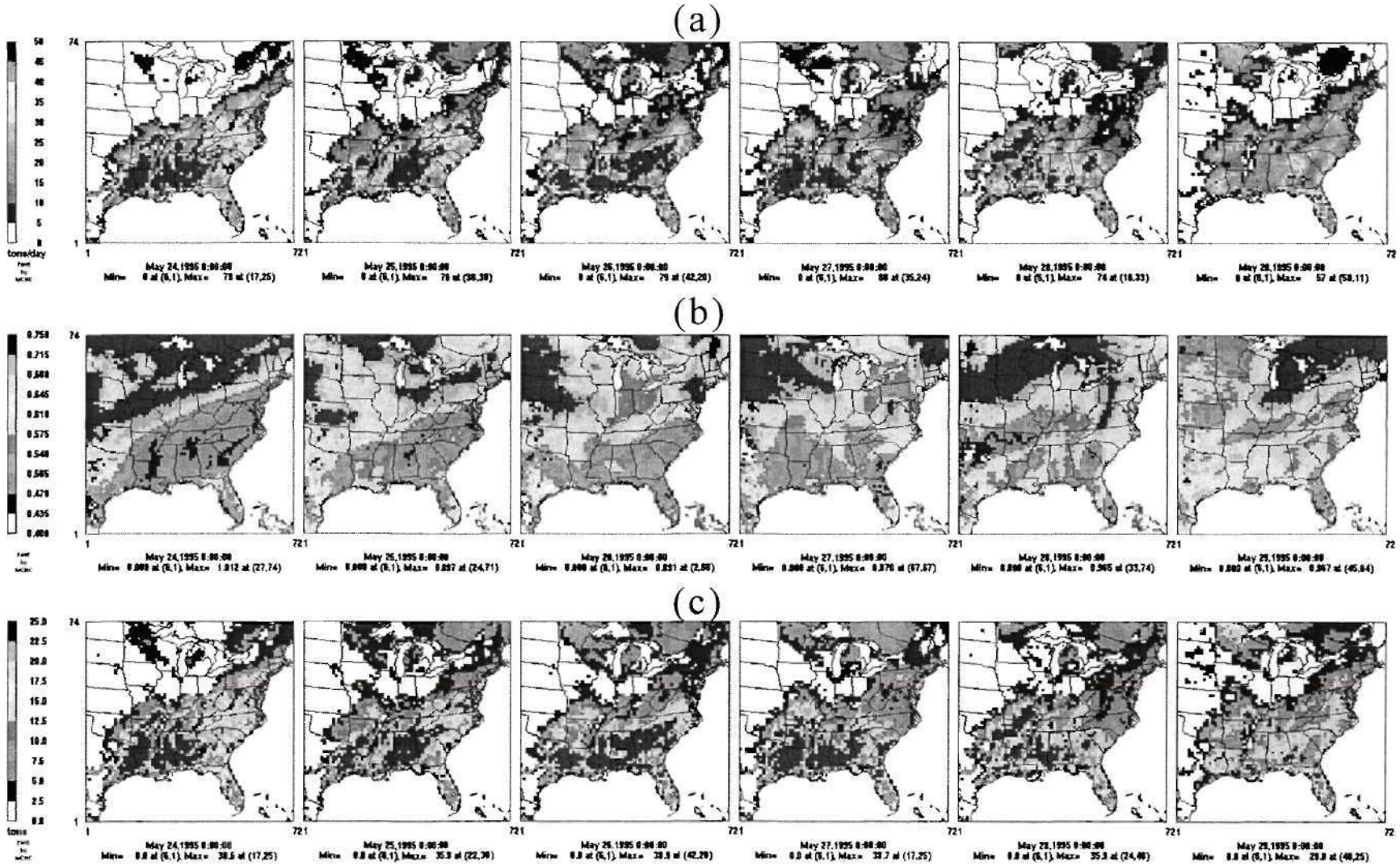

Figure 5-19.
Summary of BEIS3 isoprene emissions for 24-29 May 1995. (a) mean daily emissions (tons/day). (b) coefficient of variation in daily emissions. (c) standard deviation of daily emissions (tons).

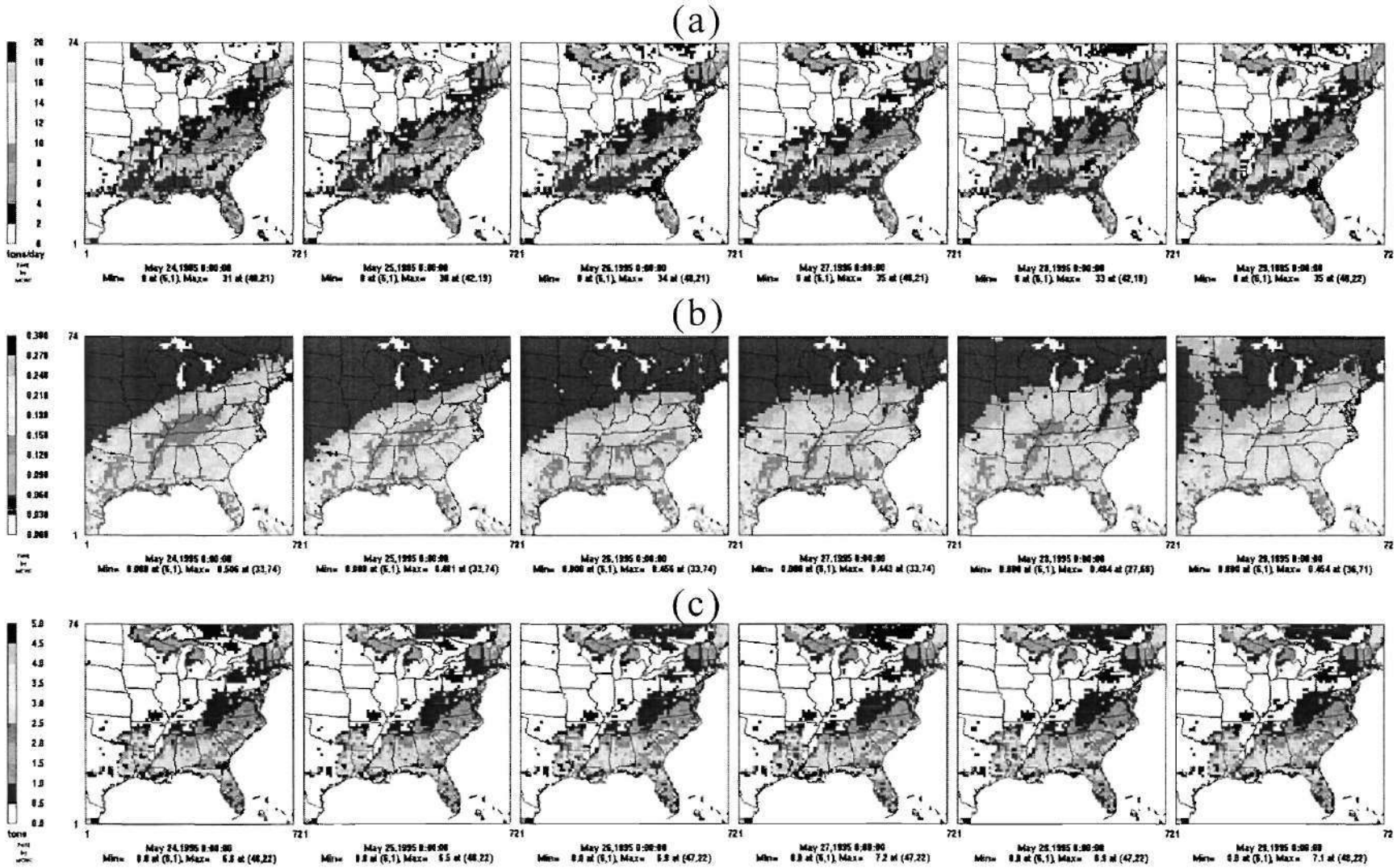

Figure 5-20.
Summary of BEIS3 monoterpene emissions for 24-29 May 1995. (a) mean daily emissions (tons/day). (b) coefficient of variation in daily emissions. (c) standard deviation of daily emissions (tons).

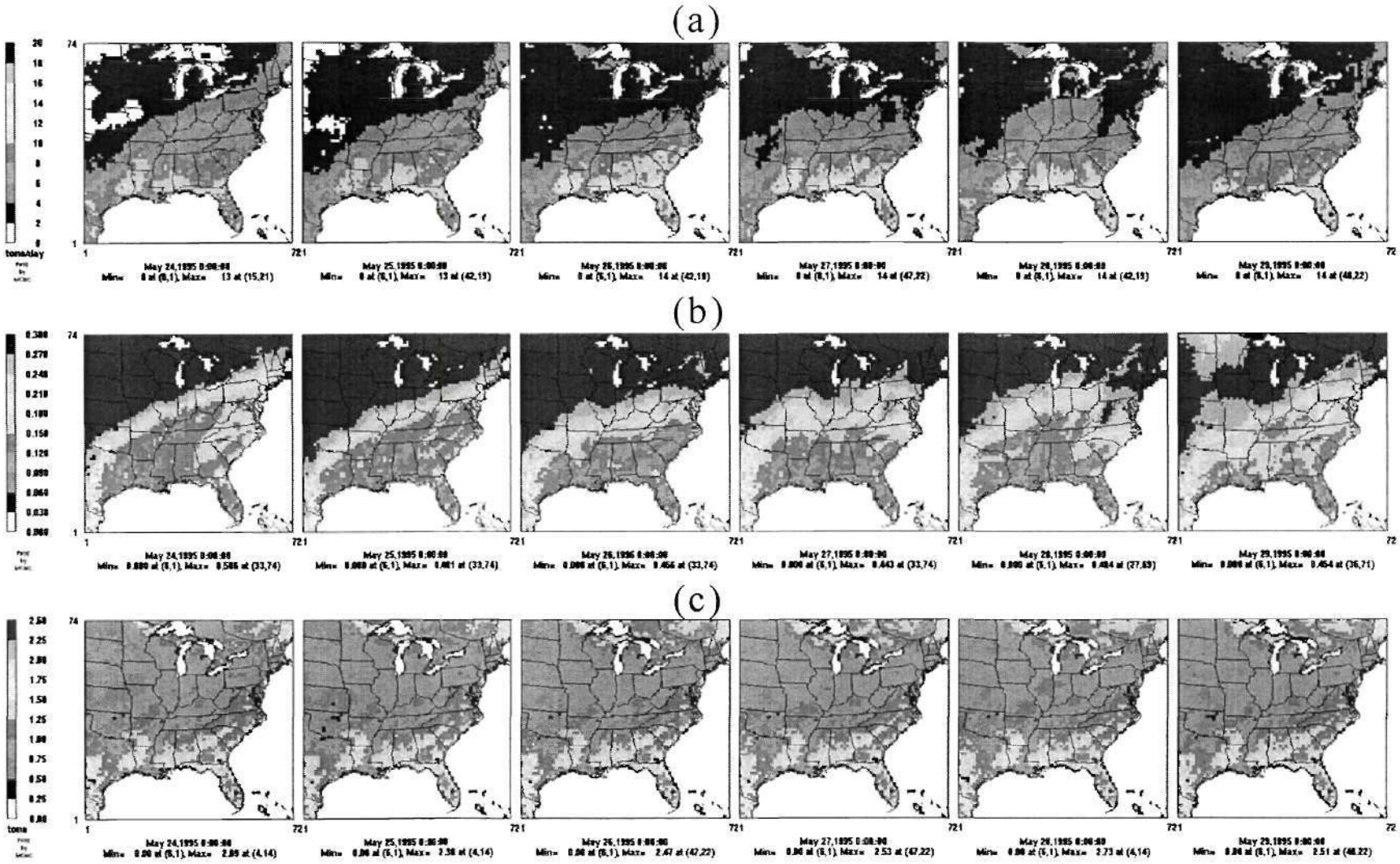

Figure 5-21.
Summary of BEIS3 OVOC emissions for 24-29 May 1995. (a) mean daily emissions (tons/day). (b) coefficient of variation in daily emissions. (c) standard deviation of daily emissions (tons).

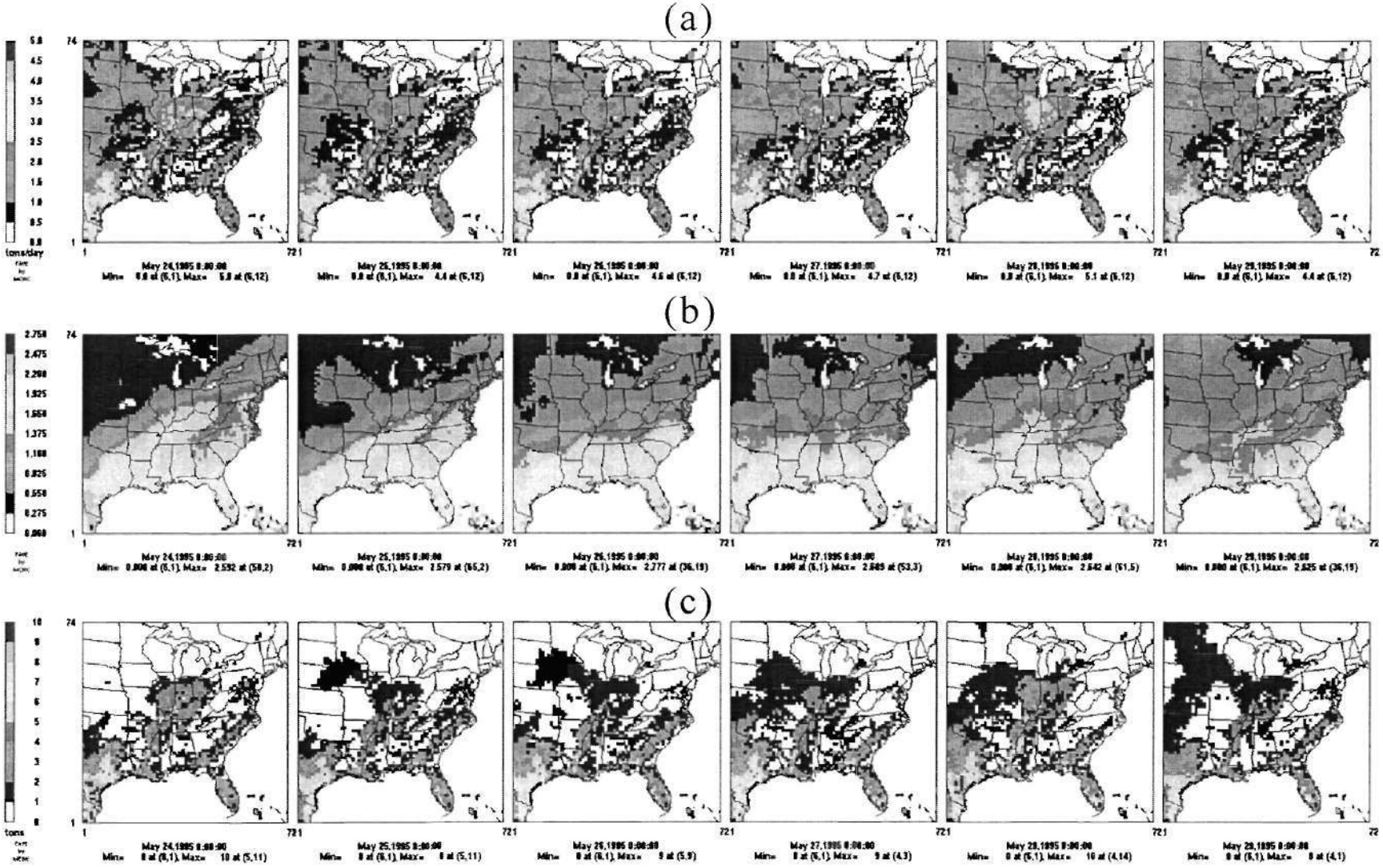

Figure 5-22.
Summary of BEIS3 NO_X emissions for 24-29 May 1995. (a) mean daily emissions (tons/day). (b) coefficient of variation in daily emissions. (c) standard deviation of daily emissions (tons).

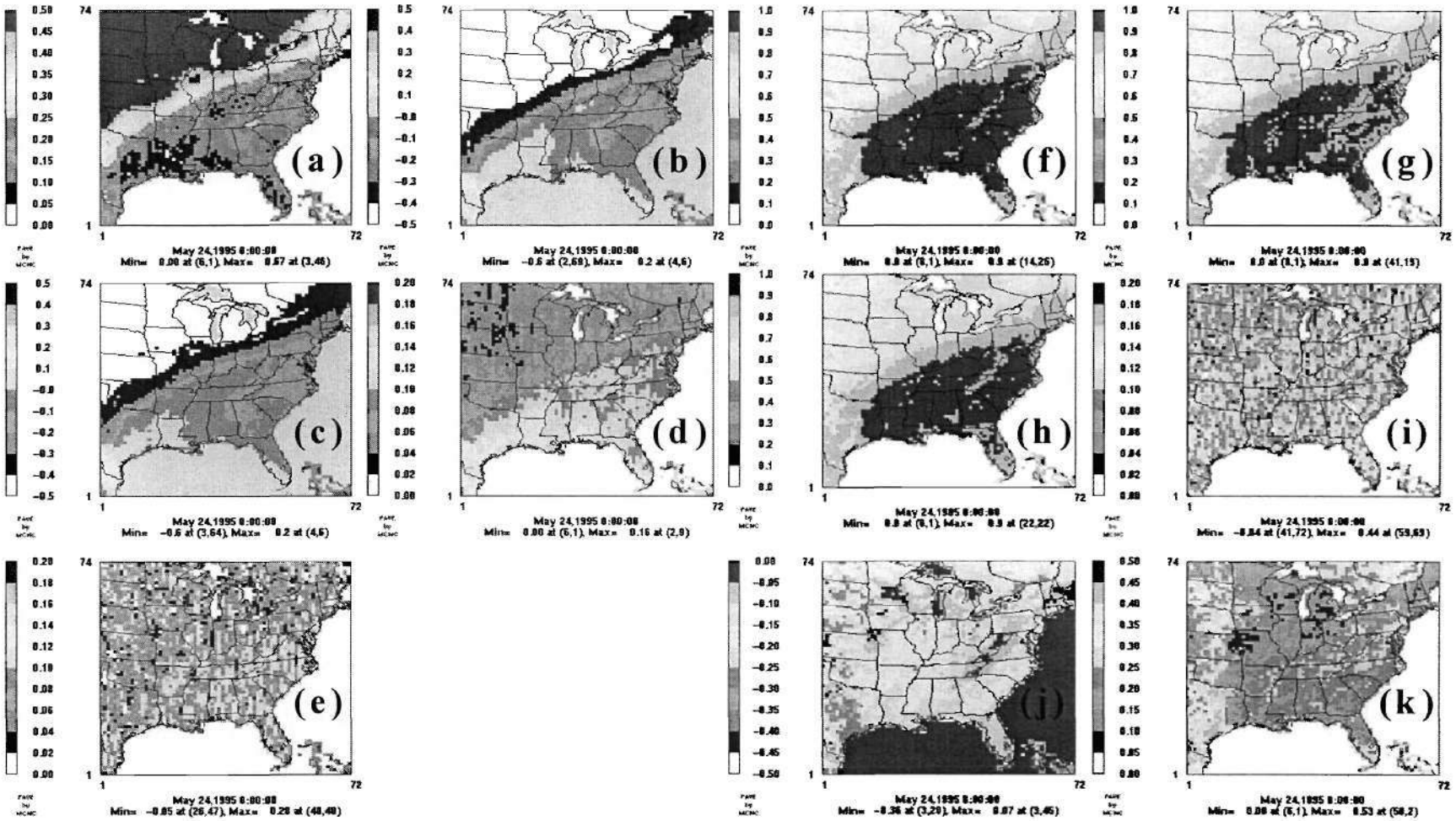

Figure 5-23.
Correlation coefficients of BEIS3 isoprene model parameters and model data inputs to BEIS3 isoprene emissions estimates for 24 May 1995. (a) C_T to BEIS3 isoprene emissions estimates; (b) c_{T1} to BEIS3 isoprene emissions estimates; (c) c_{T2} to BEIS3 isoprene emissions estimates; (d) T_M to BEIS3 isoprene emissions estimates; (e) T to BEIS3 isoprene emissions estimates; (f) C_L to BEIS3 isoprene emissions estimates; (g) α to BEIS3 isoprene emissions estimates; (h) c_{L1} to BEIS3 isoprene emissions estimates; (i) L to BEIS3 isoprene emissions estimates; (j) LAI to BEIS3 isoprene emissions estimates; and (k) E_S to BEIS3 isoprene emissions estimates.

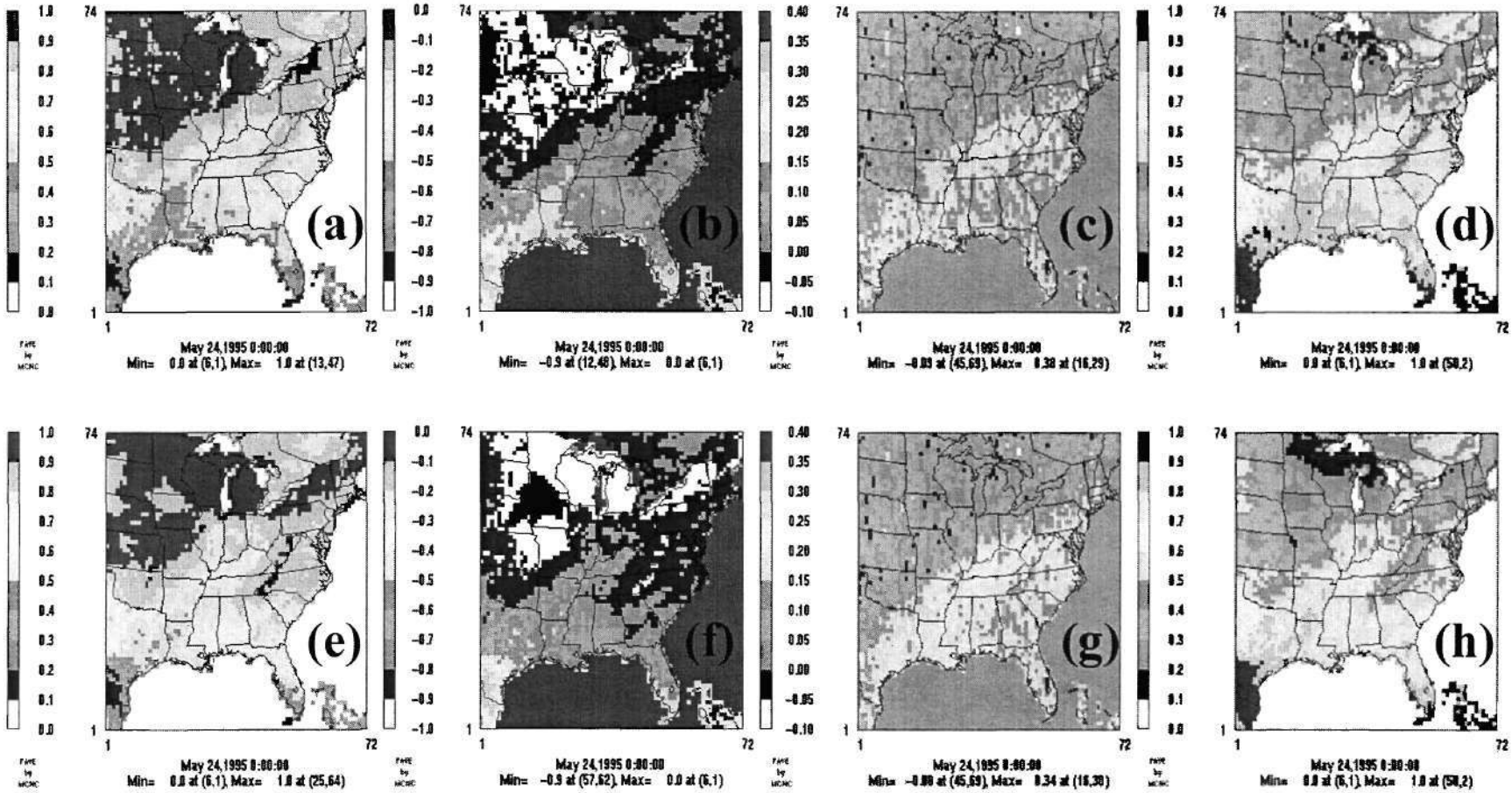

Figure 5-24.
Correlation coefficients of BEIS3 monoterpene and OVOC model parameters and model data inputs to BEIS3 monoterpene and OVOC emissions estimates for 24 May 1995. (a) C_T to BEIS3 monoterpene emissions estimates; (b) β to BEIS3 monoterpene emissions estimates; (c) T to BEIS3 monoterpene emissions estimates; (d) E_S to BEIS3 monoterpene emissions estimates; (e) C_T to BEIS3 OVOC emissions estimates; (f) β to BEIS3 OVOC emissions estimates; (g) T to BEIS3 OVOC emissions estimates; and (h) E_S to BEIS3 OVOC emissions estimates.

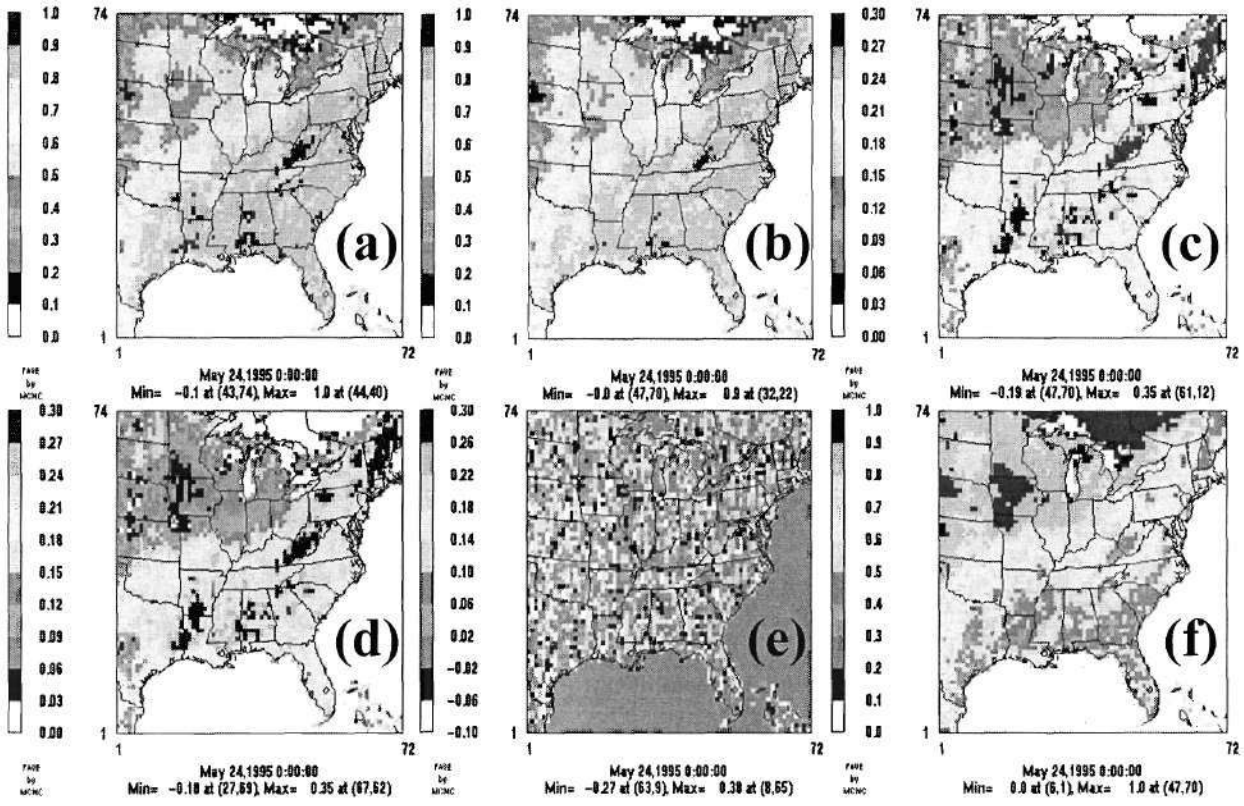

Figure 5-25.
Correlation coefficients of BEIS3 NO_X model parameters and model data inputs to BEIS3 NO_X emissions estimates for 24 May 1995. (a) C_T to BEIS3 NO_X emissions estimates; (b) T_1 to BEIS3 NO_X emissions estimates; (c) T_2 to BEIS3 NO_X emissions estimates; (d) T_3 to BEIS3 NO_X emissions estimates; (e) T to BEIS3 NO_X emissions estimates; and (f) E_S to BEIS3 NO_X emissions estimates.